

Research Report RR-12-01



Sheth-Uicker Convention Revisited

A Normal Form for Specifying Mechanisms

Bertold Bongardt, 07/2012

Research Report RR-12-01

German Research Center for Artificial Intelligence (DFKI) GmbH

Editorial Board: Prof. Dr. Frank Kirchner, Prof. Dr. Prof. h.c. Andreas Dengel, Prof. Dr. Hans Uszkoreit, Prof. Dr. Dr. h.c. mult. Wolfgang Wahlster

Bibliographic information published by the German National Library

The German National Library lists this publication in the German National Biography; detailed bibliographic data are available in the internet at <http://dnb.ddb.de>.

Editorial Board:

Prof. Dr. Frank Kirchner

Prof. Dr. Prof. h.c. Andreas Dengel

Prof. Dr. Hans Uszkoreit

Prof. Dr. Dr. h.c. mult. Wolfgang Wahlster

© German Research Center for Artificial Intelligence (DFKI) GmbH, 2012

This work may not be copied or reproduced in whole or in part for any commercial purpose. Permission to copy in whole or in part without payment of fee is granted for nonprofit educational and research purposes provided that all such whole or partial copies include the following: a notice that such copying is by permission of the German Research Center for Artificial Intelligence (DFKI) GmbH, Kaiserslautern, Federal Republic of Germany; an acknowledgement of the authors and individual contributors to the work; all applicable portions of this copyright notice. Copying, reproducing, or republishing for any other purpose shall require a licence with payment of fee to German Research Center for Artificial Intelligence (DFKI) GmbH.

Issue RR-12-01 (2012)

ISSN 0946-008x

German Research Center for Artificial Intelligence
Deutsches Forschungszentrum für Künstliche Intelligenz
DFKI GmbH

Founded in 1988, DFKI today is one of the largest nonprofit contract research institutes in the field of innovative software technology based on Artificial Intelligence (AI) methods. DFKI is focusing on the complete cycle of innovation – from world-class basic research and technology development through leading-edge demonstrators and prototypes to product functions and commercialization.

Based in Kaiserslautern, Saarbrücken and Bremen, the German Research Center for Artificial Intelligence ranks among the important 'Centers of Excellence' worldwide. An important element of DFKI's mission is to move innovations as quickly as possible from the lab into the marketplace. Only by maintaining research projects at the forefront of science DFKI has the strength to meet its technology transfer goals.

The key directors of DFKI are Prof. Wolfgang Wahlster (CEO) and Dr. Walter Olthoff (CFO). DFKI's research departments are directed by internationally recognized research scientists:

- Knowledge Management (Prof. A. Dengel)
- Cyber-Physical Systems (Prof. R. Drechsler)
- Robotics Innovation Center (Prof. F. Kirchner)
- Innovative Retail Laboratory (Prof. A. Krüger)
- Institute for Information Systems (Prof. P. Loos)
- Embedded Intelligence (Prof. P. Lukowicz)
- Agents and Simulated Reality (Prof. P. Slusallek)
- Augmented Vision (Prof. D. Stricker)
- Language Technology (Prof. H. Uszkoreit)
- Intelligent User Interfaces (Prof. W. Wahlster)
- Innovative Factory Systems (Prof. D. Zühlke)

In this series, DFKI publishes research reports, technical memos, documents (eg. workshop proceedings), and final project reports. The aim is to make new results, ideas, and software available as quickly as possible.

Prof. Wolfgang Wahlster
Director

Sheth-Uicker Convention Revisited

A Normal Form for Specifying Mechanisms

Bertold Bongardt

07/2012

Research Report RR-12-01 des
Deutschen Forschungszentrums für Künstliche Intelligenz (DFKI)

Abstract

In this survey, different conventions for specifying kinematics of mechanisms and their properties are reviewed with emphasis on the convention developed by Sheth and Uicker in 1971. This convention partitions displacements in joint- and link displacements and decomposes these displacements into three axial screw displacements. Because of this systematic construction, the convention of Sheth and Uicker features several practical and theoretical preferences which are reflected in this article. For doing so, two comparisons are conducted: first, the Sheth-Uicker convention is compared to other kinematic conventions. Second, the convention – as the Dual Euler Angle representation of finite spatial displacements – is placed into context of three other popular displacement representations. For enabling these comparisons in a rather self-consistent text, notations of necessary entities are assembled, adapted, or newly defined. In general, this article is intended as a contribution to the development of a common normal form for kinematics of mechanisms.

Zusammenfassung

In diesem Übersichtsartikel werden verschiedene Konventionen zur Spezifikation von Mechanismen und ihre Eigenschaften verglichen. Dabei steht die Konvention von Sheth und Uicker aus dem Jahr 1971 im Vordergrund: Bei dieser Konvention werden die relativen Posenversätze einer Kinematik in Versätze der Gelenke und Versätze der Gliedmaße aufgeteilt und jeder relative Versatz wird in drei lineare Schrauben zerlegt. Aufgrund dieser systematischen Behandlung ergeben sich für diese Konvention unterschiedliche praktische und theoretische Vorzüge, die in diesem Artikel vorgestellt werden. Dafür werden zwei Vergleiche erarbeitet: Zunächst wird die Sheth-Uicker Konvention mit anderen kinematischen Konventionen verglichen. Außerdem wird die Konvention – als Repräsentation über duale Eulerwinkel – in den Kontext von drei anderen populären Repräsentationen für relative Posenversätze gestellt. Um die Vergleiche in einem konsistenten Text durchzuführen, werden Notationen der notwendigen Größen zusammengestellt, angepasst oder neu eingeführt. Allgemein soll dieser Artikel zur Entwicklung einer einheitlichen Normalform für Kinematiken von Mechanismen beitragen.

Contents

| | |
|--|------------|
| Abstract | iii |
| 1 Introduction | 1 |
| 2 Mechanisms and Kinematics | 4 |
| 2.1 Mechanisms and Graphs | 4 |
| 2.1.1 Links and Joints | 4 |
| 2.2 Kinematic Specification | 5 |
| 2.3 Frames and Poses | 5 |
| 2.3.1 Pose Sets and Frame Sets | 6 |
| 2.3.2 Kinematic Conventions | 6 |
| 2.4 Classic Kinematic Problems | 7 |
| 3 Representations for Finite Displacements | 9 |
| 3.1 Homogeneous-Linear Representation | 9 |
| 3.1.1 Rotation Matrix | 9 |
| 3.1.2 Homogeneous Matrix | 10 |
| 3.1.3 Active and Passive Interpretation | 10 |
| 3.2 Vectorial Representations | 11 |
| 3.2.1 Angle and Axis | 11 |
| 3.2.2 Geometry of Lines | 12 |
| 3.2.3 Geometry of Screws | 14 |
| 3.2.4 Finite Twists | 16 |
| 3.3 Symmetric Representation | 18 |
| 3.3.1 Quaternions | 18 |
| 3.3.2 Dual Quaternions | 18 |
| 3.4 Sequential Representations | 20 |
| 3.4.1 Euler Angles in Bunge Convention | 20 |
| 3.4.2 Dual Euler Angles in Bunge Convention | 20 |
| 3.5 Other Representations | 21 |
| 4 Kinematic Modeling Conventions | 22 |
| 4.1 Prerequisites | 22 |
| 4.2 Two-Frame Convention | 23 |
| 4.3 Denavit-Hartenberg Conventions | 24 |
| 4.4 Augmented Convention | 25 |
| 4.5 Other Modeling Conventions | 27 |
| 5 Example | 30 |
| 5.1 Description of the Example Mechanism | 30 |
| 5.2 Comparison | 30 |
| 6 Comparisons | 33 |
| 6.1 Sheth-Uicker as a Kinematic Convention | 33 |
| 6.1.1 Screw, Planar, and Spatial Displacements | 33 |
| 6.1.2 Sheth-Uicker and Parallel Mechanisms | 33 |
| 6.1.3 Applications for Sheth-Uicker and Denavit-Hartenberg | 34 |
| 6.2 Sheth-Uicker as a Representation for Displacements | 35 |
| 6.2.1 Planar Displacements | 35 |
| 6.2.2 Spatial Displacements | 36 |
| 6.2.3 Principles of Sheth-Uicker and Finite Twist Decompositions | 40 |
| 7 Conclusion | 42 |
| Appendix | 43 |
| A Homogeneous Coordinates | 43 |

| | |
|--|-----------|
| B Vectors and Matrices | 43 |
| B.1 Matrixification and Vectorization | 43 |
| B.2 Exponential and Logarithmic Function for Rotation Matrices | 44 |
| C Geometry of Lines, Screws, Twists | 45 |
| C.1 Closest Points via Parametric Form | 45 |
| C.2 A Tetrahedron | 45 |
| C.3 An Overview of Screw Types | 46 |
| C.4 Three Basic Screw Displacements | 47 |
| D Augmented Convention as Exchange Format | 48 |
| E Tables, Figures, Methods, Symbols | 49 |
| References | 52 |

1 Introduction

Motivation. This survey article reviews different *conventions* which were developed to specify and to compute the kinematics of mechanisms. In particular, these conventions – which here are briefly called *Kinematic Conventions* – deliver sets of parameters that first and foremost can be used to parametrize the displacements which appear in the computational routines of kinematics. Next to this main purpose, kinematic convention fulfill another important function since they serve as *normal forms* of mechanisms. A ‘normal form’ is briefly characterized as a way of representing objects such that a *comparison* with other objects of the same type is enabled (see, e.g., [35, Sec. 1.2]). This ‘mathematical characterization’ of a normal form gains a special meaning in context of the science and engineering of mechanisms: in particular, the development of new machines often is an interdisciplinary effort which is conducted by teams of people with different background, e.g., by *industrial designers, mechanical engineers, simulation and control specialists*, as well as *mathematicians* and *computer scientists*. Throughout the entire development process – which typically consists of a sequence of iterations of designs, trials, and errors, or, in other terms, of synthetical and analytical steps – the involved people need to discuss their findings about function and form, and in particular, about the topology and the geometry of a certain prototype of a mechanism. For this process, a table which is created according to a certain kinematic convention should be considered as a medium¹ that allows to imagine, communicate, document and modify the kinematics of a mechanism prototype – briefly, as a way to *compare* kinematics.

This overview about ‘normal forms of kinematics’ emphasizes the convention developed by Sheth and Uicker in 1971. It points out the practical and theoretical preferences that this convention features for computational and for comparative purposes, since this was not provided systematically by literature to the author’s knowledge. Instead, the Seth-Uicker convention sometimes was considered as ‘complicated niche-convention’ that ‘could be useful’ for dealing with parallel mechanisms. However, as explained here, the convention features the *right degree of complexity* to represent arbitrary mechanisms conveniently.

Because of the mentioned interface-function of kinematic conventions, this article is intended to be valuable for a heterogeneous audience: independent to the reader’s prior knowledge and his working discipline, he should be guided along the useful features of Sheth and Uicker’s convention. Of course, from this follows that some parts of this text might be neither new nor interesting for a reader with an established theoretical background, while for others, the presentation might be quite compact and therefore not simple to understand. In particular, Section 3 is a comprehensive summary about displacement representations that contains (slightly) more material than necessarily required for the remainder of the text. In both cases, the reader is free to skip this section or to skim through it briefly, at first.² Later, the section might be read in more detail for looking up certain relations, or for using it as a compact guide or tutorial through the literature of representation theory. To increase readability, a lot of concepts in this article are introduced by providing sketches which illustrate their geometry.

Concept and Contribution. In this survey, four conventions for specifying kinematics of mechanisms and their properties are compared in detail. First, the property of Sheth and Uicker’s convention of partitioning displacements in *joint-* and *link* displacements, is formalized by a convention, that is named here as *two-frame* convention, since two-frames per joint are used. Subsequently, the well-known classic Denavit-Hartenberg convention and its modified variant are presented. Finally, Sheth-Uicker convention is introduced. By introducing a notation that is based on frame sets which are indexed using a graph-related scheme, a convenient comparison of the four conventions is obtained: it is shown how Seth-Uicker’s convention can seamlessly be interpreted as the *augmentation* of (1) the *two-frame* convention (2) the well-known *classic* Denavit-Hartenberg (DH) convention, and (3) the *modified* Denavit-Hartenberg convention. Therefore, here the Sheth-Uicker convention is briefly called *augmented convention*.

By means of the two-frame convention, the augmented convention is also interpreted as a representation for finite spatial displacements and compared against three other common representations. From this viewpoint, the augmented convention can be interpreted as an affine generalization of z - x' - z'' Euler angles. It is remarkable that Yang published articles in 1969 where the same geometric decomposition was applied. Here, it is argued that the decomposition of the augmented convention should be considered as a *complementary convention* to the description of a finite displacement via a finite twist. The argumentation is based on the fact that Dual Euler Angles representation and Finite Twist representation together form a certain spatial triangle. The geometry of this triangle is analyzed.

¹– next to physical setups, technical drawings, and, static and dynamic visualizations –

²Displacement representations are independent of ‘mechanism kinematics’, but not the other way round.

Next to this spatial comparison, Sheth-Uicker’s convention is analyzed as a representation for planar displacements: it is elaborated that also for this more simple case, Sheth-Uicker’s convention features advantages compared against the popular Denavit-Hartenberg convention.

Stemming from these theoretical findings, practical advantages of Sheth-Uicker’s convention can deduced and are illustrated: next to the property of be useful for parallel mechanisms, it is illustrated that on line of a table of Sheth-Uicker parameters reflect the geometry of a link geometry. Therefore, it is not only useful for parallel mechanisms, but also for every kinematic chain that contains spatial displacements. In particular, this article provided a detailed example for a chain that features a skew link geometry.

New light is shed on the augmented convention by showing connections to line, screw, and graph theory. Additionally, it is shown that – next to its theoretical solidity – the *augmented convention* provides several advantages for practical modeling tasks compared to a modeling based on other conventions. Since all computations – that are needed to derive the description of a mechanism in terms of the augmented convention – can be implemented in software, the convention is easy to use without manual effort. Finally, because Sheth-Uicker’s convention is a generalization of the other three mentioned conventions, it can be used as a tool for transferring the specification of a mechanism from one convention to another.

Structure. This document is structured as follows: In Section 2, a set of definitions is introduced for dealing with *mechanisms*. Here, a *frame-based* and *graph-based* notation is prepared for the succeeding sections. In particular, the problem of the *kinematic specification of a mechanism* is established (Problem A). In Section 3, four types of representations of displacements are presented. We use the terms *homogeneous-linear*, *vectorial*, *symmetric*, and *sequential* to describe these types. All four representations are popular and are used in the comparison section (Section 6). Additionally in Section 3, facts about the *geometry of lines* and *screws* is compiled.

In Section 4, the central *Sheth-Uicker* (SU) convention is introduced, next to the two-frame, the classic and the modified Denavit-Hartenberg (DH) convention. Here, the preparations from the first two sections (Section 2 and Section 3) are used. Each of the four conventions is introduced, first, in matrix form, second, in terms of a frame-placing procedure, and, third, if possible, by means of finite twists. In Section 5, an example is provided to illustrate Section 4: it shows the usage of the *augmented convention* in comparison to classic and modified DH conventions. The example mechanism features a link whose joint axes define a ‘skew line geometry’.

Section 6 is somehow the central section of this article: first, the augmented convention is compared as kinematic convention (Section 4 with regard to Section 2), second, the augmented convention is compared as a displacement representation (Section 4 with regard to Section 3). By doing so, the properties of the Sheth-Uicker convention are worked out. In the final Section 7, a comprehensive overview is provided.

Style. This document should be readable as a descriptive survey, but also as an article that introduces *novel* comparisons and outlines based on a *unified* notation (based on frame-sets, tuple indices, and triple indices). In general, the reader shall be guided by a lot of *geometric* insight. The notation has been adapted to deal with aspects from different disciplines. For the sake of brevity, not every conversion formula between representations is contained. Other great articles exist, that contain those. For example, the exp-log connection is missing. Also, the topics *quaternions* and *dual quaternions* are only introduced for reasons of completeness, and not thoroughly. Finally, the proper handling of ‘terminal frames’ (frames at the first ‘base’ link and last ‘end-effector’ links) is missing.

Notation. Throughout this article, several conventions for notation are used. Here, they are briefly introduced. A vector is denoted by a small bold letter, e.g., \mathbf{a} , a matrix by capital bold letter, e.g., \mathbf{M} . Sets and other nested ‘container’ data types are represented with fractional letters, like \mathcal{S} . Lines, screws, displacements, links, joints, and frames are denoted by capital letters. Names of methods are set in typewriter font, e.g., \mathbf{f} . An entity that is normalized is attached with a hat, like $\hat{(\cdot)}$. The imaginary unit is denoted with $i = \sqrt{-1}$, the imaginary vector unit is denoted with $\mathbf{i} = (i, j, k)^T$, such that $i^2 = j^2 = k^2 = ijk = -1$.

The dual unit is named as $\epsilon = \sqrt{0}$, a dual entity is equipped with a tilde as $\tilde{(\cdot)}$. The dual part of a dual entity is indicated by a ring $\overset{\circ}{(\cdot)}$. Time variant entities are marked as $\overline{(\cdot)}$, time invariant entities as $\underline{(\cdot)}$. The vectors on the standard axes are denoted as $\mathbf{e}_x, \mathbf{e}_y, \mathbf{e}_z$. For operations, the following are needed: the sign \cdot indicates a scalar, vector, or matrix multiplication. Multiplications of dual entities are marked with a ring, as \odot . The operator $(\cdot)^\otimes$ creates the skew-symmetric matrix that corresponds to a vector; in the other

direction, the operator $(.)^\oplus$ extracts the axis vector from a skew-symmetric matrix. The operator $(.)^*$, swaps primal and dual part of a dual entity.

In this article, the notation of transposing $(.)^T$ is not used for vectors: instead of writing $\mathbf{a}^T \cdot \mathbf{b}$, a shorter notation is used with the symbol \star to indicate the sum of element-wise multiplications, such that $\mathbf{a} \star \mathbf{b} = \sum a_i \cdot b_i$. Two orthogonal projections are used in this article. First, the orthogonal projection of a vector $\mathbf{b} \in \mathbb{R}^d$ onto some vector $\mathbf{a} \in \mathbb{R}^d$ is denoted as $\pi_{\mathbf{a}}(\mathbf{b})$.

$$\pi_{\mathbf{a}}(\mathbf{b}) = \frac{\mathbf{b} \star \mathbf{a}}{\mathbf{a} \star \mathbf{a}} \cdot \mathbf{a} = \underset{\kappa \cdot \mathbf{a}, \kappa \in \mathbb{R}}{\operatorname{argmin}} \operatorname{dist}(\kappa \cdot \mathbf{a}, \mathbf{b}) . \quad (1)$$

Second, the orthogonal projection of a vector $\mathbf{b} \in \mathbb{R}^d$ into the orthogonal complement $\mathbf{a}^\perp \subset \mathbb{R}^d$ of some vector \mathbf{a} is denoted as $\tau_{\mathbf{a}}(\mathbf{b})$

$$\tau_{\mathbf{a}}(\mathbf{b}) = \mathbf{b} - \frac{\mathbf{b} \star \mathbf{a}}{\mathbf{a} \star \mathbf{a}} \cdot \mathbf{a} = \underset{\mathbf{p} \in \mathbf{a}^\perp \subset \mathbb{R}^d}{\operatorname{argmin}} \operatorname{dist}(\mathbf{p}, \mathbf{b}) . \quad (2)$$

2 Mechanisms and Kinematics

In this section, basically standard terms and problems are introduced by means of specific definitions and notations. After introducing the terminology for mechanisms and graphs in Section 2.1, the problem of *kinematic specification* is introduced in Section 2.2. In particular, this problem is expressed by means of frame sets. Additionally, in Section 2.4 frame sets are used for the formulation of classic kinematic problems.

2.1 Mechanisms and Graphs

2.1.1 Links and Joints

A characterization of mechanisms by Phillips ([36, § 1.09]) reads “[..] *It can be said [..] (a) that all motion in constrained mechanism is determined by the real members or links of the mechanism, in contact with one another at the joints of the mechanism; and (b) that, in mechanism, there is no thing existing which cannot be seen as a link or a joint.*” In this article, this characterization is kept and the meaning of ‘a mechanism’ is further constrained: in particular, other aspects of machinery, like actuators or dynamic properties (mass, inertia, friction) are neglected. Therefore, the characterization may be formalized by the following definition.

Definitions 1 (Mechanism (Type), Links and Joints). A (type of a) mechanism³ \mathcal{M} is defined as the tuple $\mathcal{M} = (\mathcal{L}, \mathcal{J})$ where \mathcal{L} denotes the set of sorted links and \mathcal{J} the set of sorted joints as

$$\mathcal{L} = \{L_1, L_2, \dots, L_n\} \quad \mathcal{J} = \{J_{i_1, j_1}, J_{i_2, j_2}, \dots, J_{i_m, j_m}\}. \quad (3)$$

Thereby, a joint⁴ $J_{i_k, j_k} \in \mathcal{J}$ physically connects a link $L_{i_k} \in \mathcal{L}$ with a link $L_{j_k} \in \mathcal{L}$.

Remark: For convenience, the sorting of links can be conducted according to a spanning tree of the mechanism. The naming of joints can be standardized by the convention that $i_k < j_k$ holds $\forall J_{i_k, j_k} \in \mathcal{J}$.

Definitions 2 (Variables and Parameters). The vector of *configuration variables* is denoted as $\mathbf{q} \in \mathbb{Q}$ where \mathbb{Q} is the *configuration space* of \mathcal{M} . The vector of *design parameters* is denoted as $\mathbf{d} \in \mathbb{D}$ where \mathbb{D} is the *design space* of \mathcal{M} .

Definition 3 ((Euclidean) Mechanism). A (Euclidean) mechanism⁵ $\underline{\mathcal{M}}$ is defined as the tuple of mechanism type and the vector of design parameters $\underline{\mathcal{M}} = (\mathcal{M}, \mathbf{d})$.

Remark: The configuration variables and the design parameters do not form a simple ‘vector’ but incorporate the topology of the mechanism defined in Definition 1. Kinematic conventions deal with the best way to denote a mechanism together with its variables \mathbf{q} and its parameters \mathbf{d} (see Problem A).

Definition 4 (Mechanism with a Configuration). Given a Euclidean mechanism $\underline{\mathcal{M}}$, and a configuration vector $\mathbf{q} = \mathbf{q}(t)$ of some timestep t , the ‘mechanisms in that configuration’ can formally be denoted as

$$\underline{\mathcal{M}}(\mathbf{q}(t)) = ((\mathcal{L}, \mathcal{J}), (\mathbf{d}, \mathbf{q}(t))) \quad (4)$$

Remark: Given a configuration, the posture of the mechanism is *not* unique, since the mechanism might be arrangeable in multiple postures for one configuration. This is explained in more detail in Section 2.4 where the forward kinematics problem (Problem B) is introduced.

³– or \mathcal{M} is the *topology* or the *combinatorics* of a mechanism –

⁴– or often called a *pair* –

⁵– or $\underline{\mathcal{M}}$ is a *realization* of the mechanism type \mathcal{M} –

Graphs and Euclidean Graphs. A graph is a pair $\mathcal{G} = (\mathcal{V}, \mathcal{E})$ of sets such that $\mathcal{E} \subseteq \mathcal{V} \times \mathcal{V}$: The elements of the set \mathcal{V} are called *vertices*, the elements of the set \mathcal{E} are called *edges* (e.g. [12]). The combinatorics of a graph are defined by means of an incidence or adjacency structure. Specifically, in application to kinematics, graph theory provides the tools to distinguish between *kinematic chains*, *trees*, and *graphs*. The definition of the mechanism type from Definition 1 can seamlessly be interpreted as the ‘link graph’ of that mechanism $\mathcal{M} \cong \mathcal{G}_{\mathcal{L}} = (\mathcal{L}, \mathcal{J})$ (since $\mathcal{V} = \mathcal{L}$). In Section 6.1.2, it is illustrated how this simple graph can systematically be extended to *Special Euclidean Graphs* (in the sense that nodes are attributed with poses, edges attributed with spatial displacements) by means of the two-frame and the augmented convention.

Complexity of Mechanisms. Complexity of mechanisms can be split into the categories *combinatorics*, *link geometries*, and *joint types*. The pure, non-Euclidean combinatorics of mechanisms is covered by the graph concept. In Section 6, it is illustrated that the Sheth-Uicker convention provides advantages compared to Denavit-Hartenberg convention in presence of mechanisms with *skew* link geometries and kinematic *loops*. Generally, Sheth-Uicker allows a concise modeling of mechanisms, in the sense that the ‘Euclidean displacement graphs’ directly correspond to the combinatorics of the mechanism. This allows the definition of hierarchies by modeling of a kinematic loop as a complex joint (see also [36, §2.37-2.41]). The focus of this survey is explaining the aspects combinatorics and link geometries, and drawing comparisons, whereas the argumentation for joints is constrained to *simple* joints. Therefore, this article complements the original work by Sheth and Uicker [48] that also covers other joints types (namely spherical, planar, and gear joints) and provides an example on the ‘epicyclic gear train’.

2.2 Kinematic Specification

Problem A (Kinematic Specification of Mechanism). Given an arbitrary, physical mechanism $\underline{\mathcal{M}}$, a specification of $\underline{\mathcal{M}}$ is needed that enables to create

- (A) a physical copy of the mechanism featuring the same kinematic properties without knowing the original mechanism,
- (B) a software model of the mechanism featuring the same kinematic properties without knowing the original mechanism.

Additionally, as motivated in the introduction, the specification should be human-readable, compact, and should reflect topology and geometry of the mechanism.

2.3 Frames and Poses

A frame F is a simple term for *local coordinate system*. Here, a frame ‘remains the same’ if it moves over time. Therefore, additionally the term ‘pose’ is introduced which is only valid for a certain timestep.

Pose. A *pose* $P \in SE(3)$ describes the rotation and the translation relative to the origin. If a frame is associated with some frame it is marked as $P = P_F$. In matrix notation a pose is given as

$$P = \begin{pmatrix} \mathbf{x} & \mathbf{y} & \mathbf{z} & \mathbf{p} \\ 0 & 0 & 0 & 1 \end{pmatrix}, \quad (5)$$

where $\mathbf{x}, \mathbf{y}, \mathbf{z}$ and \mathbf{p} are elements of \mathbb{R}^3 . In general, the pose of a frame P_F is a function of time (this can be indicated by the overline notation \overline{P}) and of the mechanism (its links and joints, the design parameters and configuration variables) $P_F = P_{F_{\mathcal{M}}}(t)$. We omit the pose, and only speak about the frame $F = F_{\mathcal{M}}$, if (a) the concrete pose is not needed, or (b) the initial pose (at time step $t = 1$) of the frame is meant.

Poses via Lines. The pose P of a frame F can alternately be denoted by the set of the *lines* X, Y, Z of the axes of the frame, so that simply $P = \{X, Y, Z\}$. In Section 3.2.2, lines are formally introduced. The location \mathbf{p} of the frame F can be determined as $\mathbf{p} = X \cap Y \cap Z$.

Frame Axes Principle. In kinematics, the axes of frames are ordered and interpreted according to a common principle: Let F be a frame as defined in Equation 5. Optionally, let F be attached to some simple joint J .

1. The z -axis is the major axis of F . It indicates the *dominant* direction of a frame. In case that F is attached to J , the line Z of the z -axis coincides with the joint axis.⁶
2. The x -axis is the minor axis of F . It indicates the *secondary* direction of a frame. In case that F is attached to J , the configuration of J is indicated by the line X of the x -axis.
3. The y -axis is the redundant axis of F . Its direction follows from the right-hand rule, i.e., $\mathbf{y} = \mathbf{z} \times \mathbf{x}$.

2.3.1 Pose Sets and Frame Sets

The ambiguous situation from Definition 4 can be solved by using frame sets.

Definitions 5 (Pose Sets and Frame Sets). Let $\mathcal{F} = (F_1, F_2, \dots, F_k)$ be some set of frames of cardinality $|\mathcal{F}| = k$, then $\mathcal{P} = \mathcal{P}(\mathcal{F})$ denotes the set of poses of these frames, with $\mathcal{P} \in SE(3)^k$, as

$$\mathcal{P}(\mathcal{F}) = (P_1, P_2, \dots, P_k) = (P(F_1), P(F_2), \dots, P(F_k)).$$

As for single poses, the following additional notation is convenient also for sets of poses: 1). If the initial pose at timestep $t = 1$ is meant, then instead of using the symbol \mathcal{P} , simply \mathcal{F} can be used. 2). If the time variance of a pose shall be indicated the overline notation is used: $\overline{P} = P(t) = P(\mathcal{F}(t))$.

Definitions 6 (Link Covers and Minimal Link Covers). Let \mathcal{F}_L denote the set of the frames that are attached to some link $L \in \mathcal{F}$.⁷ Then, a frameset \mathcal{F} is called *covering* if $|\mathcal{F}_L| > 0 \forall L \in \mathcal{L}$. A covering frameset is denoted as $\hat{\mathcal{F}}$. A frameset \mathcal{F} is called *minimal* if $|\mathcal{F}_L| = 1 \forall L \in \mathcal{L}$.

Definition 7 (Mechanism with Unique Posture). Given a Euclidean mechanism $\underline{\mathcal{M}}$, and a covering frame set $\hat{\mathcal{F}}$ together with the set of poses of these frames at some timestep t , $\hat{\mathcal{P}} = P(\hat{\mathcal{F}}, t)$. Then, this covering pose set defines a unique posture, such that ‘the mechanism in that unique posture’ $\hat{\mathcal{P}}$ can formally be denoted as

$$\underline{\mathcal{M}}(\hat{\mathcal{P}}(t)) = (\mathcal{L}, \mathcal{J}, \hat{\mathcal{P}}(t)). \quad (6)$$

If the time is not important (‘in most of the cases treated’), but the (Euclidean) mechanism shall be described in its initial posture at timestep $t = 1$, (thus, for short $\hat{\mathcal{P}} = \hat{\mathcal{P}}(1)$) the former equation simplifies to

$$\hat{\underline{\mathcal{M}}} = (\mathcal{L}, \mathcal{J}, \hat{\mathcal{F}}), \quad (7)$$

hereby, \mathcal{L} denotes the set of links and \mathcal{J} denotes the set of joints, as introduced in Equation 3. Therefore, the *unique posture* can be denoted as $\hat{\mathcal{P}} = \hat{\mathcal{P}}_{\underline{\mathcal{M}}} = P(\hat{\mathcal{F}}_{\underline{\mathcal{M}}})$.

Remark: The posture $\hat{\mathcal{P}}$ of the mechanism is unique *in contrast* to Definition 4, since the frame set $\hat{\mathcal{F}}$ delivers a unique description in Euclidean space.

2.3.2 Kinematic Conventions

Specification by Frames. By means of using frames (i.e., by Definition 6 and Definition 7) the *Problem of Kinematic Specification* (Problem A) boils down to the following two questions:

1. What frames shall be selected to describe the posture of the links?
2. How shall a displacement between a pair of frames be represented?

⁶E.g. the rotation, translation, or spindle axis.

⁷The overall frame set \mathcal{F} can be partitioned as $\mathcal{F} = \mathcal{F}_{L_1} \cup \mathcal{F}_{L_2} \cup \dots \cup \mathcal{F}_{L_n}$.

Purposes of Kinematic Notation Conventions. As of today, the problem of kinematic specification has not yet been solved. With regard to that, Thomas et al. resumed “*till now, (...) a common notation for parallel manipulators has not been accepted*” [53], and Roth stated that “*essentially what remains is largely a question of notation.*” [43]. It is about choosing an appropriate convention: since each notation convention has different characteristics, it may not be the best for all purposes. In this paragraph, similar to [53], a listing of several properties of kinematic conventions is provided to help judging about the quality of notation conventions for a certain case.

To describe the properties of a convention C , a formal mapping SPEC_C is introduced. Given some mechanism of type \mathcal{M} with a unique pose $\hat{\mathcal{P}}$, therefore given $\hat{\mathcal{M}}$, the mapping SPEC_C assigns the specification of the mechanism in form of a table \mathcal{T} according to some notation convention C .

$$\text{SPEC}_C : \hat{\mathcal{M}} = (\mathcal{L}, \mathcal{J}, \hat{\mathcal{P}}) \mapsto \mathcal{T}_C(\hat{\mathcal{M}}).$$

With respect to that definition, the following properties are introduced.

1. *Uniqueness* – One mechanism specification table should only be valid for one specific mechanism and no other. Then, the mapping SPEC_C is right-unique with respect to $\hat{\mathcal{M}}$.
2. *Generality* – The specification convention should be applicable to a *large* class of different types of mechanisms. In the best case, SPEC_C is left-total, meaning that all existing mechanisms can be specified.
3. *Minimality & Compactness* – In general, a short table $\mathcal{T}_C(\hat{\mathcal{M}})$ is preferred.⁸ However, to measure the length of the table, different entities can be counted: frames, twists, or used parameters.
4. *Unconditionality* – The quality of the computation of the mechanism’s specification $\mathcal{T}_C(\hat{\mathcal{M}})$ is high if it can be conducted by only a small number of *conditions* (case-by-case analyses).
5. *Intuitiveness* – The mechanism specification $\mathcal{T}_C(\hat{\mathcal{M}})$ should reflect the *combinatorics* and the *geometry* of the mechanism SPEC_C in an intuitive way.⁹
6. *Flexibility* – The zero posture, thus $\mathbf{q} = \mathbf{0}$, should be assignable freely to each of the postures the mechanism $\hat{\mathcal{P}}$ can have, i.e., for all possible poses $\hat{\mathcal{P}}$ the routine SPEC_C should compute a valid, unique table $\mathcal{T}_C(\hat{\mathcal{M}})$.
7. *Modularity* – The mechanism specification should allow the substitution of a loop, or a subchain, by a complex joint, influencing the structure of the entire table as little as possible.
8. *Extendability* – The mechanism’s specification should be extendable to incorporate other (e.g., dynamic) properties of the mechanism.¹⁰

These properties should be kept in mind for Section 4 and Section 6.

2.4 Classic Kinematic Problems

This section illustrates how a concise definition of classic kinematic problems is easily derived by means of frame sets.

The Forward Kinematics Problem. A characterization of the Forward Kinematics Problem by Waldron and Schiedeler ([55]) reads “[...] *the forward kinematics problem is to find the relative position and orientation of any two designated members given the geometric structure of the manipulator and the values of a number of joint positions equal to the number of degrees of freedom of the mechanism.*”

Definition 8 (Forward Kinematics Map). Given a mechanism $\underline{\mathcal{M}}$, the forward kinematics map of $\underline{\mathcal{M}}$ is the map which sends a configuration vector $\mathbf{q} \in \mathbb{Q}$ to a set of poses \mathcal{P}

$$\text{FK}_{\underline{\mathcal{M}}}(\mathbf{q}) \mapsto \mathcal{P}.$$

Often (e.g., in robotic textbooks), it is assumed that the FK is a *function* (thus, it has a unique solution); however, generally, e.g., for parallel mechanism with different assembly modes, this is not true: it is a *map*. The solution set \mathcal{P} can be a discrete set $\mathcal{P} = \{P^{(1)}, P^{(2)}, \dots, P^{(n)}\}$ or also an uncountable set, in particular some semi-algebraic set.

Problem B (Forward Kinematics). Given a mechanism $\underline{\mathcal{M}}$ and a configuration vector \mathbf{q} , determine the set of poses $\mathcal{P}_{\text{FK}} \subseteq \mathcal{P}$ so that

$$\mathcal{P}_{\text{FK}} = \mathcal{P}_{\text{FK}}^{(\underline{\mathcal{M}})}(\mathbf{q}) = \{P \mid P \in \text{FK}_{\underline{\mathcal{M}}}(\mathbf{q})\}.$$

⁸Corresponds to a short overall description length.

⁹Then, a human ‘has to perform only a small number of case-by-case analyses’ to understand it.

¹⁰See the term *comprehensiveness* from [53].

Briefly, the problem of Forward Kinematics is to determine the image of the map FK for a certain configuration vector \mathbf{q} .

The Inverse Kinematics Problem. A characterization of the Inverse Kinematics Problem by Waldron and Schiedeler ([55]) reads ‘[.] given the relative positions and orientations of two members of a mechanism, find the values of all of the joint positions. This amounts to finding all of the joint positions given the homogeneous transformation between the two members of interest.’

Definition 9 (Inverse Kinematics Map). Given a mechanism $\underline{\mathcal{M}}$, the inverse kinematics map of $\underline{\mathcal{M}}$ is the map which sends a pose $P \in SE(3)$ to some set of configuration vectors \mathcal{Q} .

$$\text{IK}_{\underline{\mathcal{M}}}(P) \mapsto \mathcal{Q}$$

The solution set \mathcal{Q} can be a discrete set $\mathcal{Q} = \{\mathbf{q}^{(1)}, \mathbf{q}^{(2)}, \dots, \mathbf{q}^{(n)}\}$ or also an uncountable set, in particular some semi-algebraic set.

Problem C (Inverse Kinematics). Given a mechanism $\underline{\mathcal{M}}$ and a pose P , determine the set of configurations $\mathcal{Q}_{\text{IK}} \subseteq \mathcal{Q}$ so that

$$\mathcal{Q}_{\text{IK}} = \mathcal{Q}_{\text{IK}}^{(\underline{\mathcal{M}})}(P) = \{\mathbf{q} \mid \mathbf{q} \in \text{IK}_{\underline{\mathcal{M}}}(P)\}.$$

Briefly, the problem of Inverse Kinematics is to determine the image of the inverse kinematics map IK for a certain pose vector P .

Two Classes of Problems. Kinematic problems split up in two complexity classes: simple (\mathcal{P}) and hard (\mathcal{NP}) problems. For example, the computation of forward kinematics of chains and trees is simple. E.g., in [5], the forward kinematics computation routine for *kinematic trees* is described by following the two-frame convention. A multitude of different algorithmic approaches exists for solving hard kinematic problems and this article does not intend to cover the related algorithmic questions. However, it is pointed out that certain algorithms exist¹¹ that respect the topological and geometrical structure quite directly: for example, in the class of *heuristics*, the *cyclic coordinate descent* method for computation of inverse kinematics of chains (see e.g., [7]), and, in the class of *global approaches*, the *CUIK* suite for position analysis (see e.g., [37, 38]). Both algorithms work near to the concrete kinematic specification of the mechanism, so that for these algorithms, the Sheth-Uicker convention can be advantageous.

¹¹– in contrast to more general approaches where the problem is seen as a general mathematical optimization problem –

3 Representations for Finite Displacements

In this section, four different kinds of representations of finite spatial displacements in $SE(3)$ are presented: At first, the most common representation by a homogeneous matrix form is defined in Section 3.1. In addition, the term spatial displacement is introduced as a synonym for the passive interpretation of a transformation. Then, in Section 3.2, vectorial representations of displacements are explained: in particular, they are needed later in Section 3.4. As third, in Section 3.3, the symmetric representation is presented. This elegant representation – which is closely related to vectorial descriptions via twists of Section 3.2 – is briefly introduced for reasons of completeness. At last, the sequential representations are presented in Section 3.4: later, it is shown in Section 4 and Section 6, how the kinematic conventions are related to this representation. For all presented four representations of displacements in $SE(3)$, the linear equivalent for $SO(3)$ of the representation is introduced.

Motivation. Given a pair of frames, F_a and F_b with pose matrices \mathbf{P}_a and \mathbf{P}_b with respect to the standard basis, the task is to derive a description of the displacement between the two frames. As an example, consider the poses of two frames given by the matrices

$$\mathbf{P}_a = \begin{pmatrix} 1 & 0 & 0 & 0 \\ 0 & 1 & 0 & 0 \\ 0 & 0 & 1 & 0 \\ 0 & 0 & 0 & 1 \end{pmatrix} \quad \mathbf{P}_b = \begin{pmatrix} 1 & 0 & 0 & 2 \\ 0 & \sqrt{2} & \sqrt{2} & 1 \\ 0 & \sqrt{2} & -\sqrt{2} & 2 \\ 0 & 0 & 0 & 1 \end{pmatrix}.$$

The two frames are displayed in Figure 1. In this section, four different popular ways of describing the displacement are compiled.¹²

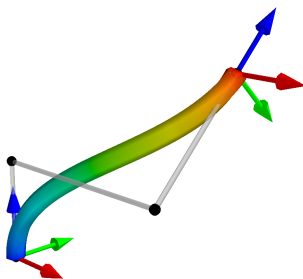


Figure 1: Two frames F_a and F_b with skew z -axes z_a and z_b are depicted. The lines G_a and G_b of the z -axes and their common orthogonal $\overline{G_a G_b}$ are indicated. Additionally, a tube is drawn in rainbow colors to support an intuitive imagination of the skew displacement. The tube may represent a trajectory or a link between the two frames. For a clear view, the lengths of the frame axes vectors are shrunk.

3.1 Homogeneous-Linear Representation

Matrices are one main entity of linear algebra (see, e.g., [15]). Quadratic matrices form the general linear group $GL(n)$.

3.1.1 Rotation Matrix

A rotation matrix $\mathbf{R} \in GL(3)$ represents a linear map which has the properties that $\mathbf{R} \cdot \mathbf{R}^T = \mathbf{I}_3$ and that $\det \mathbf{R} = 1$. In particular, the first property expresses the orthogonality of a matrix, i.e., the three columns of \mathbf{R} are a set of orthogonal unit vectors. From this follows that a rotation preserves absolute values of angles. From the second property follows that a rotation preserves volume and orientation. These two features are expressed by the two conditions

$$|\det \mathbf{R}| = 1 \quad \det \mathbf{R} > 0.$$

¹²Anticipating the topic of kinematic conventions (Section 4), one observes that the displacement *cannot* be represented by four classic or modified Denavit-Hartenberg parameters since the z -axes of the two frames are neither identical, intersecting, or parallel, but skew. For this, it would be necessary that either the two z -axes, or one z - and one x -axis share at least one common point.

3.1.2 Homogeneous Matrix

The homogeneous matrix of a displacement is an element of $GL(4)$; for such a matrix, here, the symbol \mathbf{M} is used. A homogeneous matrix \mathbf{M} incorporates a linear rotation (via rotation matrix $\mathbf{R} \in GL(3)$) and an affine linear translation (via the translation vector $\mathbf{t} \in \mathbb{R}^3$ that is linearized by the addition of the fourth dimension), denoted as

$$\mathbf{M} = \begin{pmatrix} \mathbf{R} & \mathbf{t} \\ \mathbf{0} & 1 \end{pmatrix}. \quad (8)$$

Any finite spatial displacement $D_{(a,b)}$ can be represented by means of a homogeneous matrix. This *homogeneous-linear type* representation is characterized as:¹³

$$\text{"Homogeneous Matrix := Rotation Matrix + Translation Vector"} \quad (\text{A})$$

3.1.3 Active and Passive Interpretation

A matrix \mathbf{M} can be used as a linear operator in two basic ways: either, it is used with right-multiplication $\mathbf{M} \cdot \mathbf{r}$, so that it acts as $\mathbf{r} \mapsto \mathbf{M}\mathbf{r}$, or it is used with left-multiplication $\mathbf{l}^T \cdot \mathbf{M}$, so that it acts as $\mathbf{l} \mapsto \mathbf{l}^T \mathbf{M}$. For rigid body displacements, thus for a matrix with shape $\mathbf{M} = \begin{pmatrix} \mathbf{R} & \mathbf{t} \\ \mathbf{0} & 1 \end{pmatrix}$ as in Equation 8, this corresponds to the *active* and the *passive* interpretation of a displacement (see e.g., [11]). To tighten notation, in this survey, for these, the terms ‘spatial displacement’ and ‘temporal displacement’ are introduced: spatial displacements describe the ‘relative, finite, spatial offset’ between two poses at the *same timestep*; whereas temporal displacements describe the ‘relative, finite, temporal offset’ between two poses of the *same body*. In this survey, *always* the passive interpretation is the one of interest.

Spatial Displacements. The term *spatial displacement* is used as a synonym for a proper rigid body transformation in its passive interpretation. Let t be a fixed and arbitrary timestep, let F_D and F_A be two frames in the same global coordinate system. Let $\mathbf{P}_D^{(t)}$ and $\mathbf{P}_A^{(t)}$ be the matrices (see Section 3.1) that describe the poses of these frames at this timestep t . Then, the *spatial displacement* $D_{(D,A)}^{(t)}$ and its matrix $\mathbf{M}_{(D,A)}^{(t)}$ between the two frames from F_D to F_A is expressed via

$$D_{(D,A)}^{(t)} : F_D^{(t)} \xrightarrow{\text{p}} F_A^{(t)} \quad \mathbf{M}_{(D,A)}^{(t)} = (\mathbf{P}_D^{(t)})^{-1} \cdot \mathbf{P}_A^{(t)}. \quad (9)$$

The passive interpretation is indicated by the usage of the symbol $\xrightarrow{\text{p}}$. This notation is chosen so that it matches the notation in classic robotics textbooks (e.g., [44]): The forward kinematics map (see Definition 8) of a kinematic chain is computed by composition from left-to-right as $\mathbf{M}_{(0,n)} = \mathbf{M}_{(0,1)} \cdot \mathbf{M}_{(1,2)} \cdot \dots \cdot \mathbf{M}_{(n-1,n)}$.

In other words, a ‘passive map from frame F_D to frame F_A ’, is equivalent to a *basis change transform* from basis F_A to basis F_D . According to this definition, poses (introduced in Section 2.3) can be interpreted as certain spatial displacements: a pose of a frame F_X describes a ‘spatial displacement relative to the global coordinate frame F_O ’ so that $\mathbf{P}_X = \mathbf{M}_{O,X} = (\mathbf{P}_O^{(t)})^{-1} \cdot \mathbf{P}_X^{(t)} = \mathbf{P}_X^{(t)}$.

Temporal Displacements. The term *temporal displacement* is used as a synonym for a proper rigid body transformation in its active interpretation. Let F_X be a frame, with poses $\mathbf{P}_X^{(t)}$ and $\mathbf{P}_X^{(u)}$ at timestep t and u , with $t < u$. Then, the *temporal displacement* $D_X^{(u,t)}$ and its matrix $\mathbf{M}_X^{(u,t)}$ between the two poses $\mathbf{P}_X^{(t)}$ and $\mathbf{P}_X^{(u)}$ is expressed via

$$D_X^{(u,t)} : F_X^{(u)} \xleftarrow{\text{a}} F_X^{(t)} \quad \mathbf{M}_X^{(u,t)} = \mathbf{P}_X^{(u)} \cdot (\mathbf{P}_X^{(t)})^{-1}. \quad (10)$$

The temporal displacement $D_X^{(u,t)}$ describes an *active interpretation* of the transformation, the usage of the symbol $\xleftarrow{\text{a}}$ indicates that: the temporal displacement describes the ‘movement’ object X between timestep t to timestep u . This notation is chosen so that it matches the classical matrix multiplication from right-to-left. Several temporal displacements can be composed as: $\mathbf{M}^{(t,0)} = \mathbf{M}^{(t,t-1)} \cdot \dots \cdot \mathbf{M}^{(2,1)} \cdot \mathbf{M}^{(1,0)}$.

¹³This type of characterization appears frequently in this survey.

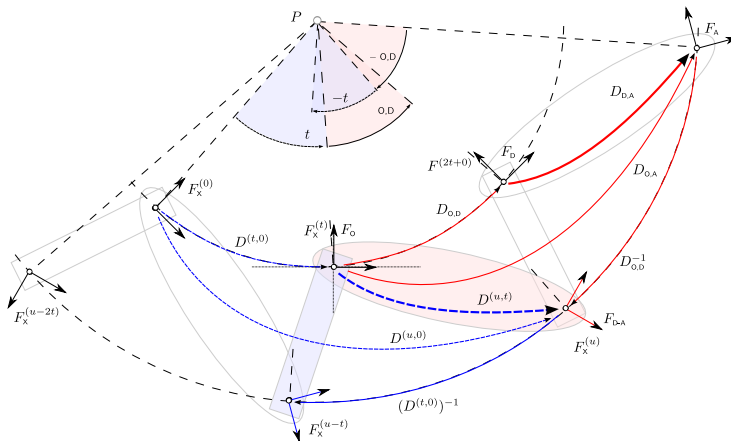


Figure 2: For illustrating the conjugation duality between relative spatial (red) and relative temporal (blue) displacements, $D_{D,A}$ and $D^{(u,t)}$ are marked by bold arrows: they are chosen to describe the same offset, once in spatial, and once in temporal domain. To allow a comparison between spatial and temporal domain, the frames F_O and $F_X^{(t)}$ coincide at the origin. The *spatial displacement* $D_{D,A}$ describes how frame F_A differs from frame F_D (both attached to an (ellipse) object) at the same timestep. It is integrated in left-to-right concatenation to compute the overall spatial displacement $D_{O,D}$ as $D_{O,D} = D_{O,D} \circ D_{D,A}$ starting from F_O . The *temporal displacement* $D^{(u,t)}$ describes how (bar) object X has moved between timesteps t and u . It is integrated in right-to-left concatenation to compute the overall temporal displacement $D^{(u,0)}$ as $D^{(u,0)} = D^{(u,t)} \circ D^{(t,0)}$ starting from $F^{(0)}$. Both representation matrices, of $D_{D,A}$ and of $D^{(u,t)}$, can be found in the sketch. A matrix contains the coordinates of a displacement relative to a basis. By definition, the bases F_O and $F_X^{(t)}$ are of interest for $D_{D,A}$ and $D^{(u,t)}$. The matrix of relative spatial displacement $D_{D,A}$ is given by frame F_{D-A} – which is dual to the ‘temporal offset’ object X between timestep t and u . The matrix of relative temporal displacement $D^{(u,t)}$ is given by frame $F_X^{(u-t)}$ – which is dual to the ‘spatial offset along’ object X between F_O and F_X .

Connection. The relative spatial displacement from Equation 9 is suited for left-to-right concatenations. The relative temporal displacement from Equation 10 is suited for right-to-left concatenations. For a moment, the introduced semantics about space and time are disregarded. By introducing $P_I = P_D = P^{(t)}$ and $P_{II} = P_A = P^{(u)}$ for the poses, and $M_S = M_{(D,A)}^{(t)}$ and $M_T = M_X^{(u,t)}$ for the displacements, by definition, the equation

$$M_S = P_I \cdot M_T \cdot (P_I)^{-1}$$

holds. Relative spatial displacement M_S and relative temporal displacement M_T are conjugated of each other – they are similar with respect to the initial offset P_I . This duality relation is illustrated in Figure 2.

3.2 Vectorial Representations

This section starts with the vectorial representation of spatial *rotation* in Section 3.2.1. Finally, vectorial representation of spatial *displacement* is treated in Section 3.2.4. In between, necessary and useful aspects of geometry of lines and screws is presented. For the topic of *vectorial representation*, also see the excellent articles [54] and [3].

3.2.1 Angle and Axis

Theorem 1 (Euler’s Rotation Theorem) *Any displacement of a rigid body such that a point on the rigid body, say O , remains fixed, is equivalent to a rotation about a fixed axis ω through the point O . [27]*

¹⁴Figure 2 is inspired by a pair of figures from [11, Fig. 4.2]. It unites those two separate drawings.

Proof of Euler's rotation theorem are provided, e.g., in [4] and [32]. The vector $\boldsymbol{\omega}^\#$ that lies on the rotation axis together with its length $\|\boldsymbol{\omega}^\#\|$ can be computed as

$$\boldsymbol{\omega}^\# = (\mathbf{R} - \mathbf{R}^T)^\oplus \quad \|\boldsymbol{\omega}^\#\| = 2 \cdot \sin \phi . \quad (11)$$

The rotation angle ϕ and the unit vector $\hat{\boldsymbol{\omega}}$ of the rotation axis can be derived as

$$\phi = \arccos \left(\frac{\text{tr}(\mathbf{R}) - 1}{2} \right) \quad \hat{\boldsymbol{\omega}} = \begin{cases} \boldsymbol{\omega}^\# / \|\boldsymbol{\omega}^\#\| & \text{if } \sin \phi \neq 0 \\ \mathbf{0} & \text{if } \sin \phi = 0 \end{cases} . \quad (12)$$

The tuple $(\phi, \hat{\boldsymbol{\omega}})$ delivers a representation for any spatial rotational displacement, like

$$\text{"Rotation := Rotation Angle + Rotation Axis"} . \quad (\text{B})$$

About this characterization, it is important to note that the orientation of the rotation axis determines the direction of rotation.¹⁵ As for planar rotations, the angle value of a rotation is made unique, if a modulo operation to an half-open interval, e.g., $[0, 2\pi)$, is applied.

3.2.2 Geometry of Lines

For our purposes, lines are one-dimensional affine-linear subspaces of \mathbb{R}^3 . Algebraically, two forms of lines are very common and are presented here: these are the parametric and the homogeneous form.

Parametric Form of Lines.

Let G be a line passing through two points \mathbf{a} and \mathbf{b} . Define $\boldsymbol{\omega}_L := \mathbf{b} - \mathbf{a}$. Then the parametric form of the line reads as

$$G = G(\mathbf{a}_L, \boldsymbol{\omega}_L) = \mathbf{a}_L + \lambda_L \cdot \boldsymbol{\omega}_L \quad (13)$$

whereby \mathbf{a}_L denotes an *anchor point* of the line, and $\boldsymbol{\omega}_L$ denotes the *direction vector*¹⁶ of the line. Briefly, we also refer to the anchor point of a line as the *location* of a line and to \mathbf{u}_L as the *direction* of the line.

In the parametric form, a line can be interpreted like

$$\text{"Line := Anchor + Direction"} . \quad (\text{C})$$

Homogeneous Form of Lines. Again, let G be a line passing through two points $a = (a_0, \mathbf{a})$ and $b = (b_0, \mathbf{b})$. Then the homogeneous form of the line reads

$$G = G(a, b) = (a_0, \mathbf{a}) \wedge (b_0, \mathbf{b}) = (a_0 \mathbf{b} - b_0 \mathbf{a}, \mathbf{a} \times \mathbf{b}) = (\boldsymbol{\omega}, \mathbf{v}_0) \quad (14)$$

The coordinates of the homogeneous form are also called Plücker coordinates. In this article, vector $\boldsymbol{\omega}$ is referred to as the *direction*, and \mathbf{v}_0 as the *orthogonal moment* of the line. The homogeneous coordinates fulfill the Grassmannian condition (see e.g., [25]) $\boldsymbol{\omega} \star \mathbf{v}_0 = 0$. Homogeneous lines are elements of a projective space and can be thus be interpreted as equivalence classes as

$$G = [\boldsymbol{\omega}, \mathbf{v}_0] = [\omega_1 : \omega_2 : \omega_3 : (v_0)_1 : (v_0)_2 : (v_0)_3] . \quad (15)$$

The homogeneous coordinates of a line also have a representation as a dual entity \tilde{G} like

$$\tilde{G} = \mathbf{g} + \epsilon \cdot \hat{\mathbf{g}} = \boldsymbol{\omega} + \epsilon \cdot \mathbf{v}_0 . \quad (16)$$

This relation is also referred to as 'Study map', e.g., in [39]. It is generalized by the concept of dual quaternions, see Section 3.3. In this article, both representations of lines are used. The conversion from homogeneous to parametric form can be derived by setting $\mathbf{a}_L = \frac{\mathbf{v}_0 \times \boldsymbol{\omega}}{\|\boldsymbol{\omega}\|^2}$ and $\boldsymbol{\omega}_L = \boldsymbol{\omega}$, see e.g., [45, Sec. 6.2]. A sketch of a line in homogeneous coordinates is provided in Figure 3(a). Further visualizations can be found, e.g., in [13, Sec. 11.3.1, Sec. 12.1.1].

¹⁵In the considered usecase of mechanism kinematics, the orientation of the rotation axes is defined by the way the joints are assembled within the overall mechanisms.

¹⁶The symbol $\boldsymbol{\omega}$ is chosen to be consistent with screw notation: In those cases, the angular velocity is expressed by $\boldsymbol{\omega}$.

| Configuration | Symbol | Common Points | Directions | Distance | Special Points |
|---------------------|--------|---------------|--------------------|----------|-----------------------------|
| <i>coincident</i> | | infinite | linear dependent | $d = 0$ | anchor midpoint |
| <i>parallel</i> | | none | linear dependent | $d > 0$ | anchor midpoint projections |
| <i>intersecting</i> | | one | linear independent | $d = 0$ | intersection point |
| <i>skew</i> | | none | linear independent | $d > 0$ | closest points |

Table 1: Four relative poses (coincident, parallel, intersecting, skew) of two lines together with some characteristic entities.

Definition 10 (Line Scalar Product). The scalar product $\langle (\cdot), (\cdot) \rangle_{\otimes}$ of two lines $\tilde{G}^{(1)} = (\boldsymbol{\omega}^{(1)}, \mathbf{v}_0^{(1)})$ and $\tilde{G}^{(2)} = (\boldsymbol{\omega}^{(2)}, \mathbf{v}_0^{(2)})$ is defined as

$$\langle \tilde{G}^{(1)}, \tilde{G}^{(2)} \rangle_{\otimes} = \frac{1}{2} \cdot (\boldsymbol{\omega}^{(1)} \star \mathbf{v}_0^{(2)} + \mathbf{v}_0^{(2)} \star \boldsymbol{\omega}^{(1)}) . \quad (17)$$

Lines are self-dual with respect to the scalar product that means: $\langle \tilde{G}, \tilde{G} \rangle_{\otimes} = \frac{1}{2} \cdot (\boldsymbol{\omega} \star \mathbf{v}_0 + \mathbf{v}_0 \star \boldsymbol{\omega}) = \boldsymbol{\omega} \star \mathbf{v}_0 = 0$, so that the Grassmannian condition from above is recovered. The normalization of a line to a *unit line* $\hat{G} = (\hat{\boldsymbol{\omega}}, \hat{\mathbf{v}}_0)$ with $\|\hat{\boldsymbol{\omega}}\| = 1$ is possible; it is explained below together with the normalization for screws. In the homogeneous form, a line can be interpreted like:

$$\text{“Line := Direction + Orthogonal Moment”} . \quad (D)$$

Poses of Lines. In Table 1, the four possible poses of a pair of lines are compared. By means of homogeneous coordinates and the scalar product (Definition 10), these four poses can be conveniently analyzed: The lines are coplanar (coincident, parallel, or intersecting) if and only if

$$\langle \tilde{G}^{(1)}, \tilde{G}^{(1)} \rangle_{\otimes} = \frac{1}{2} \cdot (\boldsymbol{\omega}^{(1)} \star \mathbf{v}_0^{(2)} + \mathbf{v}_0^{(1)} \star \boldsymbol{\omega}^{(2)}) = 0 \quad (18)$$

Translational and rotational distance of two lines $\tilde{G}^{(1)}, \tilde{G}^{(2)}$ can be computed together via the dual scalar product of Definition 14 as

$$\langle \tilde{G}^{(1)}, \tilde{G}^{(2)} \rangle_{\tilde{G}} = \cos \phi - \epsilon \cdot d \cdot \sin \phi$$

See e.g., [39] and [13, Sec. 11.7.1], for further details about the analysis by homogeneous coordinates. See e.g., [49] for numerically stable computations. See e.g., [56], [51] robotic modeling with respect to Grassman-Cayley algebras.

Closest Points and Common Perpendicular.

Skew Lines. In case of two given lines G and H that are skew, for each line, one can find a point that has *closest distance* to the other line. For example, the closest point on G to H will be denoted by $\pi_G(H)$ via the orthogonal projections for lines¹⁷ as

$$\pi_G(H) = \operatorname{argmin}_{\mathbf{p} \in G} \operatorname{dist}(\mathbf{p}, H) . \quad (19)$$

If two lines G and H are *skew*, then there is a unique line GH that connects the lines L and G with minimal length. This line is called ‘the common perpendicular’ $GH = \perp(G, H)$ and defined as

$$GH = \perp(G, H) = \pi_G(H) + \lambda_{GH} \cdot \boldsymbol{\omega}_{GH} . \quad (20)$$

The distance of two lines can be computed by means of the closest points $\pi_G(H)$ and $\pi_H(G)$ as

$$d = \operatorname{dist}(G, H) = \|\pi_G(H) - \pi_H(G)\| . \quad (21)$$

¹⁷In accordance to orthogonal projections for vectors, see Equation 1, that is $\pi_{\mathbf{x}}(\mathbf{y}) = \operatorname{argmin}_{\kappa \cdot \mathbf{x}, \kappa \in \mathbb{R}} \operatorname{dist}(\kappa \cdot \mathbf{x}, \mathbf{y})$.

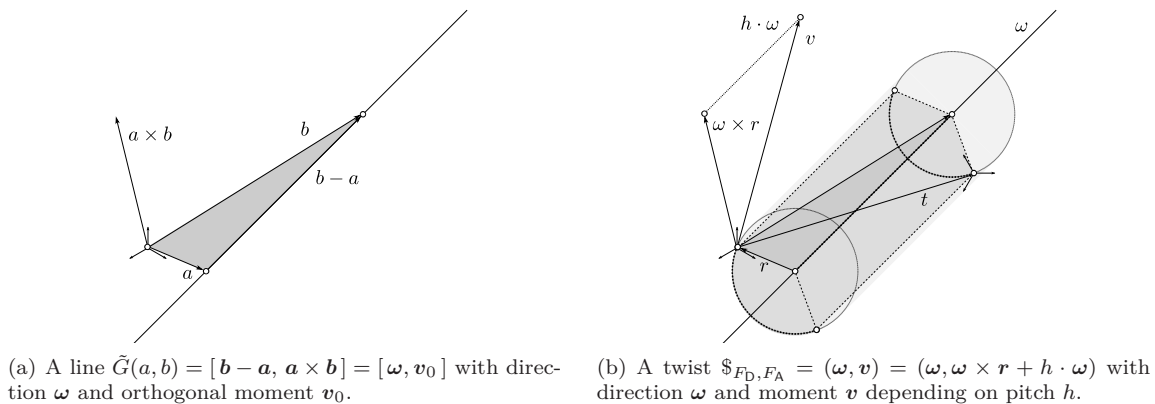


Figure 3: Visualization of a line $\tilde{G}(a, b)$ and a twist $\$,$ with screw axis $S^0 = \tilde{G}$.

Coplanar Lines. In this paragraph, the definitions of closest points and common perpendicular are adjusted by ‘generalized variants’ for lines lying in a common plane. For the case of *intersecting* lines, the closest points $\pi_G(L)$ and $\pi_L(G)$ coincide with the intersection point $L \cap G$. The distance of intersecting lines is $\text{dist}(P, H) = 0$. In case of *coincident* and *parallel* lines, neither $\pi_G(H)$ nor $\pi_H(G)$ can be determined from the geometry, since all points provide the same (minimal) distance to the other line. However, if an anchor point of the line is defined (which happens in kinematics applications in the following sections), the following ‘trick’ can be used: given the anchor points \mathbf{a}_G and \mathbf{a}_H of the lines, the midpoint \mathbf{m}_{GH} of those two $\mathbf{m}_{GH} = \frac{1}{2}(\mathbf{a}_G + \mathbf{a}_H)$ is determined. Then, the closest points of G to this midpoint \mathbf{m}_{GH} is determined as $\pi_G(\mathbf{m}_{GH})$ and defined to be ‘the’ closest point $\pi_G(\mathbf{m}_{GH})$ on G to H . For the other line H , the computation works analogously.

Definition 11 (Generalized Closest Points). Given two lines G_{ij} and G_{jk} with anchor points \mathbf{p}_{ij} , \mathbf{p}_{jk} , the *generalized closest point* $\pi_{G_{ij}}^*(G_{jk})$ on G_{ij} to G_{jk} is defined as

$$\pi_{G_{ij}}^*(G_{jk}) = \begin{cases} \pi_{G_{ij}}(G_{jk}) & \text{if lines } G_{ij}, G_{jk} \text{ are intersecting or skew,} \\ \frac{1}{2} \cdot \pi_{G_{ij}}(\mathbf{p}_{ij} + \mathbf{p}_{jk}) & \text{if lines } G_{ij}, G_{jk} \text{ are coincident or parallel.} \end{cases} \quad (22)$$

The generalized closest point $\pi_{G_{ij}}^*(G_{jk})$ on G_{ij} equals (1) the *closest point* on line G_{ij} in case of *skew* lines, (2) the *intersection point* in case of *intersecting* lines, (3) the *midpoint* of the *anchor points* in case of *coincident* lines, (4) the *projection midpoint* of the *anchor points* in case of *parallel* lines, see Table 1.

Definition 12 (Generalized Perpendicular Direction). Given two lines G_{ij} and G_{jk} with directions ω_{ij} , ω_{jk} and anchor points \mathbf{p}_{ij} , \mathbf{p}_{jk} , the *generalized perpendicular direction* $\omega_{(ij),(jk)}^*$ is defined as

$$\omega_{(ij),(jk)}^* = \perp^*(\omega_{ij}, \omega_{jk}) = \begin{cases} \omega_{ij} \times \omega_{jk} & \text{if lines } G_{ij}, G_{jk} \text{ are intersecting or skew,} \\ \tau_{\omega_{ij}}(\mathbf{p}_{jk} - \mathbf{p}_{ij}) & \text{if lines } G_{ij}, G_{jk} \text{ are coincident or parallel.} \end{cases} \quad (23)$$

By the preceding two definitions, the *generalized common perpendicular* $\perp^*(G, H)$ can be defined as follows.

Definition 13 (Generalized Common Orthogonal). Given two lines G_{ij} and G_{jk} and with directions ω_{ij} , ω_{jk} and anchor points \mathbf{p}_{ij} , \mathbf{p}_{jk} . The line that passes through generalized closest points $\pi_{G_{ij}}^*(G_{jk})$ and $\pi_{G_{jk}}^*(G_{ij})$ has direction $\omega_{(ij),(jk)}^*$ and reads in parametric form as

$$G_{(ij),(jk)}^* = \perp^*(G_{ij}, G_{jk}) = \pi_{G_{ij}}^*(G_{jk}) + \lambda_{GH} \cdot \omega_{(ij),(jk)}^*. \quad (24)$$

By means of the last three definitions, it is possible to determine a ‘shortest connection’ between two lines with given anchors, independently of how these are opposed to each other.

3.2.3 Geometry of Screws

To derive a definition of a screw, the concept of lines is enriched with a pitch. A pitch describes the relation between translational and rotational displacements; for details, see below in Section 3.2.4. For the moment,

it is sufficient that a pitch h is a scalar that expresses the ‘slope’ of the screw. In a simple terms, the object screw can be geometrically characterized as

$$\text{“Screw := Line + Pitch”}. \quad (\text{E})$$

In addition to pitch h , a screw incorporates a radius vector \mathbf{r} that points from the screw axis line to the origin with an orthogonal angle. With these two entities, a screw reads formally as

$$S = (\boldsymbol{\omega}, \mathbf{v}) = (\boldsymbol{\omega}, \boldsymbol{\omega} \times \mathbf{r} + h \cdot \boldsymbol{\omega}). \quad (25)$$

Thereby, notation of \mathbf{v}_0 is chosen such that it corresponds with the line notation of Equation 14, for a pitch that equals zero, $h = 0$. The algebraic interpretation for a screw (Equation 25) is expressed as

$$\text{“Screw := Direction + Moment”}. \quad (\text{F})$$

While screws are ‘still’ members of a projective space, a screw is – in contrast to a line – not self-dual. Thus in general, for $h \neq 0$,

$$\langle S, S \rangle_{\otimes} = \frac{1}{2} \cdot (\boldsymbol{\omega} \star \mathbf{v} + \mathbf{v} \star \boldsymbol{\omega}) = \boldsymbol{\omega} \star \mathbf{v} \neq 0. \quad (26)$$

Scalar Product. The scalar product for screws is an extended version of the product for lines $\langle \tilde{G}^{(1)}, \tilde{G}^{(2)} \rangle_{\otimes}$ from Definition 10. It is defined in accordance with scalar products of other dual entities, in particular of dual quaternions (Definition 16).

Definition 14 (Screw Scalar Product $\langle \tilde{S}^{(1)}, \tilde{S}^{(2)} \rangle_{\tilde{G}}$). The scalar product of the screws $\tilde{S}^{(1)}$ and $\tilde{S}^{(2)}$ is defined as

$$\begin{aligned} \langle \tilde{S}^{(1)}, \tilde{S}^{(2)} \rangle_{\tilde{G}} &= \langle \tilde{S}^{(1)}, \tilde{S}^{(2)} \rangle_{\mathcal{G}} + \epsilon \cdot 2 \cdot \langle \tilde{S}^{(1)}, \tilde{S}^{(2)} \rangle_{\otimes} \\ &= \boldsymbol{\omega}^{(1)} \star \boldsymbol{\omega}^{(2)} + \epsilon \cdot (\boldsymbol{\omega}^{(1)} \star \mathbf{v}^{(2)} + \mathbf{v}^{(1)} \star \boldsymbol{\omega}^{(2)}) \end{aligned} \quad (27)$$

The expression $\langle \dots \rangle_{\mathcal{G}}$ represents vector multiplication of the primal parts $\langle \tilde{S}^{(1)}, \tilde{S}^{(2)} \rangle_{\mathcal{G}} = \boldsymbol{\omega}^{(1)} \star \boldsymbol{\omega}^{(2)}$. The line scalar product $\langle \tilde{S}^{(1)}, \tilde{S}^{(2)} \rangle_{\otimes}$ is defined as in Equation 17.

Normalization. Just like lines, screws are elements of a projective space, so that $S = [\boldsymbol{\omega}, \mathbf{v}]$: the geometric object ‘screw’ S is invariant to a scalar multiplication of the screw coordinates. Therefore, the norm of a screw vector $S = (\boldsymbol{\omega}, \mathbf{v})$ can be

- (i) set to a *normal* value: the screw coordinates can be scaled such that $\|\hat{\boldsymbol{\omega}}\| = 1$, or they can be scaled such that $\|\hat{\boldsymbol{\omega}}\| = 0$ and $\|\hat{\mathbf{v}}\| = 1$ for pure translations;
- (ii) used to encode the *magnitude* of a finite displacement that it represents¹⁸.

Option (i) is described in the following paragraph, the following Section 3.2.4 is dealing with option (ii).

Normal Screw Coordinates. In Section 3.2.1, it is described how a unit vector $\hat{\boldsymbol{\omega}}$ describing the axis of the angle-axis representation of rotation is computed. This is generalized to derive the *normal screw* \hat{S} featuring the properties of option (i) above: Given some screw $S = (\boldsymbol{\omega}, \mathbf{v})$, the corresponding unit screw $\hat{S} = (\hat{\boldsymbol{\omega}}, \hat{\mathbf{v}})$ can be computed via the two equations

$$\hat{\boldsymbol{\omega}} = \begin{cases} \boldsymbol{\omega} / \|\boldsymbol{\omega}\| & \text{if } \sin \phi \neq 0 \\ \mathbf{0} & \text{if } \sin \phi = 0 \end{cases} \quad \hat{\mathbf{v}} = \begin{cases} \mathbf{v} / \|\boldsymbol{\omega}\| & \text{if } \sin \phi \neq 0 \\ \mathbf{v} / \|\mathbf{v}\| & \text{if } \sin \phi = 0 \end{cases} \quad (28)$$

For a normal screw \hat{S} , the scalar products $\langle \hat{S}, \hat{S} \rangle_{\tilde{G}}$ and $\langle \hat{S}, \hat{S}^* \rangle_{\tilde{G}}$, according to Definition 14, become simple in both cases: In case of a proper screw, with $\sin \phi \neq 0$, it holds that $\langle \hat{S}, \hat{S} \rangle_{\tilde{G}} = 1 + \epsilon \cdot 2 \cdot h^{\#}$ and $\langle \hat{S}, \hat{S}^* \rangle_{\tilde{G}} = h^{\#} + \epsilon \cdot (1 + (\frac{\|\mathbf{v}\|}{\|\boldsymbol{\omega}\|})^2)$ (for $h^{\#}$, see Equation 31). In case of a pure translation, with $\sin \phi = 0$, it holds that $\langle \hat{S}, \hat{S} \rangle_{\tilde{G}} = 0$ and $\langle \hat{S}, \hat{S}^* \rangle_{\tilde{G}} = \epsilon$.

¹⁸In the instantaneous case, the norm of the screw can be set to represent the *intensity* of the associated physical entity.

3.2.4 Finite Twists

Screw Displacements. In the last two sections, Section 3.2.2 and Section 3.2.3, facts about the geometry of lines and screws were presented; therefore, the *vectorial representation* of displacements, the representation via *twists*, can be introduced. The following famous Chasles Theorem is a generalization both of the theorem about *rotation axis* of spatial rotations (Theorem 1) and of the theorem about *rotation pole* of planar displacements (Theorem 3).

Theorem 2 (Chasles) *The most general rigid body displacement can be produced by a translation along a line followed (or preceded) by a rotation about that line. [27]*

A proof of Chasles' Theorem can be found in [4]. In particular, the theorem states that an affine *line* (that generalizes the rotation pole and the (linear) rotation axis) together with a translation and a rotation, in short, a twist, can be found. In this article, the 'translation along a line' is referred to as *absolute translation*¹⁹ and denoted by \mathbf{s} . The length of the absolute translation is referred to as *shift* $s = \|\mathbf{s}\|$. The 'rotation about that line' is shortly referred to as *spin* and denoted by ϕ . Since a line with six homogeneous coordinates only contains four 'effective' parameters, a version which is scaled by a certain factor can be used to describe a twist along that line. In other words, with a finite spin ϕ and a finite shift $s = \|\mathbf{s}\|$ it can be written:

$$\$_G(\phi, \mathbf{s}) = \$_G(\tilde{\phi}) \cong (\phi, \hat{\omega}, s, \hat{\mathbf{v}}_0). \quad (29)$$

We reach the following *external* characterization of a *twist*: a screw displacement can be interpreted as a *segment* with angle (spin) ϕ and height (shift) s of a *cylinder* with radius r , aligned along (the axis G of) a screw. In Figure 3(b), this cylinder segment is also indicated.

$$\text{"Twist := Line + Spin + Shift"} \quad (G)$$

Given a displacement in terms of a rotation matrix \mathbf{R} and a translation vector \mathbf{t} , Equation 12 provides the way to compute axis direction $\omega^\#$ and spin ϕ . The next paragraph describes how to compute the absolute translation \mathbf{s} and orthogonal translation \mathbf{t}_0 via orthogonal decomposition of the translation vector \mathbf{t} .

Orthogonal Decomposition of Translation. The translation vector \mathbf{t} can be decomposed into absolute translation \mathbf{s} along the screw axis, and orthogonal translation \mathbf{t}_0 that lies in the plane orthogonal to the screw axis as

$$\mathbf{t} = \pi_{S^0}(\mathbf{t}) + \tau_{S^0}(\mathbf{t}) = \mathbf{s} + \mathbf{t}_0. \quad (30)$$

Standard Twist. The pitch $h^\#$ of standard twist is the fraction of shift s and spin ϕ and is computed as

$$h^\# = \frac{s}{\phi} = \frac{\omega^\# \star \mathbf{v}^\#}{\omega^\# \star \omega^\#}. \quad (31)$$

In accordance to determination of $\omega^\#$ in Equation 11, the moment vector $\mathbf{v}^\#$ of the classic twist can be computed as (see [11])

$$\mathbf{v}^\# = ((\hat{\mathbf{t}} \cdot \mathbf{R}) - (\hat{\mathbf{t}} \cdot \mathbf{R})^T)^\oplus. \quad (32)$$

Similar to the computation of the orthogonal translation \mathbf{t}_0 , the orthogonal moment $\mathbf{v}_0^\#$ can be determined. It can be computed in two ways; either in the manner of the former Equation 32, or via orthogonal decomposition (see Equations 1, 2) as

$$\mathbf{v}_0^\# = ((\hat{\mathbf{t}}_0 \cdot \mathbf{R}) - (\hat{\mathbf{t}}_0 \cdot \mathbf{R})^T)^\oplus \quad \mathbf{v}_0^\# = \mathbf{v}^\# - h \cdot \mathbf{v}^\# = \mathbf{v}^\# - \pi_\omega(\mathbf{v}) = \tau_\omega(\mathbf{v}). \quad (33)$$

Hereby, the norms of these two expressions do not equal. However, this is not an issue since, in the given context, one is only interested in the normalized orthogonal moment $\hat{\mathbf{v}}_0 = \mathbf{v}_0^\# / \|\mathbf{v}_0^\#\|$. According to [21], the standard twist $\$_\#$ can be defined by the multiplication of a unit line vector \hat{G} with a dual angle $\hat{\phi} = (\phi + \epsilon \cdot s)$ like

$$\$_\# = (\omega^\#, \mathbf{v}^\#) = \tilde{\phi} \odot \hat{G} = (\phi + \epsilon \cdot s) \odot (\hat{\omega} + \epsilon \cdot \hat{\mathbf{v}}_0). \quad (34)$$

¹⁹For the term 'Rodrigues' absolute translation' see [57].

Method I. M2T – Matrix to Twist Conversion.

(In) Homogeneous matrix M representing a spatial displacement $D \in SE(3)$, a pitch concept $\eta(\phi, s)$.

(Out) Twist \mathcal{S}^h representing that spatial displacement D with pitch h according to η , twist axis S_0 .

1. Spin ϕ of the twist and unit direction of the screw axis $\hat{\omega}$ are computed according to Equation 12.
 2. Shift s of the twist is computed via an orthogonal decomposition of \mathbf{t} along $\hat{\omega}$ according to Equation 30.
 3. Orthogonal moment $\mathbf{v}_0^\#$ is computed by one of the two possibilities in Equation 33.
 4. Classic twist $\mathcal{S}^\# = (\boldsymbol{\omega}^\#, \mathbf{v}_0^\#)$ is computed with $\tilde{\phi} = (\phi, s)$ according to Equation 34.
 5. Twist axis $S_0 = (\boldsymbol{\omega}^\#, \mathbf{v}_0^\#)$ is determined. A unit line \hat{S}_0 is computed as $\hat{S}_0 = S_0 / \|S_0\|$.
 6. Pitch $h = \eta(\phi, s)$ of the screw is computed according to Equation 35.
 7. A representative of h -screw $S^h = (\boldsymbol{\omega}^h, \mathbf{v}^h)$ is computed by setting $\boldsymbol{\omega}^h = \boldsymbol{\omega}^\#$ and $\mathbf{v}^h = \mathbf{v}_0^\# + h \cdot \boldsymbol{\omega}^\#$.
 8. Twist intensity $\rho = \rho^\eta(\phi, s)$ is computed as $\rho = d(\phi) / \|\boldsymbol{\omega}^\#\|$, with $d(\phi)$ as in Equation 35.
 9. Twist $\mathcal{S}^h = \rho \cdot S^h$ corresponding to displacement D is computed by scaling h -screw S^h with intensity ρ .
- Alternatively (Equation 34), twist \mathcal{S}^h is directly computed via unit twist axis \hat{S}_0 from step 5 as $\mathcal{S}^h = \tilde{\phi} \odot \hat{S}_0$.

The interpretation of Equation 34 reads like

$$\text{“Standard Twist := Unit Line + Spin + Shift”}. \quad (\text{H})$$

The coordinates of twists with *different* pitch-models can be computed from this standard twist. It is briefly sketched in the next paragraph.

Other Pitch Definitions. The classic screw from the last section is *one* of the possibilities for defining the pitch of a screw. In the past, a multitude of different pitch concepts were developed. For this, see e.g., [33, 21, 54, 10, 46, 34, 47]. Common to all these different pitch concepts is that in the infinitesimal case, finite twists correspond to instantaneous twists. Additionally, all pitch concepts express the ‘slope of the screw’ (see Section 3.2.3). That means that they relate the finite rotation displacement to the finite absolute translation, the shift.²⁰ In particular, all pitch concepts η can be computed as a fraction of some function $n = n(s)$ over some function $d = d(\phi)$.

$$h = \eta(\phi, s) = \frac{n(s)}{d(\phi)}. \quad (35)$$

Computation. If a displacement is given in terms of a homogeneous matrix as in Equation 8, the computation of a twist with a certain pitch concept can be conducted with method Method I.²¹ The computation of the twist vector by scaling the screw S^h with an intensity ρ (as in Method I) motivates the well-known geometric interpretation of a twist.²²

$$\text{“Geometric Twist := Screw + Magnitude = Line + Pitch + Magnitude”}. \quad (\text{I})$$

Here, this characterization is only listed for reasons of completeness. In the following, all screw displacements are specified via a spin ϕ and a shift s , only. Therefore, no particular pitch definitions are needed and interpretation (G) is sufficient.

Properties. For the remainder of this article, two additional properties of screws are needed. Namely, these are *orthogonality* and *linearity* of twists (and screws and lines).

Orthogonality. Two lines G_1, G_2 , two screws S_1, S_2 , or two twists $\mathcal{S}_1, \mathcal{S}_2$ are *orthogonal* if their directions $\boldsymbol{\omega}_1, \boldsymbol{\omega}_2$ are orthogonal. In particular, if the following equality is fulfilled:

$$\boldsymbol{\omega}_1 \star \boldsymbol{\omega}_2 = 0. \quad (36)$$

Linearity. A line L , screw S , or twist \mathcal{S} that fulfills the property $\|\mathbf{r}\| = 0$ is called *linear*, otherwise it is called *affine*. A line L , screw S , or twist \mathcal{S} that is linear and its direction is aligned to one of the standard axes e_x, e_y , or e_z is called *axial*. In particular, in the remainder of this article, an axial twist is marked as $\mathcal{S}_x, \mathcal{S}_y$, or \mathcal{S}_z . In [14, Appendix A], the efficient algorithmic treatment of axial twists is described.

²⁰The question if there is a ‘correct’ way to do so is raised in [2].

²¹The described computation routine is a generalized version of the one in [11, Sec. 4.6.4]. However, degenerate cases (e.g., $\sin \phi = 0$) are not respected, here.

²²Characterization (I) can also be read as the ‘internal’ interpretation, in contrast to the ‘external’ characterization (G): a twist is regarded as a *segment (of the ‘trajectory curve’) of a certain screw*.

3.3 Symmetric Representation

In this section, the ‘symmetric’ representation of displacement via dual quaternions is briefly introduced. Rooney judges that “*the chief advantage in adopting a dual quaternion representation for a screw displacement lies in its simplicity and economy*” ([42]). Next to their simplicity and economy, dual quaternions feature algebraic properties that can effectively be used for solving practical problems, see e.g., [23].

3.3.1 Quaternions

Quaternions are generalized complex numbers. A quaternion $q \in \mathbb{H}$ can be denoted in Gaussian form as

$$q = q_0 + \mathbf{i} \star \mathbf{q} . \quad (37)$$

Definition 15 (Quaternion Scalar Product). The scalar product $\langle \cdot, \cdot \rangle_{\mathbb{H}}$ of two quaternions $q^{(1)}$ and $q^{(2)}$ as in Equation 37 is defined as

$$\langle q^{(1)}, q^{(2)} \rangle_{\mathbb{H}} = q^{(1)} \star q^{(2)} .$$

Therefore, the norm of a dual quaternion is

$$\|q\|^2 = \|q\|_{\mathbb{H}}^2 = \langle q, q \rangle_{\mathbb{H}} = q \star q . \quad (38)$$

In polar form, as $q = \|q\| \cdot (\cos \frac{\phi}{2} + \sin \frac{\phi}{2} \cdot \mathbf{i} \star \hat{\omega})$, where next to absolute value $\|q\|$ and argument $\frac{\phi}{2}$ a rotation axis $\hat{\omega}$ needs to be defined. Like lines (Section 3.2.2), quaternions are elements of a projective space, so that the rotation that is encoded in the quaternion is invariant to the quaternion norm (modulo a volume scaling). Therefore, for a finite rotational displacement $R \in SO(3)$, the corresponding quaternion is normalized to the *unit quaternion* $\hat{q} = q / \|q\|$ with $\|\hat{q}\| = 1$.

$$\hat{q} = \cos \frac{\phi}{2} + \sin \frac{\phi}{2} \cdot \mathbf{i} \star \hat{\omega} . \quad (39)$$

Essentially, unit quaternions contain angle and axis of the rotation R (see Section 3.2.1) in a ‘renormalized’ manner, such that the vector is element of a sphere element $\hat{q} \in S(3) \subset \mathbb{R}^4$. A simple characterization is stated:

$$\text{“Unit Quaternion := Rotation Angle + Rotation Axis”} . \quad (J)$$

3.3.2 Dual Quaternions

Generally, a dual quaternion consists \tilde{q} of the sum of a primal quaternion q and a dual quaternion \mathring{q} , so that it can be denoted in Gaussian form as

$$\tilde{q} = q + \epsilon \cdot \mathring{q} = q_0 + \mathbf{i} \star \mathbf{q} + \epsilon \cdot (\mathring{q}_0 + \mathbf{i} \star \mathring{\mathbf{q}}) . \quad (40)$$

Conjugations, Dualization, Scalar Product. Two kinds of conjugations can be conducted for dual quaternions: first, a complex conjugation $\bar{\tilde{q}}$ is defined that negates all complex elements of \tilde{q} so that $\bar{\tilde{q}} = q_0 - \mathbf{i} \star \mathbf{q} + \epsilon \cdot (\mathring{q}_0 - \mathbf{i} \star \mathring{\mathbf{q}})$, second, a dual conjugation $\underline{\tilde{q}}$ is defined that negates all dual elements of \tilde{q} so that $\underline{\tilde{q}} = q_0 + \mathbf{i} \star \mathbf{q} - \epsilon \cdot (\mathring{q}_0 + \mathbf{i} \star \mathring{\mathbf{q}})$. The geometric effects of these operations are derived in [23] and are depicted and described with respect to geometry of twists (of the previous section) in Figure 4. The complex conjugation occurs in the definition of the dual quaternion scalar product, below. In accordance to twists, screws and lines, the ‘dualization’ of a dual quaternion swaps primal and dual part. The scalar product for dual quaternions is a generalization of Definition 14 for screws and of Definition 16 for quaternions.

Definition 16 (Dual Quaternion Scalar Product). The scalar product $\langle \cdot, \cdot \rangle_{\mathbb{H}}$ of two dual quaternions $\tilde{q}^{(1)}$ and $\tilde{q}^{(2)}$ as in Equation 40 is defined as

$$\begin{aligned} \langle \tilde{q}^{(1)}, \tilde{q}^{(2)} \rangle_{\mathbb{H}} &= \frac{1}{2} \cdot (\tilde{q}^{(1)} \odot \bar{\tilde{q}}^{(2)} + \tilde{q}^{(2)} \odot \bar{\tilde{q}}^{(1)}) \\ &= \langle q^{(1)}, q^{(2)} \rangle_{\mathbb{H}} + \epsilon \cdot \left(\langle \mathring{q}^{(1)}, q^{(2)} \rangle_{\mathbb{H}} + \langle q^{(1)}, \mathring{q}^{(2)} \rangle_{\mathbb{H}} \right) \end{aligned} \quad (41)$$

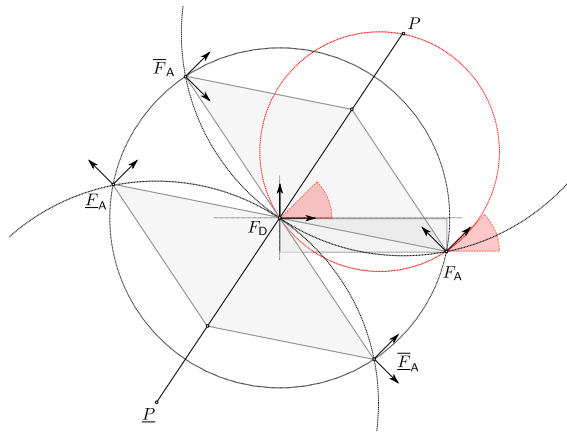


Figure 4: Depiction of dual quaternion conjugations for a displacement $\mathbf{R} = R_z(\pi/4)$, $\mathbf{t} = (5, 1, 0)^T$. The complex conjugation \bar{q} inverts the displacement. In other terms, it inverts the *direction* of the twist. The dual conjugation \underline{q} inverts the *location* of the twist from P to \underline{P} . The combination of complex and dual conjugation $\bar{\underline{q}}$ inverts *direction and location* of the twist.

Therefore, the squared norm of a dual quaternion is defined as

$$\|\tilde{q}\|^2 = \langle \tilde{q}, \tilde{q} \rangle_{\mathbb{H}} = \left(\|q\| + \epsilon \cdot \frac{\langle q, \hat{q} \rangle}{\|q\|} \right)^2.$$

Dual quaternions are elements of a projective space, as lines and screws, and primal quaternions are. Therefore, the displacement that is encoded in a dual quaternion is invariant to the quaternion norm (modulo a volume scaling). Therefore, for a dual quaternion \tilde{q} an equivalence class of so-called Study parameters $[\tilde{q}] = [q, \hat{q}]$ can be identified (as generalization of Equation 15 for lines). This topic is also named as *kinematic map*, see, e.g., [39, Sec. 8.2], [22].

For a finite spatial displacement $D \in SE(3)$ the corresponding dual quaternion is normalized to the dual unit quaternion (without volume scaling) $\hat{q} = \tilde{q} / \|\tilde{q}\|$ with $\|\hat{q}\| = 1$.²³ The dual unit quaternion \hat{q} can be determined by means of the dual angle $\tilde{\phi} = (\phi, s)$ and the dual vector $\hat{G} = (\hat{\omega}, \hat{\mathbf{v}}_0)$. In particular, the following description is possible (as generalization of Equation 34 and of Equation 39):²⁴

$$\hat{q} = \cos \frac{\tilde{\phi}}{2} + \sin \frac{\tilde{\phi}}{2} \cdot \hat{G} \quad (42)$$

The previous equation expands to the following

$$\hat{q} = \cos \frac{\phi}{2} + \sin \frac{\phi}{2} \cdot \mathbf{i} \star \hat{\omega} - \epsilon \cdot \left(\sin \frac{\phi}{2} \cdot \frac{s}{2} \right) + \epsilon \cdot \mathbf{i} \star \left(\cos \frac{\phi}{2} \cdot \frac{s}{2} \cdot \hat{\omega} + \sin \frac{\phi}{2} \cdot \hat{\mathbf{v}}_0 \right). \quad (43)$$

A third alternative to represent a dual unit quaternion by means of setting $q_R = \hat{q}$ from Equation 39, and $q_T = 0 + \epsilon \cdot \mathbf{i} \star \frac{s}{2}$, reads like

$$\hat{q} = q_R + \epsilon \cdot (q_R \cdot q_T). \quad (44)$$

From Equation 42 and Equation 43 an interpretation of a quaternion displacement can be derived that consists of the four geometric entities $(\phi, \hat{\omega}, s, \hat{\mathbf{v}}_0)$ that specify a twist displacement independently of the screw type that was chosen, see Equation 29: dual unit quaternions *renormalize* this information such that $\hat{q} \in \hat{S}(3) \subset \mathbb{R}^4 + \epsilon \cdot \mathbb{R}^4$. Essentially, the interpretation

$$\text{“Dual Unit Quaternion := Rotation Angle + Rotation Axis + Shift + Moment”} \quad (\text{K})$$

is deduced. A dual unit quaternion \hat{q} as representations of a finite displacement $D \in SE(3)$ stands in context with other dual and complex constructions, an overview of that is provided in Figure 5. For more information about dual quaternions, see e.g., [45, Sec. 9.3], [23, Appendix], etc. See e.g., [8] for dual complex number algebra.

²³Note that the scalar product and the norm for dual quaternions are ‘complete’ (in contrast to those for screws, before) for arbitrary screw displacements and translations.

²⁴Equation 42 can be derived via the exponential map: $\hat{q} = \exp(\frac{\tilde{\phi} \cdot \hat{G}}{2}) = \cos \frac{\tilde{\phi}}{2} + \sin \frac{\tilde{\phi}}{2} \cdot \hat{G}$, see [45, p.214].

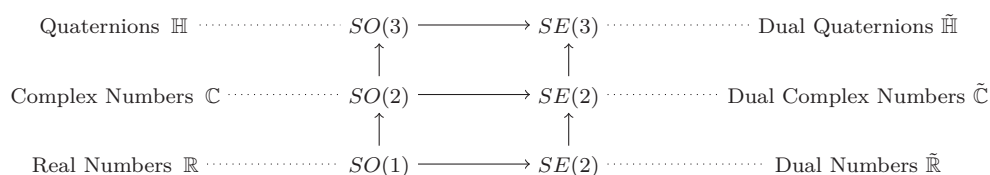


Figure 5: Complex and dual constructions for representing special orthogonal and special Euclidean groups.

3.4 Sequential Representations

3.4.1 Euler Angles in Bunge Convention

‘Passive’ Euler Angles in Bunge Convention. One classic set of Euler angles is the usage in the z - x' - z'' order (the so-called *Euler angle sequence for orbits* [26, Sec. 4.5.1] or *Bunge convention* [6]. In this sequence, the combination of three angles (γ, β, α) is applied. In the passive interpretation this means: first, a basis change from F_D to F_C about degree γ is performed, then, from F_C to F_B about the degree β , finally, from F_B to F_A about α .

$$\mathbf{R}(\gamma, \beta, \alpha) := \mathbf{R}_{\text{dyn}}^{(p)}(\gamma, \beta, \alpha) = \mathbf{R}_{\text{sta}}^{(p)}(\alpha, \beta, \gamma) = \begin{pmatrix} c_\gamma c_\alpha - s_\gamma c_\beta s_\alpha & -c_\gamma s_\alpha - s_\gamma c_\beta c_\alpha & s_\gamma s_\beta \\ s_\gamma c_\alpha + c_\gamma c_\beta s_\alpha & -s_\gamma s_\alpha + c_\gamma c_\beta c_\alpha & -c_\gamma s_\beta \\ s_\beta s_\alpha & s_\beta c_\alpha & c_\beta \end{pmatrix} \quad (45)$$

For the sake of brevity, for some angle θ the common abbreviations $s_\theta = \sin \theta$ and $c_\theta = \cos \theta$ are used in the equation above.

$$\mathbf{R}(\gamma, \beta, \alpha) := \mathbf{R}_{\text{dyn}}^{(p)}(\gamma, \beta, \alpha) = \mathbf{R}_z(\gamma) \circ \mathbf{R}_{x'}(\beta) \circ \mathbf{R}_{z''}(\alpha) \quad (46)$$

The characterization reads as

$$\text{“Euler-Bunge Rotation} := z\text{-Rotation} + x'\text{-Rotation} + z''\text{-Rotation}”. \quad (\text{L})$$

3.4.2 Dual Euler Angles in Bunge Convention

The concept of Euler angles can be generalized by dualization, so that given a displacement $D_{(D,A)}$ (Equation 9) between frames a ‘sequential representation’ can be derived. The term ‘Dual Euler Angles’ was first used in applied kinematics by Yang for the dynamic study of spatial five-link mechanisms [58], and for the dynamic study offset unsymmetric gyroscope [59]. In particular, in [58, Fig. 1] the representation of spatial displacements by Dual Euler Angles is explained. In those papers, computations are performed by means of 3x3 dual transformation matrices $\tilde{\mathbf{M}} \in \tilde{GL}(3)$ within the active interpretation.

The dual Euler parameters in Bunge convention are the ‘Yang-Sheth-Uicker’ sequence

$$\tilde{\mathbf{u}} = (\tilde{\gamma}, \tilde{\beta}, \tilde{\alpha}) = (\gamma, c), (\beta, b), (\alpha, a) \quad (47)$$

In function form / by means of axial twists (that were introduced in Section (I)):

$$D(\tilde{\gamma}, \tilde{\beta}, \tilde{\alpha}) = D_{\text{dyn}}^{(p)}(\tilde{\gamma}, \tilde{\beta}, \tilde{\alpha}) = \$_z(\tilde{\gamma}) \circ \$_{x'}(\tilde{\beta}) \circ \$_{z''}(\tilde{\alpha}) = \$_{\tilde{\gamma}} \circ \$_{\tilde{\beta}} \circ \$_{\tilde{\alpha}}. \quad (48)$$

Spoken more verbally, the following characterization is possible:

$$\text{“Euler-Yang Displacement} := z\text{-Twist} + x'\text{-Twist} + z''\text{-Twist}”. \quad (\text{M})$$

The geometry of this convention is described in more detail in Section 4.4 about the Sheth-Uicker convention.

Matrix Form. Given Dual Euler angles $\tilde{\gamma} = (\gamma, c)$, $\tilde{\beta} = (\beta, b)$, and $\tilde{\alpha} = (\alpha, a)$, the translation vector \mathbf{t} can be computed as

$$\mathbf{t} = \mathbf{t}(\tilde{\gamma}, \tilde{\beta}, \tilde{\alpha}) = c \cdot \begin{pmatrix} 0 \\ 0 \\ 1 \end{pmatrix} + b \cdot \mathbf{R}(\gamma, 0, 0) \cdot \begin{pmatrix} 1 \\ 0 \\ 0 \end{pmatrix} + a \cdot \mathbf{R}(\gamma, \beta, 0) \cdot \begin{pmatrix} 0 \\ 0 \\ 1 \end{pmatrix} \quad (49)$$

Concluding, the homogeneous matrix representation of the displacement $D_{(\mathbf{D}, \mathbf{A})}$ reads

$$\mathbf{M} = \mathbf{M}(\tilde{\gamma}, \tilde{\beta}, \tilde{\alpha}) = \begin{pmatrix} \mathbf{R} & \mathbf{t} \\ \mathbf{0} & 1 \end{pmatrix}. \quad (50)$$

with rotation matrix \mathbf{R} as defined in Equation 45 and translation vector \mathbf{t} as defined in Equation 49.

3.5 Other Representations

Other representations of spatial displacements are described and compared, e.g., in [16]. See e.g., [40] for more representations of spatial rotations. See [54] and [3] for the vectorial representations. See e.g., [46, 47] for exponential and Cayley maps.

| General notation | $F_{(ij)_i}$ | $F_{(ij)_j}$ | $F_{(ij\hat{k})_j}$ | $F_{(\hat{ij}k)_j}$ | $F_{(jk)_j}$ |
|----------------------|--------------|--------------|---------------------|---------------------|--------------|
| Two-Frame SU | ✓ | ✓ | – | – | ✓ |
| Classic DH | – | – | – | ✓ | – |
| Modified DH | – | – | ✓ | – | – |
| Augmented SU | ✓ | ✓ | ✓ | ✓ | ✓ |
| Fixed chain notation | F_{A_i} | F_{D_j} | F_{C_j} | F_{B_j} | F_{A_j} |

Table 2: Usage of frames of different conventions to describe a joint-link displacement $D_{(ijk)}$, expressing the displacements from joint J_{ij} to joint J_{jk} via link L_j . The first column represents joint frame $F_{(ij)_i}$ attached to the previous link L_i . The following four frames are attached to link L_j . These are the joint frame $F_{(ij)_j}$, the augmented frames $F_{(ij\hat{k})_j}$ and $F_{(\hat{ij}k)_j}$, and finally joint frame $F_{(jk)_j}$.

4 Kinematic Modeling Conventions

4.1 Prerequisites

In the following, in Sections 4.2–4.4, the (1) two-frame Sheth-Uicker, (2) the classic, and the (3) the modified Denavit-Hartenberg, and (4) the augmented Sheth-Uicker convention are presented in a unified notation. The link-covering frame set $\hat{\mathcal{F}}$ delivers the possibility to determine the *unique posture* (Definition 7) of a mechanism, and so to solve Problem A, since each frame is specified by (at least) one frame. Equation 7 reads like $\hat{\mathcal{M}} = (\mathcal{L}, \mathcal{J}, \hat{\mathcal{F}})$ so that a mechanism with a link-covering frame set \mathcal{F} can be determined in its *unique posture* like $\hat{P}(t) = P(\hat{\mathcal{F}}_{\hat{\mathcal{M}}}(t))$. So, for each of the four conventions, a certain link-covering frame set will be introduced. At the end of this section, in Section 4.5, four additional kinematic modeling conventions are reviewed.

Usage of Frames. The four different conventions differ according to the frames used. To establish a unified notation, four different frame sets are introduced. In particular, these are the frame set (1) of the two-frame SU convention \mathcal{F}^* , (2) of the classic DH convention \mathcal{F}^C , (3) of the modified DH convention \mathcal{F}^M , and (4) of the augmented SU convention \mathcal{F}^A . In Table 2, the usage of frames of the different conventions is shown. In particular, the equation

$$\mathcal{F}^A = \mathcal{F}^C \cup \mathcal{F}^M \cup \mathcal{F}^* \quad (51)$$

about the combinatorics of the frame sets can be read off from that table: the augmented frame set is created from the frame sets of the other three conventions.

Short Notation. In this article, links are enumerated with simple indices, while joints and their axes are enumerated with double indices to achieve a notation that reflects the topology of the mechanism (see Definition 1). In this section, pairs of lines (of joint axes) and frames located on these are considered. For this purpose, a short notation is introduced. Let Z_{ij} and Z_{jk} be two joint axes that share one index j because the two joints connect with the same link L_j . Then, the definitions

$$\mathbf{c}_{ij\hat{k}} = \pi_{Z_{ij}}^*(Z_{jk}) \quad \mathbf{c}_{\hat{ij}k} = \pi_{Z_{jk}}^*(Z_{ij}) \quad X_{ijk} = \perp^*(Z_{ij}, Z_{jk}) \quad (52)$$

shorten notation by canceling redundancy, but still reflect the necessary combinatorics.²⁵

Frames of the augmented convention are enumerated with triple indices for the same reason. To order to allow intuitive comparisons of the conventions, let an arbitrary chain of links which are connected by joints be fixed by L_i - L_j - L_k passing link L_j . Let $F_{(ij)_i}$, $F_{(ij)_j}$, $F_{ij\hat{k}}$, $F_{\hat{ij}k}$, $F_{(jk)_j}$ and $F_{(jk)_k}$ be the consecutive frames in \mathcal{F}^A associated the chain of links. Then, for the frames that are attached to link L_j , the following short notation is defined

$$F_{D_j} := F_{(ij)_j} \quad F_{C_j} := F_{ij\hat{k}} \quad F_{B_j} := F_{\hat{ij}k} \quad F_{A_j} := F_{(jk)_j} \quad (53)$$

²⁵The ‘hat’ in the used triple index $(ij\hat{k})$ can be read as a ‘not’. For example: “the point $\mathbf{c}_{(ij\hat{k})}$ belongs to the line tuple (Z_{ij}, Z_{jk}) . It is that closest point of the line pair that does *not* lie on the line which contains the index k in its name”.

Method II. TWO-SU – Frame Placings for Two-Frame Convention.

- (In) A simple joint J_{ij} (with anchor point \mathbf{a}_{ij} joint axis \mathbf{z}_{ij}) that connects a link L_i with a link L_j .
 (Out) Frames $F_{A_i} = F_{(ij)_i}$ and $F_{D_j} = F_{(ij)_j}$ that are associated to that joint and attached to link L_i and L_j .
- (p) The locations \mathbf{p}_{A_i} and \mathbf{p}_{D_j} frames F_{A_i} and F_{D_j} are located at the anchor point \mathbf{a}_{ij} of joint J_{ij} .
- (z) The \mathbf{z} -axes \mathbf{z}_{A_i} and \mathbf{z}_{D_j} of frames F_{A_i} and F_{D_j} are aligned along the joint axis \mathbf{z}_{ij} of joint J_{ij} .
- (x) The \mathbf{x} -axes \mathbf{x}_{A_i} and \mathbf{x}_{D_j} of frames F_{A_i} and F_{D_j} are chosen conveniently (e.g., in accordance with the local geometry of the link they are attached to).
- (y) The \mathbf{y} -axes \mathbf{y}_{A_i} and \mathbf{y}_{D_j} of frames F_{A_i} and F_{D_j} are aligned so that they complete right-hand systems.

Parametric and Variable Poses and Displacements. In Definitions 5, the overline notation for indicating *time variance* is introduced for poses. Similarly, if a displacement $D \in SE(3)$ is time variant (it depends on the configuration variables \mathbf{q}), the notation \overline{D} is used. Contrary, if the displacement D is time invariant (it does not depend on \mathbf{q} , but only on the design variables \mathbf{d} and the frames are attached to the same link) then the notation \underline{D} is used.

4.2 Two-Frame Convention

Idea. The idea of the two-frame convention is to achieve a partition of displacement into link and joint displacements. The practical advantages of such a partition are explained in [5]. In [48], in Section 4.4 and Section 6, the advantages of the augmented convention – that is achieved from the two-frame convention – are discussed. Since there are exactly *two* frames at each joint the convention, in total, a frame set of size $|\mathcal{F}^*| = 2 \cdot |\mathcal{J}|$ is defined. Since for each joint-link pair there is exactly one frame defined, to each link there are $|\mathcal{F}_L^*| = |\mathcal{J}_L| \geq 1$ frames attached to it, so that the two-frame convention is not minimal (Definition 6). Sheth and Uicker mention in [48] that this redundancy can be reduced by re-unifying link- and joint displacements for purposes of efficient computation. For the two-frame convention with frame set \mathcal{F}^* Equation 7 becomes

$$\underline{\mathcal{M}}^* = (\mathcal{L}, \mathcal{J}, \mathcal{F}^*) \quad (54)$$

Procedure. Method II contains a description of the frame placings routine for the Sheth-Uicker two-frame convention, TWO-SU.

Decomposition into Joint- and Link Displacements. The combined joint-link displacement D_{ijk} is decomposed into joint displacement \overline{D}_{ij} and link displacement \underline{D}_{ijk}^* like

$$D_{ijk} : F_{(ij)_i} \xrightarrow{\text{p}} F_{(jk)_j} \quad D_{ijk} = \overline{D}_{ij} \circ \underline{D}_{ijk}^* \quad (55)$$

such that the link displacement \underline{D}_{ijk}^* is an arbitrary displacement in $SE(3)$ that maps from joint frame $F_{(ij)_j}$ to joint frame $F_{(jk)_j}$ passively: $\underline{D}_{ijk}^* : F_{(ij)_j} \xrightarrow{\text{p}} F_{(jk)_j}$. It is further decomposed by the augmented convention (Section 4.4). The displacement \overline{D}_{ij} is the short notation for $\overline{D}_{(ij)_i, (ij)_j}$ that expresses the time-dependent displacement between the frames $F_{(ij)_i}$ and $F_{(ij)_j}$ at joint J_{ij} . In the passive interpretation, it can be computed as a spatial displacement as

$$\overline{D}_{ij} : F_{(ij)_i} \xrightarrow{\text{p}} F_{(ij)_j} \quad \overline{D}_{ij} = (F_{(ij)_i})^{-1} \circ F_{(ij)_j} . \quad (56)$$

In case of a simple joint, this displacement can be expressed via one finite twist as

$$\overline{D}_{(ij)} = \overline{\mathbb{S}}_{\overline{\mathbf{d}}_{ij}} = \overline{\mathbb{S}}_{\mathbf{z}}(\delta_{ij}, d_{ij}) . \quad (57)$$

The handling of other complex joint types is described in the original work by Sheth and Uicker [48].

Computation of Forward Kinematics. By means of the two-frame convention, the forward kinematics map of a kinematic chain is computed as

$$\begin{aligned} D_{(1,n)} &= \overline{D}_{1,2} \circ \underline{D}_{1,2,3}^* \circ \overline{D}_{2,3} \circ \underline{D}_{2,3,4}^* \circ \cdots \circ \overline{D}_{(n-2,n-1)} \circ \underline{D}_{(n-2,n-1,n)}^* \\ &= D_{(1,2,3)} \circ D_{(2,3,4)} \circ \cdots \circ D_{(n-3,n-2,n-1)} \circ D_{(n-2,n-1,n)}. \end{aligned} \quad (58)$$

In [5], it is discussed how the forward kinematics map for kinematic trees can be computed and how kinematic loop computations can be integrated into that by means of the two-frame convention.

4.3 Denavit-Hartenberg Conventions

Idea. For the classic DH and the modified convention with frame sets \mathcal{F}^C and \mathcal{F}^M , Equation 7 reads like

$$\underline{\mathcal{M}}^C = (\mathcal{L}, \mathcal{J}, \mathcal{F}^C) \qquad \underline{\mathcal{M}}^M = (\mathcal{L}, \mathcal{J}, \mathcal{F}^M)$$

Classic and Modified DH convention define *minimal link covering frame sets* (see Definition 6), thus $|\mathcal{F}^C| = |\mathcal{F}^M| = |\mathcal{L}|$. The classic DH convention (see [20], and e.g., [44, 50], [50]) and its modified variant (see e.g. [9, 28], [11, p.219]) represent the most popular standard for specifying a kinematic chain. Classic and modified DH convention use a set of four parameters, namely the quadruple

$$(\theta, t), (\beta, b).$$

Generally, a spatial displacement (defined by two different frames) can be specified by minimally six parameters (see the twist displacement in Section 3.2) – the ‘trick’ of the DH convention is to place the frames such that the displacement between them can be described via the four parameters θ, t, β, b . The geometric meaning is described in Table 4 and Table 5. Therefore, it has to be distinguished between the four possible cases of line configurations (see Section 3.2.2): in case of coincident and intersecting axes lines, everything ‘is nice’. In the cases of parallel and skew lines, the frames have to be ‘moved’ according to certain rules (this is also further discussed in Section 6.1.1).

Proximal and Distal. The classic DH convention is a *distal* convention in the sense that a frame j (that is attached to link L_j) is located at the *end* of the common perpendicular $X_{ijk} = \perp^*(Z_{ij}, Z_{jk})$ on joint axis Z_{jk} (see Definition 13).

The modified DH convention is a *proximal* convention in the sense that a frame j (that is attached to link L_j) is located at the *beginning* of the common perpendicular $X_{ijk} = \perp^*(Z_{ij}, Z_{jk})$ on joint axes Z_{ij} .²⁶

For a better overview of this frame alignment, see Figure 6 for classic DH, and Figure 7 for modified DH convention. Their drawing style is adapted from [50]. It is important to mind that in contrast to the preceding two frame convention, generally *neither* F_{B_i} and F_{B_j} (classic) F_{C_j} and F_{C_k} (modified) correspond to the anchor points of the joints.

Decomposition into Two Axial Twists. More concrete, each displacement can be decomposed into two *screw displacements*. By means of the frame names that were introduced in equations 53, the displacements read for the classic convention:

$$D_{ij}^C : F_{B_i} \mapsto_p F_{B_j} \qquad D_{ij}^C = \overline{\mathfrak{S}}_{\mathbf{z}}(\theta_{ij}, t_{ij}) \circ \mathfrak{S}_{\mathbf{x}}(\beta_{ijk}, b_{ijk}) \quad (59)$$

And for the modified convention:

$$D_{jk}^M : F_{C_j} \mapsto_p F_{C_k} \qquad D_{jk}^M = \mathfrak{S}_{\mathbf{x}}(\beta_{ijk}, b_{ijk}) \circ \overline{\mathfrak{S}}_{\mathbf{z}}(\theta_{ij}, t_{ij}) \quad (60)$$

Procedure. Method III displays a detailed view of the frame-placing routine CLS-DH for the classic DH convention according to the four general positions. Method IV displays a detailed view of the frame-placing routine CLS-DH for the modified convention according to the four general positions.

²⁶When using, e.g., for chains, simple joint indices, the classic convention has the unsatisfactory property that a frame j is placed on joint axis $j + 1$. To facilitate this situation, the modified version was introduced. In this article, this issue does not occur since tuple indices instead of simple indices are used to identify joints.

Method III. CLS-DH – Frame Placings for Classic DH Convention.

- (In) 1. Joint axes lines Z_{ij} and Z_{jk} of two simple joints J_{ij} and J_{jk} ,
2. classic DH frame F_{B_j} for link L_i .
- (Out) Classic DH frame F_{B_j} for link L_j .
- (\perp) The common perpendicular $X_{ijk}^* = \perp^*(Z_{ij}, Z_{jk}) = (\omega_{ijk}^*, \mathbf{v}_{ijk}^*)$ of lines Z_{ij} and Z_{jk} is computed.
- (p) The location \mathbf{p}_{B_j} of frame F_{B_j} is being fixed on line Z_{ij} . In case that the lines Z_{ij} and Z_{jk} are
1. **coincident**, \mathbf{p}_{B_j} is fixed to some point on Z_{jk} , e.g., the line anchor point \mathbf{a}_{jk} .
 2. **intersecting**, \mathbf{p}_{B_j} is fixed to some point on Z_{jk} , e.g., the line intersection point $\mathbf{c}_{ijk} = \mathbf{c}_{ijk}$.
 3. **parallel**, \mathbf{p}_{B_j} is fixed to some point on Z_{jk} , e.g., the line anchor point \mathbf{a}_{jk} .
 4. **skew**, \mathbf{p}_{B_j} is fixed to the closest point \mathbf{c}_{ijk} of Z_{ij} on Z_{jk} .
- (z) The \mathbf{z} -axis \mathbf{z}_{B_j} of frame F_{B_j} is aligned along the joint axis line l_{jk} .
- (x) The \mathbf{x} -axis \mathbf{x}_{B_j} of frame F_{B_j} is aligned perpendicular to both lines Z_{ij} and Z_{jk} . In case that the lines Z_{ij} and Z_{jk} are
1. **coincident**, \mathbf{x}_{B_j} is fixed to some direction in the plane orth. to lines Z_{ij} and Z_{jk} , e.g., along \mathbf{x}_{C_i} .
 2. **intersecting**, \mathbf{x}_{B_j} is fixed along the common perpendicular X_{ijk}^* .
 3. **parallel**, \mathbf{x}_{B_j} is fixed to some direction in the plane orth. to lines Z_{ij} and Z_{jk} , e.g., along X_{ijk}^* .
 4. **skew**, \mathbf{x}_{B_j} is fixed along the common perpendicular X_{ijk}^* .
- (y) The \mathbf{y} -axis \mathbf{y}_{B_j} of frame F_{B_j} is aligned so that it completes a right-hand system.

Method IV. MOD-DH – Frame Placings for Modified DH Convention.

- (In) 1. Joint axes lines Z_{ij} and Z_{jk} of two simple joints J_{ij} and J_{jk} ,
2. the modified DH Frame F_{C_j} for link L_i .
- (Out) Modified DH frame F_{C_j} for link L_j .
- (\perp) The common perpendicular $X_{ijk}^* = \perp^*(Z_{ij}, Z_{jk}) = (\omega_{ijk}^*, \mathbf{v}_{ijk}^*)$ of lines Z_{ij} and Z_{jk} is computed.
- (p) The location \mathbf{p}_{C_j} of frame F_{C_j} is being fixed on line Z_{ij} . In case that the lines l_{ij} and l_{jk} are
1. **coincident**, \mathbf{p}_{C_j} is fixed to some point on Z_{ij} , e.g., the line anchor point \mathbf{a}_{jk} .
 2. **intersecting**, \mathbf{p}_{C_j} is fixed to some point on Z_{ij} , e.g., the line intersection point $\mathbf{c}_{ijk} = \mathbf{c}_{ijk}$.
 3. **parallel**, \mathbf{p}_{C_j} is fixed to some point on Z_{ij} , e.g., the line anchor point \mathbf{a}_{jk} .
 4. **skew**, \mathbf{p}_{C_j} is fixed to the closest point \mathbf{c}_{ijk} of Z_{jk} on Z_{ij} .
- (z) The \mathbf{z} -axis \mathbf{z}_{C_j} of frame F_{C_j} is aligned along the joint axis line Z_{ij} .
- (x) The \mathbf{x} -axis \mathbf{x}_{C_j} of frame F_{C_j} is aligned perpendicular to both lines Z_{ij} and Z_{jk} . In case that the lines l_{ij} and l_{jk} are
1. **coincident**, \mathbf{x}_{C_j} is fixed to some direction in the plane orth. to lines Z_{ij} and Z_{jk} , e.g., along \mathbf{x}_{C_i} .
 2. **intersecting**, \mathbf{x}_{C_j} is fixed along the common perpendicular X_{ijk}^* .
 3. **parallel**, \mathbf{x}_{C_j} is fixed to some direction in the plane orth. to lines Z_{ij} and Z_{jk} , e.g., along X_{ijk}^* .
 4. **skew**, \mathbf{x}_{C_j} is fixed along the common perpendicular X_{ijk}^* .
- (y) The \mathbf{y} -axis \mathbf{y}_{C_j} of frame F_{C_j} is aligned so that it completes a right-hand system.

Discussion. Each DH displacement is expressed by only four parameters. This is achieved by the special placing of frames in \mathcal{F}^C , and \mathcal{F}^M . However, this has the consequence “*in certain circumstances, this will require placing the origin of frame i in a location that may not be intuitively satisfying, but typically this will not be the case*” as Spong and Hutchinson characterize in [50]. The mentioned ‘certain circumstances’ describe the case of skew line geometry; this is illustrated in example mechanism in Section 5 and the configuration in Figure 16, Section 6.2.1. A lot of real mechanisms feature skew line geometry. And further, if one assumes a ‘probabilistic mechanism’ (that might arise from or for a simulation), with randomly defined joint axes, skew geometries of these appear with probability one.

The property of minimal DH that the \mathbf{x} -axes of the frames need to be adjusted to so that they intersect with the ‘other’ joint axis, leads to another disadvantage: since a minimal frame set is chosen and therefore the poses of the frames are influenced by both, design parameters *and* configuration variables, the *zero pose* of the mechanism is implicitly defined by the geometries of the joint axes pairs and *cannot* be chosen freely. In particular, it is not possible to adjust the zero configuration to the poses of the integrated physical joints or to the specific wishes of the modelers.

4.4 Augmented Convention

Idea. The frames of the minimal DH conventions are located in such a manner that a displacement between the consecutive frames can be expressed by four parameters: the displacements between two successive frames in \mathcal{F}^C and \mathcal{F}^M may differ by *two* screw displacements. The frames of the two-frame convention are freely located at the joint positions. Thus the arbitrary spatial displacement between them can be minimally described by six parameters (see vectorial representation, Section 3.2, and sequential representation,

Method V. AUG-SU – Frame Placings for Augmented SU Convention.

(In) Two frames $F_{D_j} = F_{(ij)_j}$ and $F_{A_j} = F_{(jk)_j}$ at joints J_{ij} and J_{jk} and attached to link L_j .

(Out) Two augmenting frames $F_{C_j} = F_{ij\hat{k}}$ and $F_{B_j} = F_{i\hat{j}k}$ attached to link L_j .

(\perp) The common perpendicular $X_{ijk}^* = \perp^*(Z_{ij}, Z_{jk}) = (\omega_{ijk}^*, \mathbf{v}_{ijk}^*)$ of lines Z_{ij} and Z_{jk} is computed.

(p) The locations \mathbf{p}_{C_j} and \mathbf{p}_{B_j} of frames F_{C_j} and F_{B_j} are fixed to the closest points $\mathbf{c}_{ij\hat{k}}^*$ and $\mathbf{c}_{i\hat{j}k}^*$ of lines \mathbf{z}_{ij} and \mathbf{z}_{jk} . The closest points are determined by $\mathbf{c}_{ij\hat{k}}^* = \mathbf{x}_{ijk}^* \cap \mathbf{z}_{ij}$ and $\mathbf{c}_{i\hat{j}k}^* = \mathbf{x}_{ijk}^* \cap \mathbf{z}_{jk}$.

(z) The \mathbf{z} -axes \mathbf{z}_{C_j} and \mathbf{z}_{B_j} of frames F_{C_j} and F_{B_j} are aligned along the \mathbf{z} -axes \mathbf{z}_{D_j} and \mathbf{z}_{A_j} of frames F_{D_j} and F_{A_j} .

(x) Do the lines $\mathbf{z}_{D_j} = \mathbf{z}_{ij}$ and $\mathbf{z}_{A_j} = \mathbf{z}_{jk}$ of frames F_{D_j} and F_{A_j} share (at least) one common point?

Yes. (in case of coincident and intersecting \mathbf{z} -axes)

- The \mathbf{x} -axes \mathbf{x}_{C_j} and \mathbf{x}_{B_j} of frames F_{C_j} and F_{B_j} are aligned along the \mathbf{x} -axes \mathbf{x}_{D_j} and \mathbf{x}_{A_j} of frames F_{D_j} and F_{A_j} .

No. (in case of parallel and skew \mathbf{z} -axes)

- The \mathbf{x} -axes \mathbf{x}_{C_j} and \mathbf{x}_{B_j} of frames F_{C_j} and F_{B_j} are aligned along the direction of the common perpendicular ω_{ijk}^* .

(y) The \mathbf{y} -axes \mathbf{y}_{C_j} and \mathbf{y}_{B_j} of frames F_{C_j} and F_{B_j} are aligned so that they complete right-hand systems.

Section 3.4). Sheth-Uicker's uses the latter, the Dual Euler Angles representation and thus consists of a sequence of *three* screw displacements. In this section, this idea is more formalized by introducing the *augmented frame set* \mathcal{F}^A . Two consecutive frames of this frame set may differ by at least *one* screw displacement and can be described by two parameters (that together make a dual angle). Then, for the augmented convention with frame set \mathcal{F}^A the Equation 7 reads like

$$\underline{\mathcal{M}}^A = (\mathcal{L}, \mathcal{J}, \mathcal{F}^A) \quad (61)$$

Decomposition into Three Axial Twists. Decompose the link displacement \underline{D}_{ijk}^* from Equation 55 into *three* twists ($\underline{\mathcal{S}}_{\hat{c}_{ij\hat{k}}}, \underline{\mathcal{S}}_{\hat{b}_{i\hat{j}k}}, \underline{\mathcal{S}}_{\hat{a}_{ijk}}$). A sketch of the three twists is given in Figure 9. Then, the decomposition of \underline{D}_{ijk}^* can be written as

$$\underline{D}_{ijk}^* = \underline{\mathcal{S}}_{\hat{c}_{ij\hat{k}}} \circ \underline{\mathcal{S}}_{\hat{b}_{i\hat{j}k}} \circ \underline{\mathcal{S}}_{\hat{a}_{ijk}}. \quad (62)$$

Each of the screws is made up by two parameters, thus we have *six major* parameters, namely the tuple

$$(\gamma, c), (\beta, b), (\alpha, a) \quad (63)$$

The geometric meaning of these six parameters is described in Table 6. In more detail, the three twists are axial twists (see Section 3.2.4)

$$\underline{\mathcal{S}}_{\hat{c}_{ij\hat{k}}} : F_{(ij)_j} \xrightarrow{p} F_{ij\hat{k}} \quad \underline{\mathcal{S}}_{\hat{c}_{ij\hat{k}}} = \underline{\mathcal{S}}_{\mathbf{z}}(\gamma_{ijk}, c_{ijk}) \quad (64)$$

$$\underline{\mathcal{S}}_{\hat{b}_{i\hat{j}k}} : F_{i\hat{j}k} \xrightarrow{p} F_{i\hat{j}k} \quad \underline{\mathcal{S}}_{\hat{b}_{i\hat{j}k}} = \underline{\mathcal{S}}_{\mathbf{x}}(\beta_{ijk}, b_{ijk}) \quad (65)$$

$$\underline{\mathcal{S}}_{\hat{a}_{ijk}} : F_{i\hat{j}k} \xrightarrow{p} F_{(jk)_j} \quad \underline{\mathcal{S}}_{\hat{a}_{ijk}} = \underline{\mathcal{S}}_{\mathbf{z}}(\alpha_{ijk}, a_{ijk}) \quad (66)$$

Procedure. The frame-placing procedure is described in detail in Method V. It describes the frame-placing routine AUG-SU for augmented convention for a given pair of frames $F_{(ij)_j}, F_{(jk)_j} \in \mathcal{F}^*$; thus after Method II has been executed.

Discussion. The joint frames are aligned according to the Frame Axes Principle from Section 2.3. Z -lines indicate the joint axes. The decomposition takes place along these lines, thus preserving them. This is discussed in Section 6. Table 3 depicts how the pose of the line pair of joint axes can be read off from a Sheth-Uicker table.

In e.g., [30] the Sheth-Uicker convention was applied.

| Symbol | Pose of Lines | \Leftarrow | γ | c | β | b | α | a |
|--------|---------------------|--------------|----------|-------|---------|-----|----------|-------|
| | <i>coincident</i> | | $s/2$ | $s/2$ | – | – | $s/2$ | $s/2$ |
| | <i>parallel</i> | | $s/2$ | $s/2$ | – | * | $s/2$ | $s/2$ |
| | <i>intersecting</i> | | . | . | * | – | . | . |
| | <i>skew</i> | | . | . | * | * | . | . |

Table 3: Deducing the mutual line pose from SU parameters: In coincident and parallel cases, the generalized common orthogonal (Definition 13) is placed in between the frames so that the twists along the Z -line and the Z'' -line have identical twist parameters. In the other two cases, these are arbitrary. The distribution of the non-zeros (*) of the parameters β and b of β -twist along the X' -line allows a unique interpretation of the mutual pose of the lines.

Computation of Forward Kinematics. By means of the augmented SU convention, the forward kinematics map of a kinematic chain is computed as

$$\begin{aligned}
 D_{(1,n)} &= \bar{D}_{1,2} \circ \underline{D}_{1,2,3}^* \circ \bar{D}_{2,3} \circ \underline{D}_{2,3,4}^* \circ \dots \circ \bar{D}_{(n-2,n-1)} \circ \underline{D}_{(n-2,n-1,n)}^* \\
 &= \bar{\mathbb{S}}_{\bar{d}_{12}} \circ \underline{\mathbb{S}}_{c_{123}} \circ \underline{\mathbb{S}}_{\bar{b}_{123}} \circ \underline{\mathbb{S}}_{a_{123}} \circ \dots \circ \bar{\mathbb{S}}_{\bar{d}_{n-1,n}} \circ \underline{\mathbb{S}}_{c_{n-2,n-1,n}} \circ \underline{\mathbb{S}}_{\bar{b}_{n-2,n-1,n}} \circ \underline{\mathbb{S}}_{a_{n-2,n-1,n}},
 \end{aligned} \tag{67}$$

whereby the first equation is identical to Equation 58.

4.5 Other Modeling Conventions

In the final part of this section, next to the two frame convention (Section 4.2), the two variants of Denavit-Hartenberg's convention (Section 4.3), and Sheth-Uicker's augmented convention (Section 4.4), four further conventions for modeling the kinematics of mechanisms are reviewed briefly. By outlining their interconnections, a broad overview of the state-of-the-art in *kinematic modeling* shall be permitted.

Yang's Convention. Yang modeled spatial mechanisms in the works [58] and [59] by means of twists along the joint axes, and twists along common perpendiculars of consecutive pairs of these axes. In the notation of frame sets, the frame set \mathcal{F}^Y that is used by Yang contains those frames that are located in the intersections of these twists. Therefore, the set \mathcal{F}^Y can be obtained from the augmented frame set by subtracting the frames at the joints - the frames of the two-frame convention, as $\mathcal{F}^Y = \mathcal{F}^A \setminus \mathcal{F}^*$. The convention by Yang is not a *minimal* convention in terms of frames, but a minimal convention in terms of twists: twists on the same axis are 'accumulated' into one twist. There is no separation between joint and link displacements. This convention is illustrated within the example in Section 5.

Khalil-Kleininger Convention. Khalil and Kleininger developed a convention that is a '*case-sensitive blend*' between Denavit-Hartenberg's and Sheth-Uicker's convention [24]. In dependence of the topology of the mechanism (chain, tree, loop), the convention changes between the usage of only two, or more than two, twists per row. Comparing to Sheth-Uicker's convention, a number of case distinctions has to be conducted. In Section 5, the conversion of conventions is illustrated: i.e., frames of the the augmented convention can be filtered to achieve a minimal convention for a subchain of a mechanism. By doing so, similar results to Khalil-Kleininger's convention can be achieved in a way that saves the case distinctions during the 'construction phase' of the convention. Similar to this article, Khalil and Kleininger used tuple indices to enumerate elements of the mechanism. However, the set of joints was chosen as the ground set of their indexing scheme, in contrast to the set of links which is chosen here. If one applies an adjacency-based indexing together with Khalil-Kleininger's scheme for a link which connects to a multitude of k other links via k joints, the 'name' of this link becomes an impractically long tuple of – principally unrestricted – length k .²⁷

Thomas-Maciuszek-Wahl Convention. Thomas, Maciuszek, and Wahl developed a convention for handling spherical joints by extending the convention by Denavit-Hartenberg with *one* additional rotational degree of freedom to each row of the original Denavit-Hartenberg table [53]. The convention follows a one-frame convention, i.e., it uses one frame at the anchor point of each joint. In this sense, the convention by Thomas et al. is a '*total blend*' of the minimal Denavit-Hartenberg convention and the two-frame convention.

²⁷E.g., in a case of a Stewart platform, the two 'platform links' connect via six spherical joints to each of the legs. Therefore, for this example, both platform links are identified by tuples of length six.

Compared to Sheth-Uicker’s convention, the convention by Thomas et al. saves one parameter per table row. However, along with that, the strict separation of variable and constant displacements is lost – and even more repealed than in the classic Denavit-Hartenberg convention. Further – if only *five* instead of *six* parameters (Sheth-Uicker) are used to describe one joint-link displacement – the remaining of constraints on the frame-placings is inevitable. Similar to Denavit-Hartenberg’s original work, tricky situations arise for the modeling of mechanisms that feature branchings or skew line geometries. The notation by Thomas et al. is based on the link-graph $\mathcal{G}^{\mathcal{L}}$. However, since the enumeration of edges (joints) is simple, these do not reflect the combinatorics of the mechanism.

Gupta’s Zero Reference Pose Convention. The zero reference pose method by Gupta is a method by which the computation of the current pose of a kinematic structure is conducted with respect to its zero reference pose, instead of using the joint-to-joint displacements which are used by the representations explained here [18]. For that, similarity transformations are exploited. In contrast to the methods presented before, Gupta’s method is more a computation method, instead of a method about the selection, naming, location, and orientation of frames. In particular, it is a useful formalism for the computation of complex mechanisms since it is demonstrated how to analyze a complex joint “as a separate entity and then ‘add on’ this solution to the rest of the manipulator solution” [18].

| FT | Axis | Param. | Geometric Description | Alignment |
|----------------------|-----------|---------------|---|---------------------------|
| $ \mathbb{S} _{adc}$ | Z_{ij} | θ_{ij} | angular distance of \mathbf{x}_{B_i} and \mathbf{x}_{C_j} | around \mathbf{z}_{B_i} |
| | Z_{ij} | t_{ij} | linear distance of \mathbf{x}_{B_i} and \mathbf{x}_{C_j} | along \mathbf{z}_{B_i} |
| $ \mathbb{S} _b$ | X_{ijk} | β_{ijk} | angular distance of \mathbf{z}_{C_j} and \mathbf{z}_{B_j} | around \mathbf{x}_{C_j} |
| | X_{ijk} | b_{ijk} | linear distance of \mathbf{z}_{C_j} and \mathbf{z}_{B_j} | along \mathbf{x}_{C_j} |

Table 4: Geometric meaning of four minimal parameters (θ, d, α, a) of the classic Denavit-Hartenberg convention. The *four* parameters describe a combined *link-joint-link displacement*.

| FT | Axis | Param. | Geometric Description | Alignment |
|----------------------|-----------|---------------|---|---------------------------|
| $ \mathbb{S} _b$ | X_{ijk} | β_{ijk} | angular distance of \mathbf{z}_{C_j} and \mathbf{z}_{B_i} | around \mathbf{x}_{C_j} |
| | X_{ijk} | b_{ijk} | linear distance of \mathbf{z}_{C_j} and \mathbf{z}_{B_i} | along \mathbf{x}_{C_j} |
| $ \mathbb{S} _{adc}$ | Z_{jk} | θ_{jk} | angular distance of \mathbf{x}_{B_j} and \mathbf{x}_{C_k} | around \mathbf{z}_{B_j} |
| | Z_{jk} | t_{jk} | linear distance of \mathbf{x}_{B_j} and \mathbf{x}_{C_k} | along \mathbf{z}_{B_j} |

Table 5: Geometric meaning of four minimal parameters (α, a, θ, d) of the modified Denavit-Hartenberg convention. The *four* parameters describe a combined *link-joint-link displacement*.

| FT | Axis | P. | Geometric Description | Alignment |
|------------------|----------------------|----------|--|---------------------------|
| $ \mathbb{S} _d$ | $\mathbf{z}_{(ij)}$ | δ | var. angular distance of \mathbf{x}_{A_i} and \mathbf{x}_{D_j} | around \mathbf{z}_{A_i} |
| | | d | var. linear distance of \mathbf{x}_{A_i} and \mathbf{x}_{D_j} | along \mathbf{z}_{A_i} |
| $ \mathbb{S} _c$ | $\mathbf{z}_{(ijk)}$ | γ | const. angular distance of \mathbf{x}_{D_j} and \mathbf{x}_{C_j} | around \mathbf{z}_{D_j} |
| | | c | const. linear distance of \mathbf{x}_{D_j} and \mathbf{x}_{C_j} | along \mathbf{z}_{D_j} |
| $ \mathbb{S} _b$ | $\mathbf{x}_{(ijk)}$ | β | const. angular distance of \mathbf{z}_{C_j} and \mathbf{z}_{B_j} | around \mathbf{x}_{C_j} |
| | | b | const. linear distance of \mathbf{z}_{C_j} and \mathbf{z}_{B_j} | along \mathbf{x}_{C_j} |
| $ \mathbb{S} _a$ | $\mathbf{z}_{(ijk)}$ | α | const. angular distance of \mathbf{x}_{B_j} and \mathbf{x}_{A_j} | around \mathbf{z}_{B_j} |
| | | a | const. linear distance of \mathbf{x}_{B_j} and \mathbf{x}_{A_j} | around \mathbf{z}_{B_j} |

Table 6: Geometric meaning of (two plus) six parameters of the Sheth-Uicker convention. The *two* parameters δ, d describe the *joint displacement* of a simple joint. The *six* parameters ($\gamma, c, \beta, b, \alpha, a$) describe the *link displacement*.

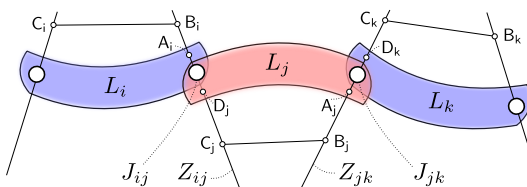


Figure 8: Line configurations of Z_{ij} and Z_{jk} for a chain of links L_i, L_j, L_k together with named frames.

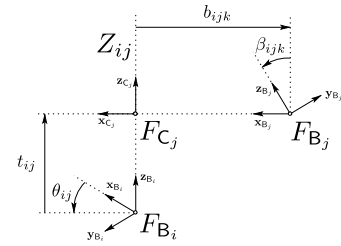


Figure 6: Classic DH parameters for a displacement between frames F_{B_i} and F_{B_j} .

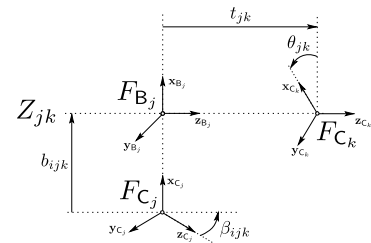


Figure 7: Modified DH parameters for a displacement between F_{C_j} and F_{C_k} .

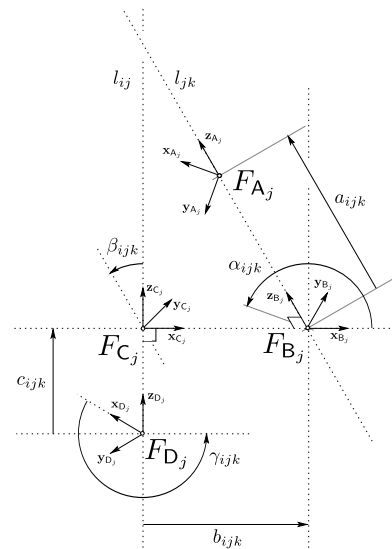


Figure 9: Augmented parameters for a displacement between frames F_{D_j} and F_{A_j} . These frames may define a pair of skew lines by their z -axes.

$$\begin{aligned}
\mathbf{S}_1 &= \begin{pmatrix} 1 & 0 & 0 & 0 \\ 0 & 1 & 0 & 0 \\ 0 & 0 & 1 & 0 \\ 0 & 0 & 0 & 1 \end{pmatrix} & \mathbf{S}_2 &= \begin{pmatrix} 1 & 0 & 0 & 0 \\ 0 & 1 & 0 & 0 \\ 0 & 0 & 1 & 1 \\ 0 & 0 & 0 & 1 \end{pmatrix} \\
\mathbf{S}_3 &= \begin{pmatrix} 1 & 0 & 0 & 0 \\ 0 & 1 & 0 & 0 \\ 0 & 0 & 1 & 2 \\ 0 & 0 & 0 & 1 \end{pmatrix} & \mathbf{S}_4 &= \begin{pmatrix} 1 & 0 & 0 & 2 \\ 0 & \sqrt{1/2} & \sqrt{1/2} & 0 \\ 0 & -\sqrt{1/2} & \sqrt{1/2} & 2 \\ 0 & 0 & 0 & 1 \end{pmatrix} \\
\mathbf{S}_5 &= \begin{pmatrix} 1 & 0 & 0 & 2 \\ 0 & \sqrt{1/2} & \sqrt{1/2} & 1 \\ 0 & -\sqrt{1/2} & \sqrt{1/2} & 3 \\ 0 & 0 & 0 & 1 \end{pmatrix} & \mathbf{S}_6 &= \begin{pmatrix} 1 & 0 & 0 & 2 \\ 0 & \sqrt{1/2} & \sqrt{1/2} & 2 \\ 0 & -\sqrt{1/2} & \sqrt{1/2} & 4 \\ 0 & 0 & 0 & 1 \end{pmatrix}
\end{aligned}$$

Figure 10: Set of matrices $\{\mathbf{S}_1, \dots, \mathbf{S}_6\}$ that determine the poses of the frames of the example mechanism.

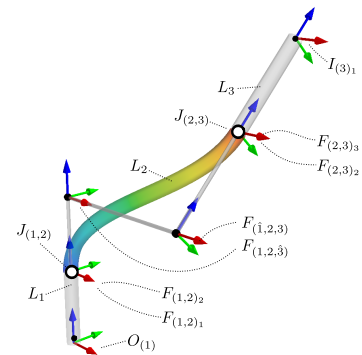


Figure 11: Example mechanism with named links, joints and frames.

5 Example

In this section, an example for the modeling with augmented Sheth-Uicker parameters in comparison to classic and modified Denavit-Hartenberg conventions is presented to clarify the similarities and differences between the concepts. For simplicity, all angles are denoted in degrees.

5.1 Description of the Example Mechanism

The example mechanism $\underline{\mathcal{M}}$ consists of three links $\mathcal{L} = \{L_1, L_2, L_3\}$. The first link is fixed and connected to some origin frame F_O , the last one can be thought of ending with some end effector, thus carrying a frame of interest F_I . The first and the third link are simple cylinders, while the second link is some curve (see below). Two simple joints J_{12} , and J_{23} , here rotative joints, are used in the mechanism. They are collected in the set $\mathcal{J} = \{J_{12}, J_{23}\}$. In Figure 11, the named entities can be read off.

Two-Frame Convention. As explained in Section 6.1.2, mechanisms can be uniquely defined ... By means of that, the mechanism $\underline{\mathcal{M}}^*$ can be specified in its unique pose via triple $\underline{\mathcal{M}}^* = (\mathcal{L}, \mathcal{J}, \mathcal{F}^*)$. The frames of the two-frame convention \mathcal{F}^* is the following

$$\mathcal{F}^* = \{F_O, F_{(1,2)_1}, F_{(1,2)_2}, F_{(2,3)_2}, F_{(2,3)_3}, F_I\}. \quad (68)$$

where the additional F_O is introduced as an invariant frame at the origin of the very first link, and F_I is introduced to indicate the pose of the tip of the last link of the chain.

The set of matrices given in Figure 10 defines the poses of all frames that appear in different representation conventions to specify the mechanism. For the two-frame convention this looks like as follows

$$P_O = \mathbf{S}_1, P_{(1,2)_1} = \mathbf{S}_2, P_{(1,2)_2} = \mathbf{S}_2, P_{(2,3)_2} = \mathbf{S}_5, P_{(2,3)_3} = \mathbf{S}_5, P_I = \mathbf{S}_6. \quad (69)$$

In Figure 12(a) the example mechanism is shown together with the frame set \mathcal{F}^2 . The Sheth-Uicker two-frame convention is not expressible in table form. The only possibility to specify the mechanism is the listing of the displacements, e.g., in form of matrices.

The Second Link. The second link L_2 was created by a multivariate Hermite spline. Start point \mathbf{p}_1 and start ‘velocity’ \mathbf{t}_1 , target point \mathbf{p}_2 and target ‘velocity’ \mathbf{t}_2

$$\mathbf{p}_1 = (0.0, 0.0, 1.0)^T \quad \mathbf{t}_1 = 3 \cdot (0.0, 0.0, 1.0)^T \quad \mathbf{p}_2 = (2.0, 1.0, 3.0)^T \quad \mathbf{t}_2 = 3 \cdot \frac{1}{\sqrt{2}} \cdot (0.0, 1.0, 1.0)^T$$

5.2 Comparison

As explained in Section 4, in different conventions different sets of frames are used. For the present example mechanism \mathcal{M} , the overall mechanism can be seen with four different frame sets in Figure 5.2. In addition to that graphical representation, the frames and their usages are also presented in Table 7.

| | | S_1 | S_2 | S_3 | S_4 | S_5 | S_6 |
|--------------|-----------------|-------|-----------|-------------------|-------------------|-----------|-------|
| Two Frame SU | \mathcal{F}^* | F_O | $J_{1,2}$ | – | – | $J_{2,3}$ | F_I |
| Classic DH | \mathcal{F}^C | F_O | – | – | L_2 | – | F_I |
| Modified DH | \mathcal{F}^M | F_O | – | L_2 | – | – | F_I |
| Augmented SU | \mathcal{F}^A | F_O | $J_{1,2}$ | $\hat{D}_{1,2,3}$ | $\hat{D}_{1,2,3}$ | $J_{1,2}$ | F_I |

Table 7: Usage of frames in different conventions and associated entities. F_O denotes the frame at the *origin*, and F_I the frame of *interest*. The table is according to the more general Table 2.

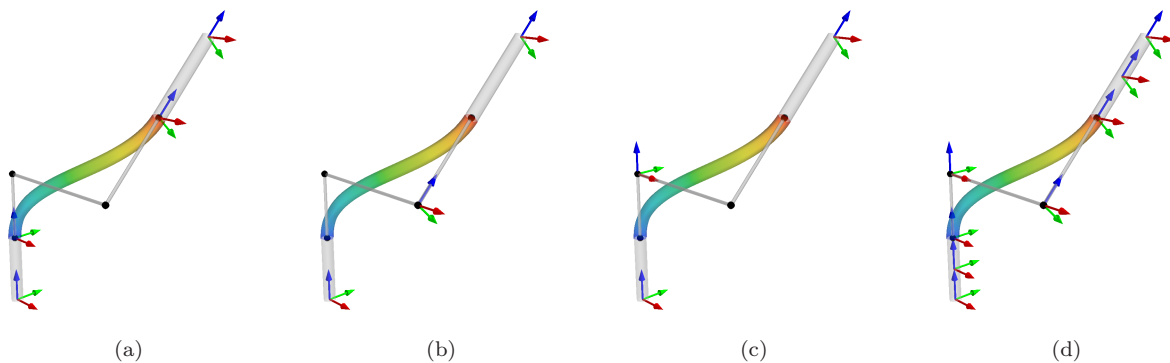


Figure 12: Usage of frames for the example in (a) *two-frame* SU, (b) *classic* DH, (b) *modified* DH, and (d) *augmented* SU convention. For a clear view, the norm of axis vectors of the frames was shrunk.

Classic and Modified DH Convention. The frame set \mathcal{F}^C for the classic DH convention consists of the following three frames

$$\mathcal{F}^C = \{F_O, F_{(\hat{1},2,3)}, F_I\}. \quad (70)$$

The frame set \mathcal{F}^M for the modified DH convention consists of the following three frames

$$\mathcal{F}^M = \{F_O, F_{(1,2,\hat{3})}, F_I\}. \quad (71)$$

Analyzing Figure 12(b) and Figure 12(c), one notices that the frame sets do not represent the link geometry, frames are in open space, no frames at the joints and joint displacements are merged. Table 8 and Table 9 show the well-known classic and modified DH parameters that can be determined via the frame sets \mathcal{F}^C and \mathcal{F}^M .

Augmented SU Convention. The augmented SU parameters are determined by the set of augmented frames \mathcal{F}^A . The frame poses are given in Figure 10.

$$\mathcal{F}^A = \{F_O, F_{(1,2)_1}, F_{(1,2)_2}, F_{1,2,\hat{3}}, F_{(\hat{1},2,3)}, F_{(2,3)_2}, F_{(2,3)_3}, F_{(2,3,\hat{4})}, F_{(\hat{2},3,4)}, F_I\}. \quad (72)$$

Observing from Figure 12(d), the dense set of augmented frames \mathcal{F}^A is indeed an approximation of the geometry of the mechanism.

| (i, j) | θ | t | β | b |
|----------|----------|-------|---------|-------|
| (1, 2) | • | 2.000 | -45.000 | 2.000 |
| (2, 3) | • | 2.828 | – | – |

Table 8: Classic DH paramters.

| (i, j) | β | b | θ | t |
|----------|---------|-------|----------|-------|
| (1, 2) | – | – | • | 2.000 |
| (2, 3) | -45.000 | 2.000 | • | 2.828 |

Table 9: Modified DH paramters.

| Index | Joint J_{ij} | Joint J_{jk} | Twist $\bar{\mathbb{S}}_{\mathbf{d}_{(ij)}}$ | | Twist $\mathbb{S}_{\mathbf{c}_{(ijk)}}$ | | Twist $\mathbb{S}_{\mathbf{b}_{(ijk)}}$ | | Twist $\mathbb{S}_{\mathbf{a}_{(ijk)}}$ | |
|-------|----------------|----------------|--|-----|---|-------|---|-------|---|-------|
| | (i, j) | (j, k) | δ | d | γ | c | β | b | α | a |
| 1 | $(--, 1)$ | $(1, 2)$ | - | - | - | 0.500 | - | - | - | 0.500 |
| 2 | $(1, 2)$ | $(2, 3)$ | • | - | - | 1.000 | -45.000 | 2.000 | - | 1.414 |
| 3 | $(2, 3)$ | $(3, --)$ | • | - | - | 0.707 | - | - | - | 0.707 |

Table 10: Augmented Sheth-Uicker parameters; the two columns of twist $\bar{\mathbb{S}}_{\mathbf{d}_{(ij)}}$ represent the variable configuration vector \mathbf{q} , the last six columns represent the vector of design parameters \mathbf{d} .

Now, the two-frame convention was augmented in such a manner that a representation by a parameter set is possible. The augmented SU parameters that are determined by the frame set \mathcal{F}^A are depicted in Table 10. (Note: Compare these results to Table 3.)

Conversion from Augmented SU to Minimal DH Parameters. Here we give an example for application of *convention conversions* that are possible with the augmented SU convention, as described in Section 4.4. In particular, we show the set of classic and modified parameters again, but in a slightly different notation, since these parameters were automatically derived from the set of augmented SU parameters (previous Table 10). Briefly, the method to derive these can be described as the action to “filter” the frames or to “accumulate” the displacements of a subchain. If this is conducted appropriately, the following two tables are derived.

| (i, j) | θ | t | β | b | (i, j) | β | b | θ | t | |
|---------------------|---------------------|-----|---------|---------|---------------------|---------------------|-------------------|----------|-------|-------|
| $(\check{0}, 1, 2)$ | $(\hat{0}, 1, 2)$ | - | 0.500 | - | $(0, 1, \check{2})$ | $(0, 1, \hat{2})$ | - | - | 0.500 | |
| $(\hat{0}, 1, 2)$ | $(\hat{1}, 2, 3)$ | • | 1.500 | -45.000 | 2.000 | $(0, 1, \hat{2})$ | $(1, 2, \hat{3})$ | - | • | 1.500 |
| $(\hat{1}, 2, 3)$ | $(\hat{2}, 3, 4)$ | • | 2.121 | - | $(1, 2, \hat{3})$ | $(2, 3, \hat{4})$ | -45.000 | 2.000 | • | 2.121 |
| $(\hat{2}, 3, 4)$ | $(\check{2}, 3, 4)$ | - | 0.707 | - | $(2, 3, \hat{4})$ | $(2, 3, \check{4})$ | - | - | - | 0.707 |

Table 11: Re-classified DH parameters.

Table 12: Re-modified DH parameters.

Table 11 and Table 12 contain the same information as the previous Tables 8 and 9 but in a slightly *exploded* form.

Conversion from Augmented SU to Yang’s Parameters. In Section 4.5, Yang’s modeling convention was characterized as that convention that uses a minimal amount of screw displacements. Once the augmented convention is computed, it is also possible to ‘filter’ to this convention. For the given example, this results in three twists whose parameters are depicted in Table 13.

| ν | n | β | b | μ | m |
|-------|-------|---------|---------|-------|-------|
| • | 2.000 | 2.000 | -45.000 | • | 4.828 |

Table 13: Yang’s Parameters.

6 Comparisons

This section consists of two parts: In the first (Section 6.1), Sheth-Uicker is compared as a kinematic convention. In the second (Section 6.2), Sheth-Uicker is compared as a displacement representation.

6.1 Sheth-Uicker as a Kinematic Convention

To compare Sheth-Uicker as a kinematic convention, in Section 6.1.1, a *geometric* comparison is conducted. Then, in Section 6.1.2, the *combinatorial* comparison of Section 4.1 is continued by relating to graph concepts. A comparison of *features* and *applications* is drawn at last, in Section 6.1.3.

6.1.1 Screw, Planar, and Spatial Displacements

Table 14 compares different kinds of displacement that can be expressed via one, two, and three finite screw displacements. Combining one aligned screw with another one that moves in an orthogonal direction increases the space of displacements that can be described. Since classic and modified DH parameters can be deconstructed into two orthogonal screws, this is a comparison against classic and modified DH conventions. If the z -axes of the two frames are not co-planar (in case of coincident, intersecting, or parallel lines), the displacement can not be described with two aligned screws.

| Symbol | Displacement | One Finite Twist | Two Finite Twists | Three Finite Twists |
|--------|-------------------------|------------------|-------------------|---------------------|
| | Coincident Z -lines | ✓ | ✓ | ✓ |
| | Parallel Z -lines | – | ✓ | ✓ |
| | Intersecting Z -lines | – | ✓ | ✓ |
| | Skew Z -lines | – | – | ✓ |
| | Examples | Simple Joints | Minimal DH | Augmented SU |

Table 14: Displacements (defined by a pair of frames) that can expressed as screw displacement of *one* finite screw, as the composition of two orthogonal screws, and as the composition of three pairwise orthogonal screws.

As described, Sheth-Uicker convention is a generalization of Denavit-Hartenberg convention: it generalizes from *two-twist* description to a *three-twist* description. Therefore, *any* finite displacement $D \in SE(3)$ can be described. Thus, also displacements with a *skew* line configuration can be displayed without changing the defining frames. Note, that since the configurations of intersecting, coincident, and parallel lines are coplanar, they are realizable in \mathbb{R}^2 : Denavit-Hartenberg displacements are only able to describe displacements $D \in SE(2)$.

6.1.2 Sheth-Uicker and Parallel Mechanisms

While the link graph $\mathcal{G}^{\mathcal{L}} = (\mathcal{L}, \mathcal{J})$ does not carry Euclidean embedding, this concept can be extended seamlessly by the triple-enumerated frame sets to ‘Geometric Graphs’. If the displacement sets

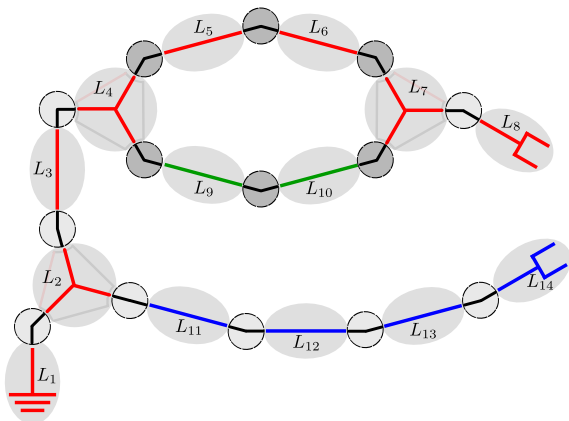
$$\mathcal{D}^* = \left\{ \overline{D}_{(ij)} \cup \underline{D}_{(ijk)}^* \quad \forall i, j, k : (J_{(ij)} \in \mathcal{J}) \wedge (J_{(jk)} \in \mathcal{J}) \right\}$$

$$\mathcal{D}^A = \left\{ \overline{D}_{(ij)} \cup \underline{D}_{\mathbf{a}_{(ijk)}} \cup \underline{D}_{\mathbf{b}_{(ijk)}} \cup \underline{D}_{\mathbf{c}_{(ijk)}} \quad \forall i, j, k : (J_{(ij)} \in \mathcal{J}) \wedge (J_{(jk)} \in \mathcal{J}) \right\}$$

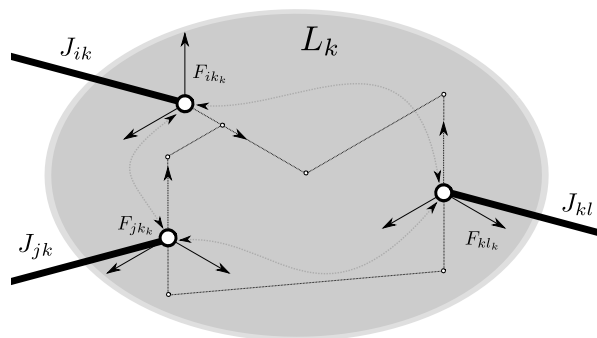
are defined, next to link graph $\mathcal{G}^{\mathcal{L}} = (\mathcal{L}, \mathcal{J})$ (see Section 2), the two-frame graph $\mathcal{G}^* = (\mathcal{F}^*, \mathcal{D}^*)$ and augmented graph $\mathcal{G}^A = (\mathcal{F}^A, \mathcal{D}^A)$ can be properly defined. All vertices and edges express poses and spatial displacements between them. Thus, these graphs can be called *Special Euclidean Graphs*. Here is a table:

| Graph | \mathcal{G} | $\mathcal{G}^{\mathcal{L}}$ | \mathcal{G}^* | \mathcal{G}^A |
|------------|---------------|-----------------------------|-----------------|-----------------|
| Vertex Set | \mathcal{V} | \mathcal{L} | \mathcal{F}^* | \mathcal{F}^A |
| Edge Set | \mathcal{E} | \mathcal{J} | \mathcal{D}^* | \mathcal{D}^A |

Table 15: Three graphs for a mechanism (type) \mathcal{M} and its Euclidean realization $\underline{\mathcal{M}}$.



(a) A schematic drawing of an example mechanism that is neither a kinematic chain (it features two end-effectors, at link L_8 and L_{14}), nor a kinematic tree (it features a kinematic loop, indicated by joint colors). The style of drawing indicates the link graph $\mathcal{G}_{\mathcal{L}} = (\mathcal{L}, \mathcal{J})$. The links are enumerated according to a spanning tree of this graph, also they are partitioned (colored) into three chain-sets that appear in the depth-first sorting of the tree. These link-chains are defined via the root link L_1 , the branching links, L_2, L_4, L_7 , and the end-effector links L_8, L_{14} .



(b) A schematic drawing of the combinatorics of links, joints, and frames for a case of a link L_k with three adjacent joints connecting to links L_i, L_j, L_l . Three sets of vertices $\mathcal{V}^{\mathcal{L}}, \mathcal{V}^*,$ and \mathcal{V}^A can be identified by three different round types of elements. The principle of the augmented DH convention for decomposing a displacement (dashed arrows) between each pair of joint frames via a set of three orthogonal twists (dotted arrows) is illustrated. This situation appears for all branching links L_2, L_4, L_7 of Figure 13(a).

Together, these graphs feature a hierarchy relationship (see also Figure 13(b)). By construction, the combinatorics of the three graphs remain similar: \mathcal{G}^* can be constructed ‘straightforward’ from $\mathcal{G}^{\mathcal{L}}$ via substitution of vertices by $|\mathcal{V}_L^*| = 2 \cdot |\mathcal{J}_L|$ sub-vertices and the edge set of the complete graph $K_{|\mathcal{J}_L|}$ (sub-edges) in between. The augmented graph \mathcal{G}^A can be constructed from two-frame graph \mathcal{G}^* via substitution of the sub-edges by a chain of three sub-sub-edges and two sub-sub-vertices. Then one link-vertex L in $\mathcal{G}^{\mathcal{L}}$ corresponds to $|\mathcal{V}_L^A| = |\mathcal{J}_L| + 2 \cdot \binom{|\mathcal{J}_L|}{2} = |\mathcal{J}_L|^2$ vertices in \mathcal{G}^A . The argumentation also holds in the opposite direction: first, the two-frame graph \mathcal{G}^* can be achieved from augmented graph \mathcal{G}^A by contracting all suitable three-chains of edges $e^A \in \mathcal{E}^A$ (concatenation of three twist displacements) ‘inside’ the links to one edge $\mathcal{E}^* \ni e^* = D_{ijk}^* \in \mathcal{D}^*$ (link displacement) – \mathcal{G}^* is called a minor of \mathcal{G}^A . Second, link graph $\mathcal{G}^{\mathcal{L}}$ can be achieved from two-frame graph \mathcal{G}^* by contracting of all edges ‘inside’ $e^* \in \mathcal{E}^*$ the links (link displacement) such that the ‘abstract’ link $\mathcal{V}^{\mathcal{L}} \ni v^{\mathcal{L}} = L \in \mathcal{L}$ ‘itself’ remains. Thus, $\mathcal{G}^{\mathcal{L}}$ is a minor of \mathcal{G}^* .

This is especially noteworthy since the concept of edge contraction and minor graphs, resp., can also be used for expressing a kinematic loop by a complex joint, as introduced in Section 2.1 (an implementation by means of the the two-frame convention is described in [5]): in particular, a subset of joints (edges of the link graph) that builds a kinematic loop is contracted into one super-edge which represents the corresponding complex joint.

6.1.3 Applications for Sheth-Uicker and Denavit-Hartenberg

In Table 16, an overall comparison for the four covered conventions is drawn. The feature *handling of branchings* is a direct consequence of the feature that the atomic displacements in the two-frame convention and in the augmented convention are clearly separated into link displacements and joint displacements. Handling of branchings, and thus the handling of parallel mechanism is explained in Section 6.1.2 above. The feature of properly handling skew lines is illustrated with an example in Section 5. The ability of the minimal DH conventions to serve as a normal representation for planar displacements $D \in SE(2)$ is only partially valid as explained in Section 6.1.1. The table partially anticipates results from the following Section 6.2. In particular, the ability of the augmented Sheth-Uicker’s convention to serve as a normal representation for spatial displacements $D \in SE(3)$ is explained in Section 6.2.1.

| Kinematic Modeling Convention | | Classic Denavit-Hartenberg | Modified \mathcal{F}^M | Two-Frame Sheth-Uicker | Augmented \mathcal{F}^A |
|-------------------------------|--|--|-----------------------------|--|--|
| (C) | Link Covering Frame Set | \mathcal{F}^C | \mathcal{F}^M | \mathcal{F}^* | \mathcal{F}^A |
| | Frames per Link $ \mathcal{F}_L $ | 1 | 1 | $2 \cdot \mathcal{J}_L $ | $4 \cdot \mathcal{J}_L $ |
| | Number of Parameters | 4 | 4 | (12) | 6 (+2) |
| (P) | Description via | 2 axial twists | | (matrices) | 3 (+1) axial twists |
| | Representable Line Pairs | coincident, parallel, intersecting | | coincident, parallel, intersecting, skew | coincident, parallel, intersecting, skew |
| | Representation of Atomic Displacements | planar* displacements $D \in SE(2)$ accumulated L - J - L displacements | | spatial* displacements $D \in SE(3)$ | separated link and joint displacements |
| (A) | Freely Assignable Zero Posture | – | – | ✓ | ✓ |
| | Preserving Joint Frames | – | – | (✓) | ✓ |
| | Simple Handling of Branchings | – | – | (✓) | ✓ |
| | Simple Handling of Skew Lines | – | – | (✓) | ✓ |
| | Geometry-Reflecting Parameters | – | – | – | ✓ |

Table 16: Comparison of combinatoric (C), principal (P), and application-relevant (A) properties of the four kinematic conventions. *Sheth-Uicker parameters are not only capable of displaying spatial, but also planar displacements. In the planar case, at least one parameter of the X' -twist simplifies to zero (see Table 3). Also in this case, as indicated in the following Section 6.2.1, the additional third twist in Sheth-Uicker’s convention allows reflecting the geometry of a planar displacement better, compared to the two twists used in Denavit-Hartenberg’s convention. While Sheth-Uicker conventions permit the convenient treatment of branchings and skew line geometries, this is not possible by means of the minimal DH conventions without further ado, concretely without moving one of the two frames such the displacement becomes planar. This does not only hold for spatial, but also for planar mechanisms, see Section 6.2.1.

6.2 Sheth-Uicker as a Representation for Displacements

In this section, the Sheth-Uicker and the Dual Euler Angles representation, resp., are compared to the Finite Twist representation. First, in Section 6.2.1 this is conducted for planar displacements $D \in SE(2)$, then, in Section 6.2.2 for spatial displacements $D \in SE(3)$. It turns out that studying the spatial setting has a lot of parallels to the planar, in particular, a spatial setting can be ‘planarized’ via orthogonal decomposition of the translation (see Equation 30).

6.2.1 Planar Displacements

Theorem 3 (Rotation Pole) “Every planar displacement $D \in SE(2)$ is a rotation about a point (rotation pole) P in the projective plane.”

The Rotation Pole Theorem is the planar version of the more general Theorem 2. A proof can be found, e.g., in [29, Theorem 2.4]. In case of pure translations, the pole lies at infinity. In the ‘finite case’, the location of the pole can be constructed by intersecting bisectors of line segments between homologous²⁸ points (another way of constructing the location of the pole works via the radius \mathbf{r} and is described below, in Section 6.2.2). The value of the rotation around the rotation pole P equals the value of rotation of the displacement without the translation. The rotation pole is not the only point where the rotation value is preserved: the rotation pole is located on a circle that preserves this rotation value. This is characterized by the following *Theorem of Inscribed Angles* which is a generalization of the *Theorem of Thales*.

Theorem 4 (Inscribed Angles) Let C' be a circle with center point M' and radius r' . Let A and B be the intersection points of a secant c with the circle C' . Then, the angle γ is constant for any triangle ABC with C any third point on C' . In particular, the angle γ equals $\frac{1}{2} \cdot \mu$ where μ is the ‘central angle’ at point M' in triangle ABM' .

PROOF The equation $\gamma = \frac{1}{2} \cdot \mu$ is combined from the equations $\gamma = \beta'' - \alpha''$ and $\mu = \beta' - \alpha'$ together with the relations $\alpha'' = \frac{1}{2} \cdot \alpha'$ and $\beta'' = \frac{1}{2} \cdot \beta'$. The latter follow from triangle sums $2 \cdot \alpha'' + (\pi - \alpha') = \pi$ and $2 \cdot \beta'' + (\pi - \beta') = \pi$.

The idea of the proof is shown in Figure 15 which is a rotated version of Figure 13 so that position of the pole (named as C) is located at $(-1, 0)^T$. Then, the idea is to apply the arguments about half-angles

²⁸in the sense of ‘corresponding’, used as in [57].

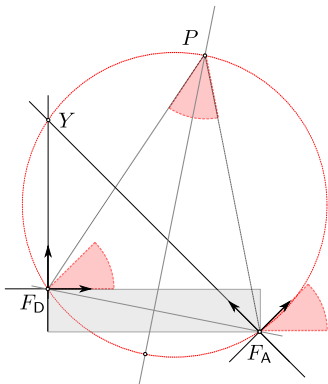


Figure 13: The rotation pole P lies in the intersection of the *isometric circle* and the perpendicular bisector of the planar translation vector. While the bisector is entirely determined by translation t_0 , the circle is determined as that circle passing F_D and F_A which preserves rotation angle ϕ .

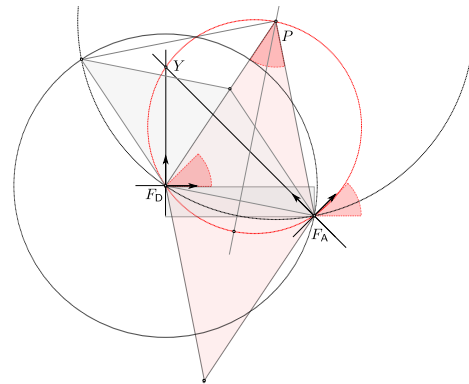


Figure 14: The radius r lies on the diagonal of a dual rhombus that is made by the location of F_D that is P_D , location of F_A that is $P_A = D_0 \circ P_D$, rotation pole P and the location $D_0^{-1} \circ P_D$.

twice (for the half-angle parametrization, see e.g., [1]). The notation in Theorem 4 was chosen so that for the radius of the screw $r = \|\mathbf{r}\|$ it holds that $r = 2 \cdot r'$, for the twist angle ϕ it holds that $\phi = \gamma = \frac{1}{2} \cdot \mu$ (see Figure 14).

Isometric Circle. The circle which the rotation pole is located on has a constant angle and in particular this angle equals the angle of the rotation of the displacement. Because of that it is here called *isometric circle*. It can be characterized to be the circle of intersection points of homologous axes.²⁹

Sheth-Uicker and Denavit-Hartenberg. The sketch in Figure 16 is a rotated and extended version of Figure 13. It depicts the same planar displacement, z -axes and x -axes are in the plane, the y -axes of the frames were chosen to be orthogonal to the plane. A direct interpretation of the sketch as a planar *link displacement* according to the two-frame convention is only possible if the frames F_D and F_A indicate locations of *slider joints*. Figure 16 shows the points Y , M and H that correspond to SU, DH conventions.

One can observe that the Sheth-Uicker point Y also lies on that circle since the z -axes are homologous axes. Therefore, the angle β between z_D and z_A equals the angle ϕ that is taken at the pole. The classic Denavit-Hartenberg point H and the modified Denavit-Hartenberg point M do *not* lie on that circle. Because of this property, it is concluded that while the two conventions – augmented Sheth-Uicker and minimal DH – are *combinatorically equivalent* for planar displacements, the SU-convention ‘specializes better to $SE(2)$ ’ and provides a geometrically *more concise* representation of planar displacements $D \in SE(2)$ than Denavit-Hartenberg.

In the interpretation of the planar displacement as a link displacement, for the case of two *rotative* joints, both joint axes would be orthogonal to the plane. For this case, in case of parallel joint axes, DH and SU conventions are equivalent. In case of *one rotative* and *one planar* joint, while the mechanism is planar, the link displacement is not planar in the sense of Theorem 3: it is not representable as an affine rotation in the plane. In this case, the joint axes are skew such that the DH is *not* able to represent that displacement without moving one of the two frames on its joint axis.

6.2.2 Spatial Displacements

A Spatial Perspective. In Figure 17, three-dimensional visualizations of a finite displacement together with the ‘discrete’ Sheth-Uicker approximation and the ‘continuous’ Finite Twist approximation are provided. In Figure 17(a), the line segments of the three axial twists are drawn, in Figure 17(b) the affine twist is drawn as a segment of the ‘trajectory’ of a certain screw (see Characterization (I)).

²⁹Homologous axes are defined in accordance with homologous points: If two homologous points P_D and P_A are chosen, then the lines $D-P_D$ and $A-P_A$ passing from the two origins D and A through the points P_D and P_A are homologous.

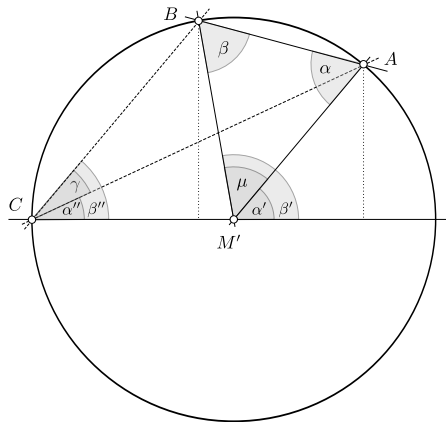


Figure 15: Sketch for proving the theorem of inscribed angles. The equality $\gamma = \frac{1}{2} \cdot \mu$ can be deduced from a twofold application of the half-angle parametrization.

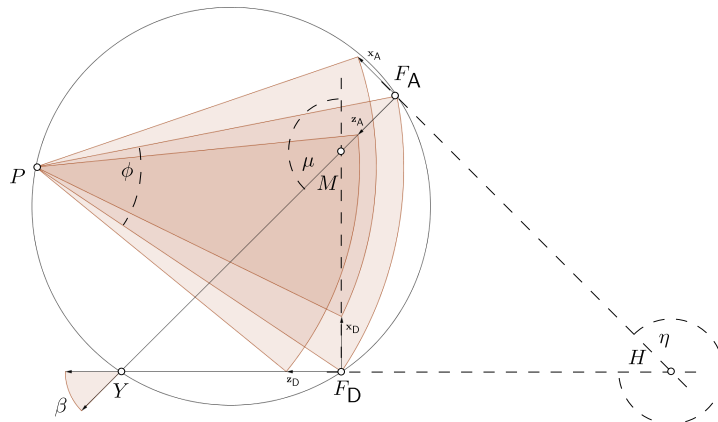


Figure 16: A planar displacement D defined by two frames F_D and F_A , $D = F_D^{-1} \circ F_A$. The equivalent rotation about pole P is illustrated by a set of three sectors of circles. The point Y is the point that corresponds to the location of frames F_C and F_B . The point H for the classic DH convention is located at the intersection of z and x'' . The analogous point M for the modified DH convention is located at the intersection of x and z'' .

Combinatoric Equivalent Decompositions

Two Simplified Perspectives. Two perspectives on the two decompositions are shown in Figure 18. In Figure 18(a), the view is aligned along the screw axis; in this case, the common orthogonal appears ‘oblique’. In Figure 18(b), the view is aligned perpendicular to the common orthogonal; in this case, the axis of finite twist appears ‘oblique’. The two decompositions of the displacement are *complementary*.

A Twist Decomposition. To compare the two descriptions in more detail, a *decomposition* of the Finite Twist representation in the same manner³⁰ as for Sheth-Uicker description is conducted below. Again, the *key ingredient* of the decomposition of Sheth-Uicker is the definition of two augmenting frames. In this case, they are named F_T and F_R and computed as in Method VI.

Method VI. DT – Decomposed Twist.

- (In) Frames F_D and F_A that define a displacement.
- (Out) Augmenting Frames F_T and F_R in the intersection of screw axis and orthogonal planes which contain \mathbf{p}_D and \mathbf{p}_A .
- (S) The twist axis S_0 is computed (via Method I)
- (p) The locations of F_T and F_R are computed as projections of the location points \mathbf{p}_D and \mathbf{p}_A onto the screw axis: $\mathbf{p}_T = \Pi_{S_0}(\mathbf{p}_D)$ and $\mathbf{p}_R = \Pi_{S_0}(\mathbf{p}_A)$.
- (R) The orientation of F_T is set identical to the orientation of F_D . The orientation of F_S is set identical to the orientation of F_A .

The decomposition of the Sheth-Uicker representation SUD was described in Equation 62. By means of the augmenting frames F_T and F_S , the decomposition of the Finite Twist representation can, analogously, be described as

$$D = \mathcal{S}_t \circ \mathcal{S}_s \circ \mathcal{S}_r . \quad (73)$$

³⁰In this paper the Sheth-Uicker convention is introduced as an augmentation of the two-frame convention.

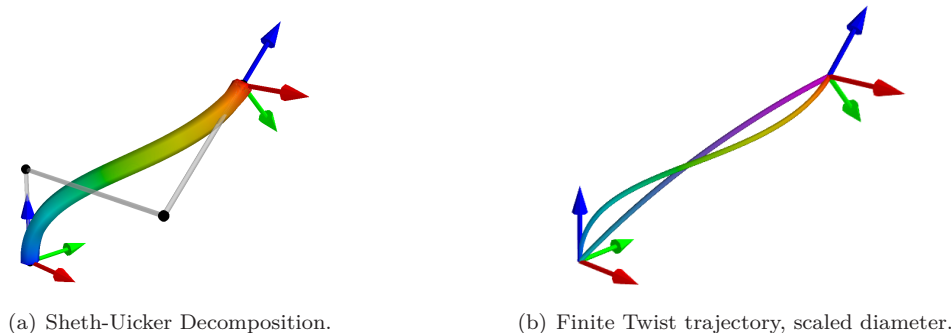


Figure 17: Visualizations of Sheth-Uicker decomposition and Finite Twist trajectory between two frames defining a spatial displacement. The displacement is identical to the link displacement of link L_2 in example of Section 5.

In this case, the general screw displacement $\$G(\phi, s)$ (see Equation 29) is decomposed into three linear screw displacements. However, in contrast to Sheth-Uicker (Equation 62), the three atomic displacements are not axial, but linear screw displacements. On the other hand, $\$t$ and $\$s$ are more special: First, they do not contain rotations. Second, the radius vector ‘is the same’³¹.

$$D = T_r^{-1} \circ \$s \circ T_r \quad (74)$$

The situation is displayed twice in Figure 18 and schematically in Figure 19.

A Spatial Triangle. Combining Equation 62 and Equation 73, the following two chains can be observed:

$$F_D \begin{cases} \xrightarrow{\$c} F_C \\ \xrightarrow{\$t} F_T \end{cases} \begin{matrix} \xrightarrow{\$b} F_B \\ \xrightarrow{\$s} F_R \end{matrix} \begin{cases} \xrightarrow{\$a} F_A \\ \xrightarrow{\$r} F_A \end{cases}$$

Computation of Angles and Radii. The spatial triangle features right angles at all frames, except for F_D and F_A . At these frames, the angle is made up between the z -axes z_D and z_A and the radius vectors r_D and r_A . If the angles are defined as

$$\psi_D = \angle(r_D, z_D) \quad \psi_A = \angle(r_A, z_A)$$

then, the inner angles ‘inside’ the triangle, compare Figure 19, are $\psi_D^\Delta = \pi - \psi_D$ and $\psi_A^\Delta = \psi_A$ such that $\psi_D^\Delta + \psi_A^\Delta = \pi$.³² To compute the angles ψ_D and ψ_A , an expression for radius vectors r_D and r_A is necessary.

One way to compute radius vector $r_D^\#$ follows from the observation that $r_D \cong v_0 \times \omega$. In particular, one can write by means of using the Lie bracket

$$r_D^\# = [v_0^\otimes, \omega^\otimes]^\oplus = (v_0^\otimes \cdot \omega^\otimes - \omega^\otimes \cdot v_0^\otimes)^\oplus, \quad (75)$$

whereby ω and v_0 can be computed by using Equation 11 and Equation 33. The radius vector $r_A^\#$ can simply be computed via $r_A^\# = R \cdot r_D^\#$. The norm of the radius r follows from triangle angle sums and the law of cosines, see Figure 13, as

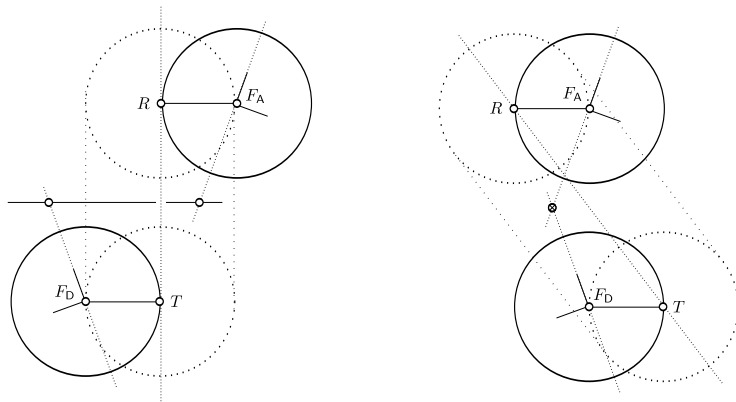
$$\|r\|^2 = \frac{\|t_0\|^2}{2 \cdot (1 - \cos \phi)}. \quad (76)$$

By studying the geometry of that sketch in Figure 14, alternative and shorter expressions for \hat{r}_D and \hat{r}_A can be deduced.

$$\hat{r}_D = R\left(\frac{3}{4}\pi - \frac{1}{2}\phi, s\right) \cdot \hat{t}_0 \quad \hat{r}_A = R\left(\frac{3}{4}\pi + \frac{1}{2}\phi, s\right) \cdot \hat{t}_0 \quad (77)$$

³¹this is described more in next paragraph

³²The angle sum equation $\psi^\Delta = \psi_D^\Delta + \psi_A^\Delta + \psi_C^\Delta + \psi_B^\Delta + \psi_T^\Delta + \psi_R^\Delta = 6\frac{\pi}{2}$ of the spatial triangle is fulfilled.



(a) The perspective is aligned along axis S_0 of the finite twist.

(b) The perspective is aligned along the common orthogonal of the Z -lines.

Figure 18: Simplified views on the decompositions of the Finite-Twist representation and of Sheth-Uicker's representation into linear twists are depicted for a displacement between two frames. The drawing of the lines was chosen to reflect the duality between the vertices and the sides of the spatial triangle which is formed by the loop of the six linear twists involved in the configuration.

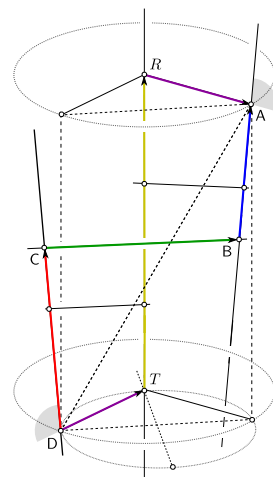


Figure 19: Simplified perspective on the spatial setting of the two decompositions including angles ψ_D and ψ_A , isometric view circle and spatial and planar translations \mathbf{t} and \mathbf{t}_0 .

Finally, with $\hat{\mathbf{r}}_D \star \mathbf{z}_D = \hat{\mathbf{r}}_A \star \mathbf{z}_A$ (see Equation 79) the angles ψ_D and ψ_A can be determined as

$$\psi_D = \angle(\mathbf{r}_D, \mathbf{z}_D) = \arccos(\hat{\mathbf{r}}_D \star \mathbf{z}_D) = \arccos(\hat{\mathbf{r}}_A \star \mathbf{z}_A) = \angle(\hat{\mathbf{r}}_A, \mathbf{z}_A) = \psi_A. \quad (78)$$

From these, the angles ψ_D^Δ and ψ_A^Δ can be determined. Thus, a full description of the spatial triangle that is built by the six displacements of the two decompositions is achieved.

Discussion. For the Sheth-Uicker Decomposition, the middle of the three screw displacements is the linear twist \mathcal{S}_b that connects the two \mathbf{z} -axes via the shortest possible route: the line of this twist \mathcal{S}_b is *in the middle* of the two Z -lines. For the other case, for the Augmented Twist Decomposition, the middle of the three screw displacements is the linear twist \mathcal{S}_s along the screw axis S_0 . This displacement also lies *in the middle* in a geometric sense: At first, the *location* of twist \mathcal{S}_s , and therefore the locations of the frames F_T and F_R , lie in the intersection of the \mathbf{r} -circles around F_D and F_A . Thus, they are equidistant to both. Following the other interpretation (see Section 6.1.1), the screw axis lies at the intersection of isometric view circle and the perpendicular bisector of the planar translation vector \mathbf{t}_0 . In this interpretation, too, the frames F_T and F_R are located at the same distance to \mathbf{p}_D and \mathbf{p}_A . Furthermore, regarding the *direction* $\hat{\omega}$ of the twist, one can deduce from Equation 11 that for $\hat{\omega}$ the following equations hold

$$\hat{\omega} \star \mathbf{z}_D = \hat{\omega} \star \mathbf{z}_A \quad \hat{\omega} \star \mathbf{x}_D = \hat{\omega} \star \mathbf{x}_A \quad \hat{\omega} \star \mathbf{y}_D = \hat{\omega} \star \mathbf{y}_A. \quad (79)$$

This indicates, that also the *direction* $\hat{\omega}$ of the twist lies equidistant to the orientation of F_D and F_A . Concluding, the geometric constructions (see Figure 18) of the two decompositions can be described as

$$\begin{aligned} \text{Sheth-Uicker Decomposition} &: \mathbf{z}\text{-axes of } F_D \text{ and } F_A &\rightarrow \text{Common perpendicular} \\ \text{Finite-Twist Decomposition} &: \mathbf{r}\text{-circles around } F_D \text{ and } F_A &\rightarrow \text{Common intersection} \end{aligned} \quad (80)$$

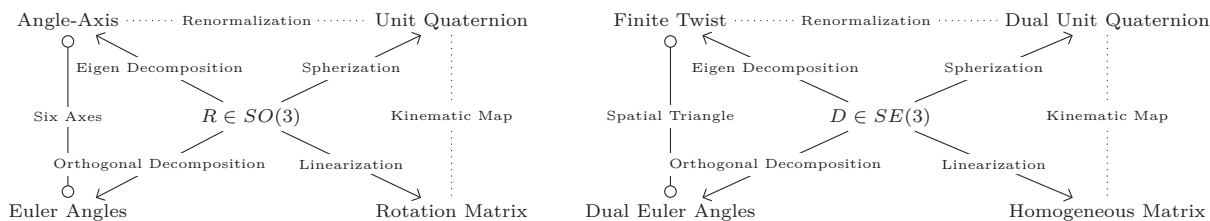
Reasoning about this analogy, one deduces two following statements: Firstly, the parameters of the one-affine-twist representation contain the ‘actual’ amount of rotation (ϕ) and the ‘actual’ rotation (shift s). And secondly, the parameters of Sheth-Uicker's three-linear-twists representation accurately reflect the original parameters, since they use a basis that is as similar, as possible. These findings lead to the following reformulation of the construction principles of the decompositions:

$$\begin{aligned} \text{Sheth-Uicker Decomposition} &: \text{Successive-orthogonal basis } \textit{preserving} \text{ the dominant axes.} \\ \text{Finite-Twist Decomposition} &: \text{Successive-orthogonal basis } \textit{equidistant} \text{ to poses of frames.} \end{aligned} \quad (81)$$

For this, Table 17 provides a comprehensive overview.

| Convention | Sheth-Uicker | Finite Twist |
|------------------------|--------------------------------|------------------------------|
| Characterization | Three-linear-twist description | One-affine-twist description |
| Interpretation | Linear-discrete | Affine-continuous |
| Basis | Preserving z -axes | Frame-symmetric screw axis |
| Parameters | Speaking / dominant | Absolute / essential |
| Related Decompositions | Orthogonal Decomposition | Eigen Decomposition |
| Advantages | Readability, Speed | Symmetry, Algebra |

Table 17: Sheth-Uicker and Finite Twist representation and their decompositions in comparison.

Figure 20: Four representations of a finite spatial rotation $R \in SO(3)$ and some interrelations.Figure 21: Four representations of a finite spatial displacement $D \in SE(3)$ and some interrelations.

6.2.3 Principles of Sheth-Uicker and Finite Twist Decompositions

Counterparts in $SO(3)$. In Section 3.2.1, the Angle-Axis representation for a rotation $R \in SO(3)$ is introduced, in Section 3.4.1 its Euler Angles representation. In summary, one can state that both conventions – the affine-one-twist and the linear-three-twist description – generalize from $SO(3)$ to $SE(3)$.

Counterparts in $SE(2)$. Also, the representation of an element in $SE(3)$ via a finite twist has a counterpart-representation in $SE(2)$: in particular, this is the *rotation pole* (see Theorem 3 and Figure 16). In Section 6.1.1, it is also shown that Sheth-Uicker holds nicely for $D \in SE(2)$ (since Y lies on the circle). In summary, one can state that both conventions – the affine-one-screw and the linear-three-screw descriptions – generalize from $SE(2)$ to $SE(3)$.

Counterparts in $GL(n)$. In previous Section 6.2.2, it was demonstrated that both, Sheth-Uicker and Finite Twist, can be understood as complementary decompositions into three linear, successive-orthogonal screw displacements. In particular, in Equation 6.2.3, the constructions were formulated with respect to some *bases*. If this is formulated in a more constructive manner, the following two principles can be observed:

- Sheth-Uicker Decomposition* : Iteratively *project* the displacement into the space of *orthogonal complements* starting from the dominant axes of the frames.
- Finite-Twist Decomposition* : Formulate the displacement as being *similar* to a linear-screw displacement along the linear *frame-equidistant* twist.

These two principles also occur in a similar manner for $GL(n)$ for well-known matrix decompositions: in particular, the Orthogonal and the Eigen Decomposition of a matrix: Thus, the Sheth-Uicker representation provides a decomposition that is describable as a (symmetrized) Orthogonal Decomposition of a displacement, thus comparable to a QR -Factorization of a matrix. And the one-twist representation provides a decomposition that is comparable to an QDQ^{-1} -Factorization of a matrix. These findings are compared and summarized in Table 22.

Conclusion. As stated in the last three paragraphs, Sheth-Uicker and Finite Twist decompositions have counterparts in $SO(3)$, in $SE(2)$ as well as in $GL(n)$. This is summarized in Diagram 23.

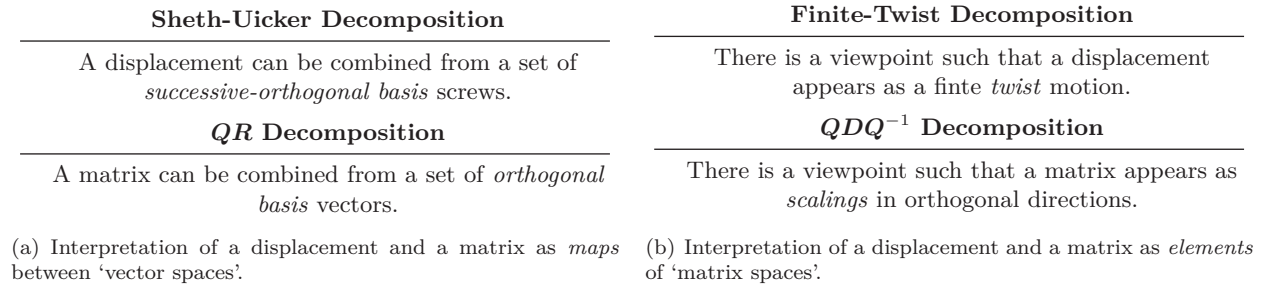


Figure 22: Analogies of decompositions for a displacement and for a matrix.

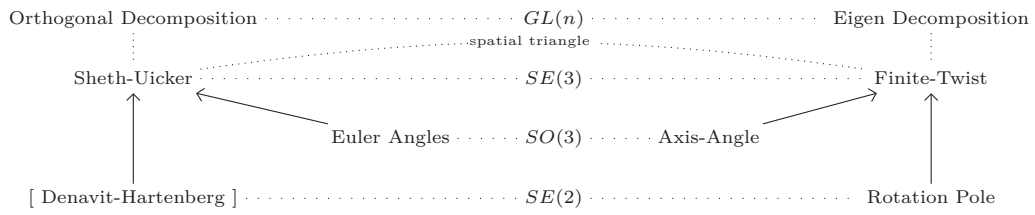


Figure 23: Connections of Sheth-Uicker's and the Finite Twist Representation for Finite Displacements.

7 Conclusion

In this survey, the convention by Sheth and Uicker from 1971 was reviewed from two different perspectives. In the first perspective, Sheth-Uicker was regarded as a convention for kinematic modeling: it was compared to three other conventions in the ‘unified notation of frames’. As explained in the first section, conventions for kinematic modeling have to deal with a ‘trade-off’ between compactness on the one hand, and generality and intuitiveness on the other hand. It was shown how the two-axial-twist description of Denavit-Hartenberg is extended to a three-axial-twist description by the Sheth-Uicker convention such that a mechanism can be described by a table that reflects the *geometry* of adjacent joint axes and that has a structure that reflects the *topology* of the mechanism type.

In particular, by the worked-out example, it was demonstrated that SU is not only useful for kinematic loops, but also for chains that feature skew geometries of joint axes. Therefore, the Sheth-Uicker convention generalizes Denavit-Hartenberg to the right amount, in the sense that it allows to cover the complexity of any mechanism with one simple convention. Finally, it was derived that Sheth-Uicker is a representation with respect to a basis that preserves the ‘dominant’ joint axes: therefore, the parameters of Sheth-Uicker provide direct insight into the geometries of the links. In summary, Sheth-Uicker’s convention is not minimal, but general and intuitive: therefore, it is optimally suited to specify the kinematics of mechanism in form of tables. The question of efficient implementations (of displacement representations) and of kinematic conventions was not covered in this article. However, it was demonstrated how Sheth-Uicker’s convention can be ‘thinned out’ in several ways to increase redundancy for efficient subsequent computation purposes.

In the second perspective, Sheth-Uicker was identified as the Dual Euler Angles representation of displacements of the two-frame convention. It was worked out in a comparison that Sheth-Uicker and Finite-Twist can be regarded as complementary decompositions, and together form a certain spatial triangle. Additionally, it was demonstrated that similar principles of both conventions can be found in more special, and in more general groups. In addition to these comparisons, the interconnections between four displacement representations were reviewed: in particular, a ‘geometric outline’ of screw theory for finite displacements was provided in this survey. Dual quaternions were motivated as the ‘algebra-ized counterpart’ of screw theory. In summary, it was shown how the Dual Euler Angle representation, and thus Sheth-Uicker’s convention, is embedded among other theoretically-solid displacement representations.

We hope that the practical and theoretical preferences of Sheth and Uicker’s convention have been explained in an coherent manner so that more people appreciate its usage. For further illustration, in future, it might be worthwhile to compile specification tables according to Sheth-Uicker’s convention of a set of mechanisms which are of the same type but feature different geometries: for example, the Sheth-Uicker tables for different Bennett mechanisms feature the same shape but different contents – depending on the set of design parameters that describe their planar, spherical, or spatial realization.

A promising direction for continuing the work about kinematic conventions could be the study of connections between Sheth-Uicker’s kinematic convention and sets of algebraic equations, as, e.g., developed by Porta et al. (see [37, 38]), and, in particular, the development of automated derivations of these equations from mechanism specifications.

The author would like to thank Prof. John Uicker and Prof. Hans-Peter Schröcker for valuable remarks on a draft version of this document.

The research presented in this report was funded by the German Ministry of Education and Research (BMBF) within the projects VI-BOT (Grant Number 01-IW-07003) and CAPIO (Grant Number 01-IW-10001).

Appendix

A Homogeneous Coordinates

Homogeneous Point Coordinates. If $\mathbf{x} = (x_1, x_2, \dots, x_d)^T$ is a point in \mathbb{R}^d , its standard homogenization is a point in \mathbb{R}^{d+1} that contains the the same d coordinates and an additional coordinate which equals one. In the most popular way, the additional coordinate is appended from back to the vector as the $(d + 1)$ -st coordinate (as done in the document). Equivalently, in the second-most popular way, the additional coordinate is appended from front as the 0-th coordinate. Then, the homogenized vector looks like the following,

$$\mathbf{v} = (1, v_1, v_2, \dots, v_d). \quad (82)$$

This has the advantage that point homogenization and line homogenization are compatible. For homogenized elements, equivalence classes can be defined - in this case, as

$$[\mathbf{v}] := \{ \mathbf{v}' \in \mathbb{R}^d : \mathbf{v}' = \lambda \cdot \mathbf{v}, \lambda \in \mathbb{R} \}. \quad (83)$$

The set of all such equivalence classes can be denoted as (see [41])

$$\mathbb{RP}^3 = \frac{\mathbb{R}^4 \setminus \{\mathbf{0}\}}{\mathbb{R} \setminus \{0\}}. \quad (84)$$

Homogeneous Line Coordinates. In Section 3.2.2 homogeneous line coordinates, the Plücker coordinates, were introduced. The two concepts of homogenization are opposed in the following tables.

| Entity | Formula |
|-------------------|---|
| Point | $\mathbf{a} \in \mathbb{R}^3$ |
| Homogeneous point | $\mathbf{a} = (1, \mathbf{a}) \in \mathbb{R}^4$ |
| Equivalence class | $[\mathbf{a}] \in \mathbb{RP}^3 \cong \mathbb{R}^4$ |
| Representative | $\hat{\mathbf{a}} = (1, \mathbf{a}) \in \mathbb{R}^4$ |

Table 18: Homogeneous coordinates for points, *the* representative of a point equivalence class is the point with *one* as additional coordinate.

| Entity | Formula |
|------------------------|--|
| Two points | $\mathbf{a}, \mathbf{b} \in \mathbb{R}^3$ |
| Two homogeneous points | $\mathbf{a}, \mathbf{b} \in \mathbb{R}^4$ |
| Equivalence class | $\mathbf{g} = [\mathbf{g}, \bar{\mathbf{g}}] \in \mathbb{RP}^5 \cong \mathbb{R}^6$ |
| Representative | $\hat{\mathbf{g}} = (\hat{\mathbf{g}}, \hat{\bar{\mathbf{g}}}) \in \mathbb{R}^6$ |

Table 19: Homogeneous coordinates for lines, *the* representative of a line equivalence class is the line with *normalized* plücker coordinats.

B Vectors and Matrices

B.1 Matrixfication and Vectorization

In this paragraph, the definitions of the operators $(\cdot)^\otimes$ $(\cdot)^\oplus$ are provided.³³ An ‘encircled cross’ \otimes in the superindex of a vector \mathbf{v} is a function that lifts the vector into the space of skew symmetric matrices. For short, the cross can also be written as an accent.

$$(\cdot)^\otimes : \mathbb{R}^3 \rightarrow se(3) \quad \boldsymbol{\omega} \mapsto \boldsymbol{\omega}^\otimes = \hat{\boldsymbol{\omega}} \quad (85)$$

An ‘encircled plus’ \oplus in the superindex of a skew-symmetric matrix \mathbf{S} is a function that extracts the direction of the the orthogonal axis. For short, the plus can also be written as an accent.

$$(\cdot)^\oplus : se(3) \rightarrow \mathbb{R}^3 \quad \mathbf{S} \mapsto \mathbf{S}^\oplus = \hat{\mathbf{S}} \quad (86)$$

The concrete definition of the skewing operation $(\cdot)^\otimes$ reads like

$$\boldsymbol{\omega} = (\omega_1, \omega_2, \omega_3)^T \quad \mapsto \quad \mathbf{S} = \hat{\boldsymbol{\omega}} = \begin{pmatrix} 0 & -\omega_3 & \omega_2 \\ \omega_3 & 0 & -\omega_1 \\ -\omega_2 & \omega_1 & 0 \end{pmatrix}. \quad (87)$$

³³The notation for this is adapted from [31]. However, in this text, a ‘hat’ is reserved for normalization and therefore a ‘cross’ and a ‘plus’ are used for matrixfication and vectorization.

The concrete definition of the axing operation $(\cdot)^\oplus$ reads like

$$\mathbf{S} = \begin{pmatrix} 0 & -S_{12} & -S_{13} \\ S_{12} & 0 & -S_{23} \\ S_{13} & S_{23} & 0 \end{pmatrix} \mapsto \boldsymbol{\omega} = \mathbf{S}^\oplus = (S_{23}, S_{13}, S_{12})^T. \quad (88)$$

B.2 Exponential and Logarithmic Function for Rotation Matrices

Let $\hat{\boldsymbol{\omega}}$ denote the unit vector along the rotation axis, $\hat{\boldsymbol{\omega}}^\otimes$ the corresponding skew-symmetric matrix (see last paragraph), and ϕ the *magnitude* (i.e., angle) of the rotation. The rotation matrix \mathbf{R} is computed as

$$\mathbf{R} = \mathbf{R}(\phi) = \exp(\phi \cdot \hat{\boldsymbol{\omega}}^\otimes). \quad (89)$$

The expression $\exp(\phi \cdot \hat{\boldsymbol{\omega}}^\otimes)$ can be computed by the well-known *Rodrigues formula*³⁴

$$\exp(\phi \cdot \hat{\boldsymbol{\omega}}^\otimes) = \mathbf{I} + \sin \phi \cdot \hat{\boldsymbol{\omega}}^\otimes + (1 - \cos \phi) \cdot (\hat{\boldsymbol{\omega}}^\otimes)^2. \quad (90)$$

In the other direction, given a rotation matrix \mathbf{R} , the rotation angle ϕ can be determined as $\phi = \arccos\left(\frac{\text{tr}(\mathbf{R})-1}{2}\right)$ and the unit vector along the rotation axis $\hat{\boldsymbol{\omega}}$ is determined via $\hat{\boldsymbol{\omega}}^\otimes = \frac{1}{2 \cdot \sin \phi} \cdot (\mathbf{R} - \mathbf{R}^T)$, see Equation 12 and Equation 11. Instead of using these explicit formulas, the angle-axis representation can also be derived via inverting the relation of Equation 89, as

$$\ln(\mathbf{R}) = \phi \cdot \hat{\boldsymbol{\omega}}^\otimes = \frac{\phi}{2 \cdot \sin \phi} \cdot (\mathbf{R} - \mathbf{R}^T). \quad (91)$$

For the computation of the logarithmic function for rotation matrices, see [52, Sec. 7], [31, Sec. 2.18] and [17].

Summarizing the last two paragraphs, one can state:

“The vectorial representation $(\phi, \hat{\boldsymbol{\omega}}) \cong \phi \cdot \hat{\boldsymbol{\omega}}^\otimes$ and the linear representation \mathbf{R} of a rotation are connected via the exponential and the logarithmic map.”

The exponential function and the logarithmic function are not only defined for the angle-axis representations of rotations but also for quaternions, see e.g., [19, chap. 18]. Also, the functions are defined for general, affine case of spatial displacements, see e.g., [31, Sec. 3.2].

³⁴See [31, Sec. 2.2.] for a derivation.

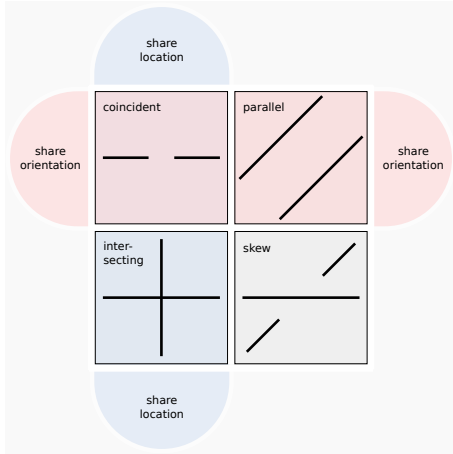


Figure 24: Four relative positions of a pair of lines, displayed with common and distinctive features.

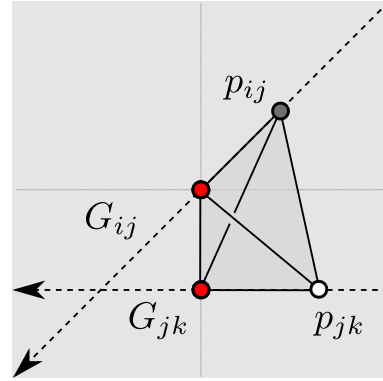


Figure 25: Tetrahedron involved in the configuration of two lines G_{ij} , G_{jk} with anchor points \mathbf{p}_{ij} , \mathbf{p}_{jk} . The four vertices of the tetrahedron are the anchors \mathbf{p}_{ij} , \mathbf{p}_{jk} and the generalized closest points $\pi_{G_{ij}}^*(G_{jk})$ and $\pi_{G_{jk}}^*(G_{ij})$ of the two lines.

C Geometry of Lines, Screws, Twists

In this appendix, the analysis of the *mutual pose of two lines* of Section 3.2.2 is supported.

C.1 Closest Points via Parametric Form

In the main body of the document, the closest points are briefly determined via orthogonal projections. Here, the closest points in terms of the parameter forms are provided.³⁵ Let two lines G_{ij} and G_{jk} be given in parametric form as

$$G_{ij} = \mathbf{p}_{ij} + \lambda_{ij} \cdot \boldsymbol{\omega}_{ij} \quad (92)$$

$$G_{jk} = \mathbf{p}_{jk} + \lambda_{jk} \cdot \boldsymbol{\omega}_{jk} \quad (93)$$

The closest points $\pi_{G_{ij}}(G_{jk})$ and $\pi_{G_{jk}}(G_{ij})$ are the points

$$\pi_{G_{ij}}(G_{jk}) = \mathbf{p}_{ij} + \lambda_{ij}^* \cdot \boldsymbol{\omega}_{ij}, \quad (94)$$

$$\pi_{G_{jk}}(G_{ij}) = \mathbf{p}_{jk} + \lambda_{jk}^* \cdot \boldsymbol{\omega}_{jk}, \quad (95)$$

whereby the parameters λ_{ij}^* and λ_{jk}^* with $\mathbf{d}_{ij,jk} = \mathbf{p}_{jk} - \mathbf{p}_{ij}$ are determined as

$$\lambda_{ij}^* = \frac{(\boldsymbol{\omega}_{ij} \times \boldsymbol{\omega}_{jk}) \cdot (\mathbf{d}_{ij,jk} \times \boldsymbol{\omega}_{jk})}{(\boldsymbol{\omega}_{ij} \times \boldsymbol{\omega}_{jk})^2}, \quad (96)$$

$$\lambda_{jk}^* = \frac{(\boldsymbol{\omega}_{ij} \times \boldsymbol{\omega}_{jk}) \cdot (\mathbf{d}_{ij,jk} \times \boldsymbol{\omega}_{ij})}{(\boldsymbol{\omega}_{ij} \times \boldsymbol{\omega}_{jk})^2}. \quad (97)$$

C.2 A Tetrahedron

When dealing with the mutual pose of *two* lines, G_{ij} and G_{jk} , that are attached to anchors, \mathbf{p}_{ij} and \mathbf{p}_{jk} , a tetrahedron can be considered (see [25, Sec. III]). Concretely, via and the generalized closest points (see Definition 6.1.2), $\mathbf{p}_{(ij\hat{k})} = \pi_{G_{ij}}^*(G_{jk})$ and $\mathbf{p}_{(i\hat{i}j)} = \pi_{G_{jk}}^*(G_{ij})$, the tetrahedron is defined as the convex combination of these four points. The situation is displayed in Figure 25.

³⁵For a derivation and more information on the parametric analysis of two lines, see, e.g., [49], <http://paulbourke.net/geometry/lineline3d/> and <http://stochastix.wordpress.com/2008/12/28/distance-between-two-lines>.

If the indexing is simplified by setting $\mathbf{v}_1 = \mathbf{p}_{ij}$, $\mathbf{v}_2 = \mathbf{p}_{jk}$, $\mathbf{v}_3 = \mathbf{p}_{(ij\hat{k})} = \pi_{G_{ij}}^*(G_{jk})$, and $\mathbf{v}_4 = \mathbf{p}_{(\hat{i}j)} = \pi_{G_{jk}}^*(G_{ij})$, and each point is denoted by unified coordinates as $\mathbf{v}_l = (x_l, y_l, z_l)^T \forall l = 1, \dots, 4$, then, the volume V of the tetrahedron is computed as

$$V = \frac{1}{6} \cdot \begin{vmatrix} x_1 & x_2 & x_3 & x_4 \\ y_1 & y_2 & y_3 & y_4 \\ z_1 & z_2 & z_3 & z_4 \\ 1 & 1 & 1 & 1 \end{vmatrix}. \quad (98)$$

Two general cases can be distinguished: Either, the four points $\mathbf{v}_l \forall l = 1, \dots, 4$ are *affine independent* or they are *affine dependent*: either the four points lie in *generic* pose, or they lie in *degenerate* pose. These two cases correspond to the tetrahedron's volume V as:

$$\left. \begin{array}{l} \text{skew lines} \\ \text{co-planar lines} \end{array} \right\} \Leftrightarrow \left\{ \begin{array}{l} V > 0 \quad \text{for affine independent } \mathbf{v}_i \\ V = 0 \quad \text{for affine dependent } \mathbf{v}_i \end{array} \right. . \quad (99)$$

This tetrahedron can be appears twice: once for Sheth-Uicker Decomposition, once for the Decomposed Finite Twist. In both cases, the regarded lines are passing through the anchors of two joint frames: in case of the Sheth-Uicker decomposition, the lines are lying along the \mathbf{z} -vectors, in case of the Finite-Twist decomposition, the lines are lying along the \mathbf{r} -vectors. Considering the tetrahedron for Sheth-Uicker decomposition, the generic case $V > 0$ corresponds to skew Z -lines / joint axes. The degenerate case $V = 0$ corresponds to co-planar Z -lines / joint axes.

Considering the tetrahedron for Finite-Twist decomposition, the tetrahedron is made by the four points of the Decomposed Twist construction (positions of frames, and the projections of these onto the axis of the twist). The degenerate cases occur, generally, if the radius vectors r_D and r_A are either co-planar, or they vanish; concretely, in the following cases:

- The rotation of the screw displacement has an angle of a *multiple of half-turns* (e.g., $\phi = 0$ or $\phi = \pi$). Then, all four vertices are located in a common plane that also contains the axis of rotation.
- The screw displacement is a *pure rotation* (zero pitch). Then, all four vertices are located in the plane perpendicular to the axis of rotation.
- The screw displacement is a *pure translation* (infinite pitch). Then, all four vertices are located on one line.
- The screw displacement is a *linear* (zero radius). Then, all four vertices are located on the axis of the screw.

C.3 An Overview of Screw Types

In Table 20 three types of screws and twists are opposed.

| Kind of Screw | Translation ($\omega = \mathbf{0}$) | Screw Motion | Rotation ($h = 0$) |
|-------------------------|---------------------------------------|--|--|
| General Form | $(\mathbf{0}, \boldsymbol{\tau})$ | $(\boldsymbol{\omega}, \boldsymbol{\omega} \times \mathbf{r} + h \cdot \boldsymbol{\omega})$ | $(\boldsymbol{\omega}, \boldsymbol{\omega} \times \mathbf{r})$ |
| Linear Form ($r = 0$) | $(\mathbf{0}, \boldsymbol{\tau})$ | $(\boldsymbol{\omega}, h \cdot \boldsymbol{\omega})$ | $(\boldsymbol{\omega}, \mathbf{0})$ |
| Axial Form \mathbf{a} | $(\mathbf{0}, \mathbf{a})$ | $(\mathbf{a}, h \cdot \mathbf{a})$ | $(\mathbf{a}, \mathbf{0})$ |
| Pitch | $h = \infty$ | $0 < h < \infty$ | $h = 0$ |
| Joint Type | Prismatic Joint | Spindle Joint | Revolute Joint |
| Example | $(0, 0, 0, 0, 0, 1)$ | $(0, 0, 1, 0, 0, h)$ | $(0, 0, 1, 0, 0, 0)$ |
| Geometric Entity | Free Vector | Screw | Line |
| Velocity Field | Parallel | Helicoidal | Planar |

Table 20: An overview of three displacement (and motion) types and their twists. The radius r is defined as $r = \|\mathbf{r}\|$. An axis vector \mathbf{a} is a vector that lies on one of the coordinate axes $\mathbf{e}_x, \mathbf{e}_y, \mathbf{e}_z$ of \mathbb{R}^3 .

C.4 Three Basic Screw Displacements

The homogeneous matrix representations of the three axial twists are defined here. The matrix of the axial finite twist along \mathbf{x} reads as

$$\mathcal{S}_{\mathbf{x}}(\phi, s) = \begin{pmatrix} 1 & 0 & 0 & s \\ 0 & c_{\phi} & -s_{\phi} & 0 \\ 0 & s_{\phi} & c_{\phi} & 0 \\ 0 & 0 & 0 & 1 \end{pmatrix}. \quad (100)$$

The matrix of the axial finite twist along \mathbf{y} reads as

$$\mathcal{S}_{\mathbf{y}}(\phi, s) = \begin{pmatrix} c_{\phi} & 0 & s_{\phi} & 0 \\ 0 & 1 & 0 & s \\ -s_{\phi} & 0 & c_{\phi} & 0 \\ 0 & 0 & 0 & 1 \end{pmatrix}. \quad (101)$$

The matrix of the axial finite twist along \mathbf{z} reads as

$$\mathcal{S}_{\mathbf{z}}(\phi, s) = \begin{pmatrix} c_{\phi} & -s_{\phi} & 0 & 0 \\ s_{\phi} & c_{\phi} & 0 & 0 \\ 0 & 0 & 1 & s \\ 0 & 0 & 0 & 1 \end{pmatrix}. \quad (102)$$

D Augmented Convention as Exchange Format

Figure 26 contains several frame sets that appeared in the main body of this document and shows relations among those. At several places in the main body of this document, it is mentioned that frame sets can be ‘thinned out’. This operation of *filtering frames* and *accumulating displacements*, resp., described explicitly in Method VII.

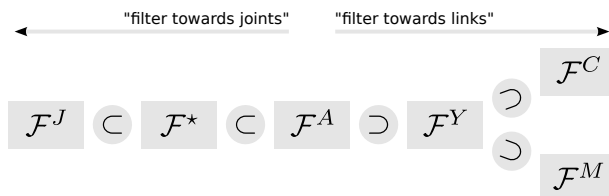


Figure 26: Frame sets and their relations: the augmented Sheth-Uicker frame set \mathcal{F}^A can be thinned out in two directions, either in a joint- or in a link-related manner. In the first direction, \mathcal{F}^A is reduced to the set \mathcal{F}^* (which contains two frames per joint) by discarding the augmenting frames. This can be further reduced to a set \mathcal{F}^J (which contains one frame per joint). In the second direction, \mathcal{F}^A is reduced to Yang’s minimal twist frame set \mathcal{F}^Y by discarding the joint frames. This can be further reduced to the classic and to the modified Denavit-Hartenberg sets \mathcal{F}^C and \mathcal{F}^M .

Within Method VII, Equation 104 can be explained by the following: Let the equalities $F_j^p = F_k^e$ and $F_{j+1}^p = F_p^e$ hold as described in Method VII. Then accumulation displacement $D_{j,j+1}^p$ is computed as

$$\begin{aligned}
 D_{j,j+1}^p &= (F_j^p)^{-1} \circ F_{j+1}^p = (F_k^e)^{-1} \circ F_p^e \\
 &= ((F_k^e)^{-1} \circ F_{k+1}^e) \circ ((F_{k+1}^e)^{-1} \circ F_{k+2}^e) \circ \dots \circ ((F_{p-1}^e)^{-1} \circ F_p^e) \\
 &= \prod_{i=k}^{p-1} (F_i^e)^{-1} \circ F_{i+1}^e = \prod_{i=k}^{p-1} D_{i,i+1}^e.
 \end{aligned} \tag{103}$$

Method VII. AC – Accumulated Displacements for Filtered Frame Sets.

(In) (1) A set of frames $\mathcal{F}^E = \{F_0^e, F_1^e, \dots, F_n^e\}$ of size $|\mathcal{F}^E| = n + 1$, and (2) a set of frames $\mathcal{F}^P = \{F_0^p, F_1^p, \dots, F_m^p\}$ of size $|\mathcal{F}^P| = m + 1$, which is a subset of the first, i.e., $\mathcal{F}^P \subset \mathcal{F}^E$ and $m < n$. Subset \mathcal{F}^P contains the same terminal frames as \mathcal{F}^E . I.e., first and last frame are identical, $F_0^p = F_0^e$ and $F_m^p = F_n^e$.

(Out) Set \mathcal{D}^P of accumulated displacements between m pairs of consecutive frames in \mathcal{F}^P .

(I) Let $\mathcal{E} = \{e_0, e_1, \dots, e_n\}$ and $\mathcal{P} = \{p_0, p_1, \dots, p_m\}$ denote the index sets of the given frame sets.

(D) Computation of n displacements $\mathcal{D}^E = \{D_{i,i+1}^e\}_{i \in \mathcal{P} \setminus \{e_n\}}$ between the frames of \mathcal{F}^E via (see Equation 9)

$$D_{i,i+1}^e = (F_i^e)^{-1} \circ F_{i+1}^e.$$

(A) Computation of m ‘accumulated’ displacements $\mathcal{D}^P = \{D_{j,j+1}^p\}_{j \in \mathcal{E} \setminus \{p_m\}}$ between the frames of the ‘filtered’ frame set \mathcal{F}^P . For F_j^p , let F_k^e denote the identical frame of \mathcal{F}^E and, for F_{j+1}^p , let F_p^e denote the identical frame of \mathcal{F}^E . Briefly, let $F_j^p = F_k^e$ and $F_{j+1}^p = F_p^e$, then for each $j \in \mathcal{E} \setminus \{e_n\}$ the accumulated displacement $D_{j,j+1}^p$ is computed via (see Equation 103)

$$D_{j,j+1}^p = \prod_{i=k}^{p-1} (F_i^e)^{-1} \circ F_{i+1}^e = \prod_{i=k}^{p-1} D_{i,i+1}^e. \tag{104}$$

E Tables, Figures, Methods, Symbols

List of Tables

| | | |
|----|---|----|
| 1 | Four relative poses of two lines. | 13 |
| 2 | Frame usages to describe a joint-link displacement. | 22 |
| 3 | Deduction of the mutual line pose from Sheth-Uicker parameters. | 27 |
| 4 | Geometric meaning of four classic DH parameters. | 29 |
| 5 | Geometric meaning of four modified DH parameters. | 29 |
| 6 | Geometric meaning of six SU parameters. | 29 |
| 7 | Usage of frames for example mechanism. | 31 |
| 8 | Classic DH paramters. | 31 |
| 9 | Modified DH parameters. | 31 |
| 10 | Augmented Sheth-Uicker parameters for example mechanisms. | 32 |
| 11 | Re-classified DH parameters. | 32 |
| 12 | Re-modified DH parameters. | 32 |
| 13 | Yang's Parameters. | 32 |
| 14 | Displacements and the linear span of one, two, and three screws. | 33 |
| 15 | Three graphs for a mechanism. | 33 |
| 16 | Comparison of combinatoric, principal, and application-relevant properties of four conventions. | 35 |
| 17 | Sheth-Uicker and Finite Twist representation and their decompositions in comparison. | 40 |
| 18 | Homogeneous coordinates for points. | 43 |
| 19 | Homogeneous coordinates for lines. | 43 |
| 20 | Three displacement (and motion) types and their twists. | 46 |

List of Figures

| | | |
|----|---|----|
| 1 | A displacement defined by two frames. | 9 |
| 2 | Conjugation duality between relative spatial and relative temporal displacements. | 11 |
| 3 | Visualization of a line $\tilde{G}(a, b)$ and a twist $\$,$ with screw axis $S^0 = \tilde{G}$ | 14 |
| 4 | Depiction of dual quaternion conjugations. | 19 |
| 5 | Complex and dual representations. | 20 |
| 6 | Classic DH parameters for a displacement between frames F_{B_i} and F_{B_j} | 29 |
| 7 | Modified DH parameters for a displacement between F_{C_j} and F_{C_k} | 29 |
| 8 | Line configurations of Z_{ij} and Z_{jk} for a chain of links L_i, L_j, L_k together with named frames. | 29 |
| 9 | Schematic sketch for augmented parameters. | 29 |
| 10 | Set of matrices of example mechanism. | 30 |
| 11 | Example mechanism with named links, joints and frames. | 30 |
| 12 | Frame usage for skew example mechanism. | 31 |
| 13 | Twist rotation axis location. | 36 |
| 14 | Twist radius vectors. | 36 |
| 15 | Theorem of inscribed angles. | 37 |
| 16 | Planar displacement with rotation pole. | 37 |
| 17 | Visualizations of Sheth-Uicker decomposition and Finite Twist trajectory. | 38 |
| 18 | Decompositions of the Finite-Twist representation and of Sheth-Uicker's representation. | 39 |
| 19 | Spatial setting of two decompositions. | 39 |
| 20 | Four representations of a finite spatial rotation $R \in SO(3)$ and some interrelations. | 40 |
| 21 | Four representations of a finite spatial displacement $D \in SE(3)$ and some interrelations. | 40 |
| 22 | Analogies of decompositions for a displacement and for a matrix. | 41 |
| 23 | Connections of Sheth-Uicker's and the Finite Twist Representation for Finite Displacements. | 41 |
| 24 | Four relative positions of a pair of lines, displayed with common and distinctive features. | 45 |
| 25 | Tetrahedron associated to two anchored lines. | 45 |
| 26 | Frame sets and their relations. | 48 |

List of Methods

| | | |
|-----|--|----|
| I | M2T – Matrix to Twist Conversion | 17 |
| II | TWO-SU – Frame Placings for Two-Frame Convention | 23 |
| III | CLS-DH – Frame Placings for Classic DH Convention | 25 |
| IV | MOD-DH – Frame Placings for Modified DH Convention | 25 |
| V | AUG-SU – Frame Placings for Augmented SU Convention | 26 |
| VI | DT – Decomposed Twist | 37 |
| VII | AC – Accumulated Displacements for Filtered Frame Sets | 48 |

List of Symbols

| | | |
|-------------------------------------|---|----|
| $\tilde{(\cdot)}$ | dual entity | 2 |
| $\overset{\circ}{(\cdot)}$ | dual part of a dual entity | 2 |
| $(\cdot)^*$ | swapping primal and dual part of a dual entity | 2 |
| $[\cdot]$ | equivalence class | 2 |
| $\hat{(\cdot)}$ | normalized entity | 2 |
| \hat{i} | omitted index, e.g., let $\mathcal{I} = \{1, 2, 3, 4\}$, then $\{1, 2, \hat{3}, 4\} = \{1, 2, 4\} = \mathcal{I} \setminus \{3\}$ | 22 |
| $(\cdot)^\otimes$ | skew-symmetric matrix of a vector | 2 |
| $(\cdot)^\oplus$ | axis vector of a skew-symmetric matrix | 2 |
| \overline{D} | time variant displacement D | 2 |
| \underline{D} | time invariant displacement D | 2 |
| $\overline{\tilde{q}}$ | complex conjugation of a dual quaternion \tilde{q} | 18 |
| $\tilde{\overline{q}}$ | dual conjugation of a dual quaternion \tilde{q} | 18 |
| \cdot | scalar, vector, or matrix multiplication | 2 |
| \star | sum of element-wise products | 3 |
| \odot | multiplication of dual entities | 2 |
| $\langle \cdot, \cdot \rangle$ | scalar product | 2 |
| $[\cdot, \cdot]$ | Lie bracket | 39 |
| $\pi_{G_{ij}}^*(G_{jk})$ | generalized closest point | 14 |
| $\perp^*(\omega_{ij}, \omega_{jk})$ | generalized perpendicular direction | 14 |
| $\perp^*(G_{ij}, G_{jk})$ | generalized orthogonal line | 14 |
| c_ζ | short for $\cos(\zeta)$ | 20 |
| \mathbf{d} | vector of design paramters | 4 |
| \mathcal{D} | set of vectors of design parameters | 4 |
| ID | space of design parameter vectors | 4 |
| $D_{(D,A)}^{(t)}$ | spatial displacement | 10 |
| $D_X^{(u,t)}$ | temporal displacement | 10 |
| \mathcal{D}^* | set of displacements according to two-frame Sheth-Uicker convention | 33 |
| \mathcal{D}^A | set of displacements according to augmented Sheth-Uicker convention | 33 |
| $\tilde{\delta}_{ij}$ | dual angle to represent the displacement of a simple joint J_{ij} | 21 |
| \mathcal{E} | set of edges of a graph | 4 |
| ϵ | dual unit | 2 |
| F_{ij_i}, F_{ij_j} | frames at joint J_{ij} | 6 |
| F_O | global coordinate frame at origin | 10 |
| F_D, F_C, F_B, F_A | short names of four consecutive frames | 22 |
| F_T, F_R | short names of two consecutive frames on twist axis | 37 |
| F_X | frame attached to a body \mathbf{X} | 10 |
| \mathcal{F} | set of frames | 6 |
| $\hat{\mathcal{F}}$ | set of frames that determines a unique posture | 6 |
| \mathcal{F}^C | set of frames according to classic Denavit-Hartenberg convention | 22 |
| \mathcal{F}^M | set of frames according to modified Denavit-Hartenberg convention | 22 |
| \mathcal{F}^* | set of frames according to two-frame Sheth-Uicker convention | 22 |
| \mathcal{F}^A | set of frames according to augmented Sheth-Uicker convention | 22 |
| G_{ij}, G_{jk} | lines | 13 |
| γ, β, α | Euler angles in Bunge convention | 20 |

| | | |
|---|---|----|
| $\tilde{\gamma}, \tilde{\beta}, \tilde{\alpha}$ | dual Euler angles in Bunge convention | 21 |
| \mathcal{G} | graph | 4 |
| h | pitch h of a screw | 17 |
| i | imaginary unit | 2 |
| \mathbf{i} | imaginary vector unit | 2 |
| J_{ij} | joint connecting L_i and L_j | 4 |
| \mathcal{J} | set of joints | 4 |
| κ | scalar variable | 13 |
| L_i | link | 4 |
| \mathcal{L} | set of links | 4 |
| M | homogeneous matrix | 10 |
| \mathcal{M} | mechanism (type) | 4 |
| $\underline{\mathcal{M}}$ | (Euclidean) mechanism | 4 |
| $\overline{\mathcal{M}}$ | (Euclidean) mechanism with unique posture | 6 |
| ω | rotation axis | 12 |
| P | pose | 6 |
| \mathcal{P} | set of poses | 6 |
| $SE(3)$ | space of poses | 6 |
| ϕ | rotation angle / spin of a twist | 12 |
| $\pi_{\mathbf{a}}(\mathbf{b})$ | orthogonal projection of \mathbf{b} onto \mathbf{a} | 3 |
| \mathbf{q} | vector of configuration variables | 4 |
| \mathcal{Q} | set of vectors of configuration variables | 4 |
| \mathbb{Q} | space of configuration variable vectors | 4 |
| q | quaternion | 18 |
| \tilde{q} | dual quaternion | 18 |
| \mathbf{R} | rotation matrix | 9 |
| \mathbf{r} | radius vector | 15 |
| s_{ζ} | short for $\sin(\zeta)$ | 20 |
| s | shift s of a twist | 17 |
| \mathbf{s} | shift vector / absolute translation | 16 |
| S | screw $S = (\boldsymbol{\omega}, \mathbf{v})$ | 15 |
| $\$$ | twist $\$_G(\tilde{\phi})$ | 16 |
| \mathcal{S} | twist coordinates with respect to pitch h | 17 |
| \mathbf{t} | translation vector | 10 |
| \mathbf{t}_0 | orthogonal translation vector | 16 |
| $\tau_{\mathbf{a}}(\mathbf{b})$ | orthogonal projection of \mathbf{b} onto \mathbf{a}^{\perp} | 3 |
| $\tilde{\theta}$ | dual angle to represent an accumulated L - J - L displacement along the joint axis of J | 21 |
| \mathbf{v} | moment of a screw | 15 |
| \mathbf{v}_0 | orthogonal moment of a line | 12 |
| \mathcal{V} | set of vertices of a graph | 4 |

References

- [1] Shreeram S. Abhyankar. *Algebraic Geometry for Scientists and Engineers*. Mathematical Surveys and Monographs. American Mathematical Society, July 1992.
- [2] Jorge Angeles. Is there a characteristic length of a rigid-body displacement? *Mechanism and Machine Theory*, 41(8):884 – 896, 2006. Special issue on CK 2005, International Workshop on Computational Kinematics.
- [3] Olivier A. Bauchau and Lorenzo Trainelli. The vectorial parameterization of rotation. *Nonlinear Dynamics*, 32(1):71–92, 2003.
- [4] Millard F. Beatty. Kinematics of finite, rigid-body displacements. *American Journal of Physics*, 34(10):949, 1966.
- [5] Bertold Bongardt. CAD-2-SIM – Kinematic Modeling of Mechanisms Based on the Sheth-Uicker Convention. In *Intelligent Robotics and Applications – 4th International Conference, ICIRA 2011*, volume I of *LNAI 7101*, pages 465–477, 2011.
- [6] Hans J. Bunge. *Texture analysis in materials science*. Butterworths, London, Boston, 1982.
- [7] Adrian A. Canutescu and Roland L. Dunbrack. Cyclic coordinate descent: A robotics algorithm for protein loop closure. *Protein Science*, 12(5):963–972, May 2003.
- [8] Harry H. Cheng and Sean Thompson. Dual polynomials and complex dual numbers for analysis of spatial mechanisms. In *Proceedings of 1996 ASME Design Engineering Technical Conference and Computers in Engineering Conference*, 1996.
- [9] John J. Craig. *Introduction to Robotics: Mechanics and Control*. Addison-Wesley Longman Publishing Co., Inc., Boston, MA, USA, 1989.
- [10] Jian S. Dai. An historical review of the theoretical development of rigid body displacements from rodrigues parameters to the finite twist. *Mechanism and machine theory*, 41(1):41–52, 2006.
- [11] Joseph K. Davidson, Kenneth H. Hunt, and Gordon R. Pennock. *Robots and Screw Theory: Applications of Kinematics and Statics to Robotics*, volume 126. ASME, 2004.
- [12] Reinhard Diestel. *Graph Theory*. Springer, 2005.
- [13] Leo Dorst, Daniel Fontijne, and Stephen Mann. *Geometric Algebra – An Object-Oriented Approach to Geometry*. Morgan Kaufmann Series in Computer Graphics. Morgan Kaufmann Publishers, 2007.
- [14] Roy Featherstone. *Rigid Body Dynamics Algorithms*. Springer, 2008.
- [15] Gerd Fischer. *Lineare Algebra. Eine Einführung für Studienanfänger*. Vieweg, 12 edition, 2000.
- [16] Janez Funda. A computational analysis of line-oriented screw transformations in robotics. Technical report, University of Pennsylvania, 1988.
- [17] Jean Gallier and Dianna Xu. Computing exponentials of skew symmetric matrices and logarithms of orthogonal matrices. *International Journal of Robotics and Automation*, 18:10–20, 2000.
- [18] Krishna C. Gupta. Kinematic analysis of manipulators using the zero reference position description. *Int. J. Rob. Res.*, 5:5–13, 1986.
- [19] Andrew J. Hanson. *Visualizing Quaternions (The Morgan Kaufmann Series in Interactive 3D Technology)*. Morgan Kaufmann Publishers Inc., San Francisco, CA, USA, 2006.
- [20] Richard S. Hartenberg and Jacques Denavit. *Kinematic Synthesis of Linkages*. 1964.
- [21] Chintien Huang. On definitions of pitches and the finite screw system for displacing a line. In *A Symposium Commemorating the Legacy, Works, and Life of Sir Robert Stawell Ball*, 2000.
- [22] Manfred L. Husty. Algebraic methods in mechanisms analysis and synthesis. *Machine Design & Research*, pages 37–48, 2006.

- [23] Ladislav Kavan, Steven Collins, Jiří Žára, and Carol O’Sullivan. Geometric skinning with approximate dual quaternion blending. *ACM Trans. Graph.*, 27(4):1–23, 2008.
- [24] Wisama Khalil and Jean-François Kleinfinger. A new geometric notation for open and closed-loop robots. In *Robotics and Automation. Proceedings. 1986 IEEE International Conference on*, volume 3, pages 1174 – 1179, apr 1986.
- [25] Felix Klein. *Elementary mathematics from an advanced standpoint: Geometry*. 1939.
- [26] Jack B. Kuipers. *Quaternions and Rotation Sequences: A Primer with Applications to Orbits, Aerospace and Virtual Reality*. Princeton University Press, 2002.
- [27] Vijay Kumar. *The Theorems of Euler and Chasles*, 2002.
- [28] Steven M. LaValle. *Planning Algorithms*. Cambridge University Press, 2006.
- [29] Matthew T. Mason. *Mechanics of Robotic Manipulation*. MIT Press, 2001.
- [30] Patrick Muir and Charles P. Neuman. Kinematic modeling of wheeled mobile robots. Technical Report CMU-RI-TR-86-12, Robotics Institute, Pittsburgh, PA, June 1986.
- [31] Richard M. Murray, S. Shankar Sastry, and Li Zexiang. *A Mathematical Introduction to Robotic Manipulation*. CRC Press, Boca Raton, FL, USA, 1994.
- [32] Bob Palais and Richard Palais. Euler’s fixed point theorem: The axis of a rotation. *Journal of Fixed Point Theory and Applications*, 2(2):215–220, December 2007.
- [33] Ian A. Parkin. Unifying the geometry of finite displacement screws and orthogonal matrix transformations. *Mechanism and Machine Theory*, 32(8):975 – 991, 1997.
- [34] Ian A. Parkin. *Advances in Robot Kinematics: Analysis and Design*, chapter Alternative Forms for Displacement Screws and Their Pitches. 2008.
- [35] Marko Petkovek, Herbert S. Wilf, and Doron Zeilberger. *A=B*. AK Peters, Ltd., January 1996.
- [36] Jack Phillips. *Freedom in Machinery: Volume 1 (1984) and Volume 2 (1990)*. Cambridge University Press, 2007.
- [37] Josep M. Porta, Lluís Ros, Tom Creemers, and Federico Thomas. Box approximations of planar linkage configuration spaces. *Journal of Mechanical Design*, 129(4):397–405, 2007.
- [38] Josep M. Porta, Lluís Ros, and Federico Thomas. A linear relaxation technique for the position analysis of multiloop linkages. *IEEE Transactions on Robotics*, 25(2):225–239, 2009.
- [39] Helmut Pottmann and Johannes Wallner. *Computational Line Geometry*. Springer-Verlag New York, Inc., Secaucus, NJ, USA, 2001.
- [40] Romain Quey. Orientation Library – The documentation for Orientation Library 2.0, 2009.
- [41] Jürgen Richter-Gebert. *Perspectives on projective geometry. A guided tour through real and complex geometry*. Springer, 2011.
- [42] Joseph Rooney. A comparison of representations of general spatial screw displacement. *Environment and Planning B: Planning and Design*, 5(1):45–88, 1978.
- [43] Bernard Roth. Overview on advanced robotics: Manipulation. In *Proceedings ICAR*, pages 569–580, 1985.
- [44] Lorenzo Sciavicco and Bruno Siciliano. *Modelling and Control of Robot Manipulators*. Kluwer Academic Publishers, 2nd edition, 1999.
- [45] Jon M. Selig. *Geometric Fundamentals of Robotics, 2nd ed.* Springer, Berlin, 2005.
- [46] Jon M. Selig. Cayley maps for $se(3)$. In *12th IFToMM World Congress, Besancon*, 2007.

-
- [47] Jon M. Selig. Exponential and cayley maps for dual quaternions. *Advances in Applied Clifford Algebras*, 20:923–936, 2010. 10.1007/s00006-010-0229-5.
- [48] Pradip N. Sheth and John J. Uicker. A generalized symbolic notation for mechanisms. *Journal of Engineering for Industry, Series B*, 93(70):102–112, 1971.
- [49] Jonathan Richard Shewchuk. Lecture notes on geometric robustness, November 2009.
- [50] Mark W. Spong, S. Hutchinson, and M. Vidyasagar. *Robot Modeling and Control*. John Wiley and Sons, Inc., 2005.
- [51] Ernesto Staffetti and Federico Thomas. Analysis of rigid body interactions for compliant motion tasks using the grassmann-cayley algebra. In *Intelligent Robots and Systems, 2000. (IROS 2000). Proceedings. 2000 IEEE/RSJ International Conference on*, volume 3, pages 2325–2332 vol.3, 2000.
- [52] John Stillwell. *Naive Lie Theory*. Undergraduate Texts in Mathematics. Springer, New York, NY, 2008.
- [53] Ulrike Thomas, I. Maciuszek, and Friedrich M. Wahl. A Unified Notation for Serial, Parallel, and Hybrid Kinematic Structures. In *ICRA*, pages 2868–2873, 2002.
- [54] Lorenzo Trainelli. The vectorial parameterization of rotation and motion. Technical report, Politecnico di Milano, 2002. DIA-SR 02-18.
- [55] Kenneth Waldron and James Schmiedeler. *Springer Handbook of Robotics*, chapter Kinematics, pages 9–33. Springer, 2008.
- [56] Neil L. White. Grassmann-cayley algebra and robotics. *Journal of Intelligent and Robotic Systems*, pages 91–107, 1994.
- [57] Thomas R. Williams and Ken R. Fyfe. Rodrigues’ spatial kinematics. *Mechanism and Machine Theory*, 45(1):15 – 22, 2010.
- [58] An Tzu Yang. Displacement analysis of spatial five-link mechanisms using (3x3) matrices with dual-number elements. *ASME Journal of Engineering for Industry*, 91:152–157, 1968.
- [59] An Tzu Yang. Analysis of an offset unsymmetric gyroscope with oblique rotor using (3x3) matrices with dual-number elements. *ASME Journal of Engineering for Industry*, 91(3):535–542, 1969.

German Research Center for Artificial Intelligence (DFKI) GmbH

DFKI Bremen

Robert-Hooke-Straße 5

28359 Bremen

Germany

Phone: +49 421 178 45 4100

Fax: +49 421 178 45 4150

DFKI Saarbrücken

Stuhlsatzenhausweg 3

Campus D3 2

66123 Saarbrücken

Germany

Phone: +49 681 875 75 0

Fax: +49 681 857 75 5341

DFKI Kaiserslautern

Trippstadter Straße 122

67608 Kaiserslautern

Germany

Phone: +49 631 205 75 0

Fax: +49 631 205 75 5030

DFKI Projektbüro Berlin

Alt-Moabit 91c

10559 Berlin

Germany

Phone: +49 30 238 95 1800

E-mail:

reports@dfki.de

Further information:

<http://www.dfki.de>